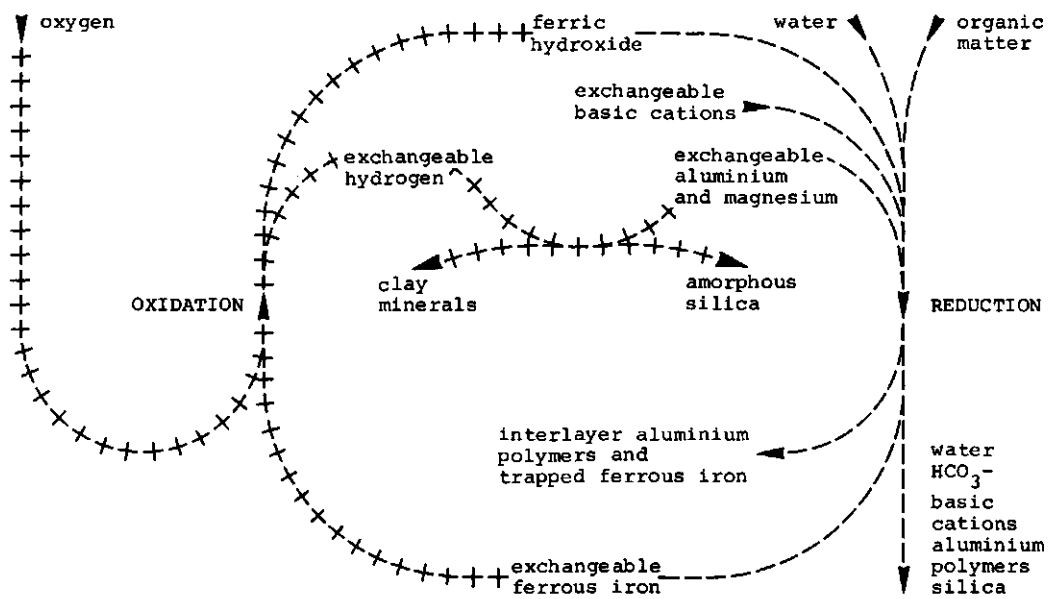


Contents

<i>Introduction</i>	1
<i>Soil descriptions, analyses and interpretation</i>	4
Summary interpretation	4
Latina	6
Hardthäuser Wald	17
Eynatten	25
Solling	42
Biebosch Valkenburg	52
Nuth	61
<i>Multiple soil-forming processes in single profiles</i>	69
The processes listed by soil profile	69
Examples of both cheluviation and ferrolysis in single profiles	70
<i>Processes taking place in surface-water gley soils, podzols and podzolic soils, and criteria for distinguishing their effects</i>	73
Existing soil terminology, classification and genetic concepts	73
Two models for the genesis of bleached eluvial horizons	77
Choice of criteria from eluvial or illuvial horizons for diagnosis and classification	81
The distinction of ferrolysis from clay translocation and desilication	82
Diagnostic characteristics for cheluviation and ferrolysis; consequences for soil classification	83
<i>Appendix</i>	88
Methods	88
Choice of units and entities	91
<i>Summary</i>	93
<i>Samenvatting</i>	98
<i>References</i>	103



Introduction

During soil surveys in the Guyana coastal plains by a joint group from FAO and the Guyana Ministry of Agriculture, 1961-1964, a question arose about the origin of the widespread acid bleached seasonally wet, silty surface horizons that occurred over more clayey subsoils. These were most evident in the Pleistocene coastal plain but were also observed in Holocene meander belts as well as in some parts of the Holocene coastal clay plains.

A group in adjacent Suriname (Pons, pers. commun., 1963) was of the opinion that the action of earthworms in combination with slight erosion by slowly moving inundation water was responsible for the loss of clay from the surface horizons. This clay would then be deposited in low-lying parts of the landscape or removed to the rivers. In the Holocene riverine areas this hypothesis appeared tenable. The Pleistocene marine clay landscape of the Guyanas contains closed depressions, the margins of which are dotted with towers of earthworm excreta, whereas the low, level centre has a silt loam or even a silt surface horizon over a silty clay subsoil and substratum. Clearly, the hypothesis of clay removal by erosion and water flow over the surface could not adequately explain these observations.

During soil surveys in Bangladesh, 1964-1966, a team from FAO and the Ministry of Agriculture found very extensive areas of soils similar to those in the Guyanas, both on Holocene floodplains and Pleistocene terrace landforms. The lower boundary of the silty material may have many shapes, appearing as if 'etched' into the underlying silty clay or clay as observed in many pits and deep excavations. The silty upper horizons thus should have been formed from the underlying clayey material, but the pedogenic process was obscure.

Already about 1962, R.B. Cate had explained to me how ferrous iron in reduced conditions could temporarily substitute for the more strongly acidic aluminium, so that exchangeable bases could be leached out as bicarbonates at a temporarily high pH value. Thus, a low base saturation could be brought about more rapidly by leaching under reduced conditions than in well-drained soils. This idea was later published (Cate & Sukhai, 1965). Regrettably, the explanation did not stick in my memory and about 1965, H. Brammer and I slowly redeveloped this concept, starting from the observation that in many seasonally wet surface horizons in Bangladesh, the soil reaction alternated between near-neutral under reduced conditions and strongly acid in the dry season or after drying in the laboratory.

During 1967-1969, while working in the semi-arid plains of Pakistan, I could not forget these soils of Bangladesh, and a hypothesis of clay destruction and interlayering under seasonally wet conditions took shape, as yet with very little analytical support. A search of the literature then turned up some data by earlier authors, from work on clay suspensions and soil columns, that illustrated most of the steps of this postulated hydro-morphic soil-forming process. Stimulating discussions, particularly with H. Brammer and

R. Dudal, clarified several aspects and helped in the invention of a suitably descriptive name for the overall process: ferrolysis (from ferrous and lysis; clay decomposition by a process based on the alternate reduction and oxidation of iron).

Ferrolysis is summarized in the frontispiece figure. In brief, iron oxides are reduced to Fe^{2+} during continued microbial decomposition of organic matter after water-saturation of the eluvial horizons. The Fe^{2+} displaces exchangeable cations, which are removed by leaching together with part of the ferrous ions. Hydrogen ions consumed during reduction are replaced by partial neutralization and polymerization of aluminium ions. Next, the pH rises from about 4-5 to about 6-7. Part of the aluminium polymers is leached, part is fixed as octahedral fragments or incomplete interlayers between the layers of swelling clay minerals; some Fe^{2+} is trapped and becomes non-exchangeable; the cation exchange capacity of the clay fraction is decreased. Upon re-entry of oxygen into the eluvial horizons, exchangeable ferrous ions are oxidized again to ferric oxides. The hydrogen ions produced during oxidation become exchangeable. The hydrogen clay is rapidly altered to an aluminium-magnesium clay by partial dissolution of cations from the clay minerals. Silica from unsupported tetrahedral sheets is partially dissolved and may reprecipitate in amorphous form when the eluvial horizons dry out. Part of the silica is removed in solution during the next period of water-saturation.

After publication of the hypothesis in 1970, I tested it by comparing its consequences with the results of morphological, chemical and mineralogical studies of samples from different acid, seasonally wet soils. A paper published in 1973 gives micromorphological and microchemical information on clay skins from a surface-water gley soil in different stages of decomposition. After the presence of secondary clay-sized quartz had been reported in that paper, it was found that at least the quartz of coarse-clay size was largely detrital, not secondary. Later studies showed the presence of amorphous silica in samples from seasonally wet soils subject to clay decomposition. A series of papers published in 1977 contain data on two acid, seasonally wet soils from Southeast Asia with an interpretation of the main processes responsible for their formation. These papers corroborated the hypothesis that ferrolysis was one of the main soil-forming processes in the seasonally wet, nearly level terrace and river plain landforms in the humid monsoon climate of Southeast Asia.

This book first gives detailed morphological, physical, chemical and mineralogical data and genetic interpretations of four European surface-water gley soils and two well-drained soils in similar materials from nearby locations. The next chapter starts with a list of the different processes identified in these soils as well as in the Southeast Asian ones reported earlier. Examples are discussed of soils in which cheluviation and ferrolysis may have occurred concurrently, but not in the same horizon; cheluviation may follow ferrolysis, not coexist with it, in a given soil horizon.

The last chapter opens with a review of earlier work and opinions on podzols and surface-water gley soils and on the processes presumed to occur in them. The distinction between these two kinds of soil, even though recognized from the beginning of this century, has not been systematically maintained in the Russian literature. Many authors thought

that one process, termed podzolization but not well defined, was responsible for their formation. In the U.S. literature, the two kinds of soil have been distinguished, but the chemical and mineralogical characteristics of surface-water gley soils have not been completely explained. The latest U.S. soil classification system relegates the surface-water gley soils to different Great Groups in different Soil Orders.

In this chapter, the processes of cheluviation and ferrollysis are described in detail in tabular form; diagnostic criteria are given for distinguishing the effects of these two, as well as for distinguishing the effects of ferrollysis from those of hydrolysis by water containing carbonic acid (desilication). The criteria refer mainly to the eluvial horizons; these are less marked by effects of fossil soil-forming processes than illuvial horizons, to which conventional criteria for soil classification mainly refer.

Use of these new criteria in soil classification would probably improve the homogeneity and practical value of the resultant groupings. Their use in studies of soil genesis should decrease the uncertainty and ambiguity often met with in attempts at identifying recent or current soil-forming processes when marks of earlier ones are present.

Soil descriptions, analyses and interpretation

This chapter comprises morphological descriptions and physical, chemical and mineralogical analyses with a genetic interpretation of European surface-water gley soils, two without and two with podzol sequa developed in the surface horizons, and of a few well-drained soils in similar materials at nearby locations. Data on these soils as well as on surface-water gley soils in Southeast Asia described earlier in separate papers (Brinkman et al., 1977 and Brinkman, 1977a en b), form the background for the following chapters.

SUMMARY INTERPRETATION

The *Latina* profile is dry or moist for most of the year. The upper horizons are wet and reduced by rain-water saturation during wet spells in winter. Saturation is due to the nearly level terrace landform and a slow or very slow subsoil permeability. The decrease in clay percentage from about 40 to less than 15 in the upper horizons of the homogeneous sediment may be ascribed for a small part to clay translocation, and mainly to (probably subsequent) ferrolysis and an unknown proportion of removal by slow sheet flow.

Besides kaolinite, illite and some quartz, the clay fractions contain slightly aluminium-interlayered smectite in the lowest horizons, and strongly aluminium-interlayered material, soil chlorite, with some trapped ferrous iron in the upper horizons.

Liming appears to have raised the pH and percentage of calcium saturation and to have eliminated exchangeable aluminium from the upper 0.4 m of the profile. The very unfavourable hydrology, drought in summer and water-saturation in wet periods, presumably was the main reason why the land around this profile and similar areas nearby are no longer cultivated.

The *Hardthäuser Wald* profile has wet, reduced upper horizons in wet winters and dries out deeply in dry summers. There is some net vertical leaching, not necessarily every year, and slow lateral water movement in wet periods. (Blume et al., 1971).

There has been considerable clay translocation; there is no proof of net clay loss from the profile. Some clay destruction is indicated by the graininess and low birefringence of argillans and papules and the presence of secondary silica in thin sections. The main component of the clay fractions, vermiculite, is slightly aluminium-interlayered in the deeper horizons and strongly interlayered in the A and E horizons; the interlayers in these upper horizons apparently contain considerable trapped ferrous iron and probably some magnesium. Morphological and chemical evidence for translocation of iron and manganese oxides and for some clay destruction indicate that ferrolysis may have occurred or may still be active. This conclusion is confirmed by the aluminium-interlayering and the

presence of excess ferrous iron in clay fractions of the upper horizons.

Trends with depth in total Ca, Mg, K and P contents of the clay fractions and in exchangeable potassium and magnesium may be due to a long period of effective nutrient cycling by forest vegetation in balance with slow leaching, followed by a short period in which acid rain has accelerated the removal of exchangeable magnesium and potassium from the upper 0.2 m.

The *Eynatten* profile is seasonally dry or moist and periodically wet for a sufficient period to bring about reduction in the upper horizons, due to the nearly level slope and the very slow permeability of the subsoil and substratum. Clay translocation and concurrent or, more probably, subsequent weathering under periodically reduced conditions have produced a surface-water gley sequum comprising a pale, silty eluvial horizon with a low cation exchange capacity, tonguing into a strongly mottled silt loam illuvial horizon containing more clay, with a very low base saturation throughout.

The very low nutrient availability has inhibited the mineralization of leaves and twigs, and given rise to litter, *forna* and humus layers on top of the mineral soil. Cheluviation by mobile organic acids originating from this material has produced a thin podzolic eluvial horizon in the upper decimetre of the eluvial horizon of the surface-water gley sequum.

The two types of eluvial horizon may be distinguished in the field by differences in colour and mottling. The analytical data for the eluvial horizons of the surface-water gley and the podzol sequa show contrasting trends in aluminium and ferrous iron contents of the clay fractions, and maximal development and preferential decomposition, respectively, of aluminium-interlayered material with ferrous iron trapped in the interlayers.

At present, the profile appears to be subject to leaching by strong mineral acid, as suggested by the high sulphate concentrations and the cation composition in soil solutions and by data from other authors on sulphate and acid in precipitation.

The *Solling* profile is much less deeply developed but otherwise similar to the *Eynatten* profile. There is no evidence for leaching by strong acid in the data for the *Solling* profile.

The *Solling Brown Earth* profile is well drained, more strongly homogenized than the *Solling* (pseudogley) profile and does not show a trace of clay illuviation. The main physicochemical process identified is desilication, hydrolysis by water containing carbon dioxide, superseded by cheluviation in the surface horizon.

The *Biebosch Valkenburg* profile is well drained; the horizons to about 0.6 m depth are strongly perforated and have common roots that are well-distributed. Deeper horizons are less porous and contain few roots. Clay illuviation features and clay produced by the transformation of mica flakes are prevalent in the lower horizons but also occur higher in the profile. The chemical and mineralogical data indicate that there has been moderate desilication throughout, followed by cheluviation in the surface horizon as in the *Solling Brown Earth* profile.

The *Nuth* profile is well drained and has no trace of present or past reduction. Besides the strong biotic perforation, clay eluviation-illuviation is evident. Part of the weatherable minerals in the sand + silt fraction has been removed, probably by desilication. Little of the clay fraction has disappeared. The decrease towards the surface of smectite recognizable by X-ray diffraction indicates that cheluviation has not played a part. Presumably, part of the smectite reflection has disappeared by desilication, part by randomly interstratified aluminium interlayering. The decrease in estimated CEC of the clay fractions towards the surface also suggests that the silica-rich clay minerals have been preferentially attacked or altered.

LATINA

FAO/Unesco Soil Units (FAO, 1974): Solodic Planosol¹

USDA Soil Taxonomy (Soil Survey Staff, 1975): Aquic Dystric Eutrochrept^{2,3}

Examined 21 December 1971 by R. Brinkman.

The site

Location near Latina, Italy. Topographic map sheet no. 158 (Latina), 4th edition, 1:100 000, coordinates 4590.7 km N, 323.5 km E. About 41°26.8' N, 12° 53.2' E (0°26.1'E of Roma meridian). About 2.6 km SSW of Latina town centre on the Latina-Mare road; about 250 m from underpass under main highway to Rome; about 200 m S of highway, 100 m W of road. Elevation about 22 m above mean sea level.

Landform and slope: level surface of extensive terrace, dissected to 2 - 5 m depth by dry, winding drainage channels at wide intervals, more closely and deeply dissected near the edge of the terrace.

Vegetation and land use: mainly abandoned farmland, locally used for housing. Land under grasses and small shrubs. The only trees are eucalypts planted along road ditches and locally seeded elsewhere. Locally some fields in use for poor arable crops, locally few very poor, stunted vines. Used fields are slightly convex with small open field drains.

Climate: mediterranean (Köppen Csa). Data from Latina (Fig. 1): mean annual temperature 15.9°C, coldest month (Jan.) 8.4°C, hottest month (Aug.) 24.2°C. Precipitation 928 mm/year, wettest months (Oct.-Jan.) about 125 mm/month, driest months (June-Aug.) about 20 mm/month.

1. marginal to Dystric Planosol.

2. marginal to Aeric Haplaquept.

Liming may have raised the base saturation and caused a shift from Aquic Dystrichrept.

3. or Aeric Albaqualf, as discussed in the section on grain-size distribution.

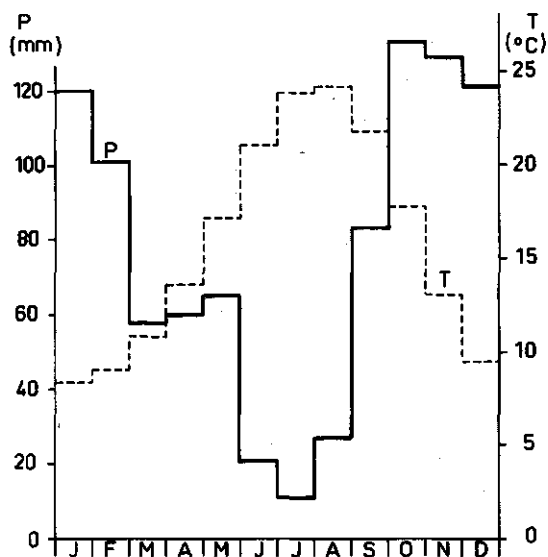


Fig. 1. Temperature and precipitation at Latina (13 m above mean sea level). Source: Istituto Centrale di Statistica, Anuario di Statistiche Meteorologiche, 1959. Roma. Quoted in Wernstedt, 1972.

General information on the soil

Parent material: old marine or lagoonal material, noncalcareous sandy clay loam to clay. In one place in the terrace a few km from the profile site, some calcareous material and pieces of limestone were observed at a depth of about 1 metre. Remmelzwaal (1978, p 230-231) estimates the age of the Latina deposits as (early) middle Pleistocene, possibly 0.5 to 0.4 m.y.

Drainage: somewhat poorly drained. Surface drainage very slow in most places, internal drainage slow or very slow. Water standing locally on fields, in occasional shallow field drains, man-made pits and road ditches some weeks after the last rain. Profile moist throughout. Ground water not observed. Serious flooding during severe or extended wet periods in some years.

No surface stones or rock outcrops. Signs of slaking and local redistribution of sand and (silt + clay) in many places on the surface and at edges of depressions and small field drains. No salinity or sodicity present.

Human influence: occasional shallow field drains, and deepened and locally straightened natural drainage channels. The surface horizon of the profile locally contains few small pieces of Bg1 material presumably brought in from field ditches. The pH profile and base saturation suggest influence of liming to about 0.4 m depth.

Brief description of the profile

Acid, greyish brown sandy loam about 0.4 m over acid, brown sandy clay with grey mottles, changing to light brownish grey mottled yellowish brown from about 0.9 m. Subsoil structure weak with very thin cutans, probably pressure faces. Few fine and very fine tubular pores in most of the profile, very few at depth.

Description of individual soil horizons

- 0-13 cm Abandoned former Ap. Greyish brown (10YR 5/2) moist sandy loam with many fine
Eg1 faint brown and dark yellowish brown mottles; very weak medium and fine subangular blocky, parts granular, upper few cm massive or very weak platy (redistribution); moist friable, wet non-plastic, slightly sticky, no cutans; occasional medium, few fine and few very fine tubular pores; locally few small pieces of Bg1 material (presumably brought in by man); many fine and very fine roots, part dead; gradual smooth boundary. Sample 72-135; thin sections 72056 (0-15 cm) and 72063 (small, 5-8 cm).
- 13-36 cm Greyish brown (10YR 5/2) moist sandy loam with few fine distinct yellowish brown
Eg2 and strong brown mottles partly along old root channels; massive; moist friable, wet non-plastic, slightly sticky; few fine, common very fine tubular pores; occasional fine black nodules; locally few medium dark grey infillings; common fine and very fine dead and living roots, occasional medium living roots; abrupt smooth boundary. Sample 72-136; thin sections 72057 (14-29 cm), 72058 (28-43 cm), 72064 and 72065 (small, about 36 cm depth).
- 36-56 cm Brown (10YR 5/3) moist sandy clay loam with many medium distinct light grey and
Bg1 many medium faint yellowish brown mottles (mainly clusters of individual fine mottles); very weak medium subangular blocky; moist friable, wet plastic and sticky; thin patchy pressure faces; common fine and very fine tubular pores, most with root remnants; occasional fine black nodules; common fine and very fine dead root remnants and occasional fine living roots; clear wavy boundary. Sample 72-137; thin sections 72058 (28-43 cm), 72059 (43-58 cm), 72064 and 72065 (small, about 36 cm) and 72066 (small, about 43 cm depth).
- 56-86 cm Light brownish grey (2.5Y 6/2) moist sandy clay with common medium distinct
Bg2 yellowish brown mottles; weak very coarse prismatic and coarse and medium angular blocky; firm in place, moist friable, wet plastic, slightly sticky; thin continuous pressure faces on peds (sand grains on ped faces not covered); few fine and very fine tubular pores mostly with root remnants; common fine and very fine, occasional medium (woody) root remnants; gradual wavy boundary. Sample 72-138; thin sections 72059 (43-58 cm), 72060 (64-79 cm), 72067 (small, about 60 cm) and 72068 (small, about 80 cm depth).
- 86-132 cm Greyish brown (2.5Y 6/2) moist sandy clay with few medium distinct yellowish
Bg3 brown mottles; weak coarse and medium angular blocky; moist firm, wet plastic, slightly sticky; thin continuous or broken pressure faces on peds (occasional sand grains on ped faces not covered) and locally patches of oblique, shiny,

ridged faces (slickensides); very few very fine and rare fine tubular pores, most with root remnants; rare patches (infillings?) of loamy sand or sandy loam, greyish brown (lighter colour than Eg); locally few dark brown fibrous remnants of fine roots and light grey remnants of very fine dead roots. Sample 72-139; thin sections 72061 (86-101 cm), 72062 (115-130 cm) and 72069 (small, about 108 cm depth).

Interpreted characteristics

The soil is highly susceptible to slaking and sheet erosion where not covered by vegetation. The slow drainage limits the periods available for cultivation. No sources of irrigation water are apparent, and irrigation would increase the hazard of severe waterlogging for extended periods.

The slow permeability, low estimated water holding capacity and apparently unfavourable aeration in wet periods make the soil poorly suited or unsuitable for vines, common dry-land field crops and common tree crops, and moderately or poorly suited for improved grassland.

If irrigation water would be available, with adequate balanced fertilizer applications the soil would be at least moderately suited for one rice crop per year. With high expenditure for major soil improvement the soil could be made moderately suited for common dry-land field crops, but the improvement may last only a few years and is probably uneconomic in present conditions.

Much of this land is being taken for housing and small industry. It is suitable for these uses if a drainage and sewage system is installed. Septic tanks and on-site infiltration pits would probably not be satisfactory.

Micromorphology

Description

Skeleton grains throughout the profile comprise mainly quartz, some feldspars, chalcidony and heavy minerals. They are not corroded and mainly occur in a random distribution pattern.

The plasma in the Eg horizons consists of clay minerals with organic matter and locally iron oxides. In lower horizons, organic matter is virtually absent. The plasma is locally skelsepic (this and other terms according to Brewer, 1964) in the Eg horizons; skelsepic, masepic, omnisepic in the Bg horizons and, at about 1.2 m depth, planar vosepic along skew planes. The plasma is irregularly distributed and fragments up to a few mm in size from lower horizons occur in the surface horizon. The lowest horizon contains clusters of papules, 50-400 μ m, with continuous orientation. The proportion of plasma increases with depth.

Voids in the moderately porous Eg horizons comprise channels, vughs, interconnected vughs and craze planes. The very compact Bg horizons additionally contain skew planes but have few interconnected vughs.

There are very few channel ferriargillans, 50-100 μm thick, and few papules, 20-100 μm , in the Bg1 and Bg2 horizons, generally totalling less than 1% but in one sample (43-58 cm) estimated more than 1%, and occasional large papules in the Bg3 horizon. The clay illuviation features generally have continuous orientation, locally in the grey areas they are grainy, mainly in the Bg2 horizon. Few matriferrargillans, 20-50 μm thick, occur around channels in the Eg horizons.

Few channel neoferrans, about 50 μm thick, are found in the Eg horizons. Ferric nodules with abrupt boundaries, a few mm in size, occur throughout the profile. They contain cutans consisting of goethite, and of isotropic ferric oxides, as well as ferriargillans covered by ferric oxides. Mainly compound ferric nodules with diffuse to abrupt boundaries, up to a few cm, occur throughout, but most are found in a mainly grey matrix in the Bg1 and Bg2 horizons. They generally contain fine (50-200 μm) roundish nodules with abrupt boundaries.

Plant remains, a few mm in size, part carbonized, some containing Ca oxalate, and organic and welded matric fecal pellets (about 50 μm diameter) are present in the Eg horizons; few are found in lower horizons.

Interpretation

Alternate swelling and shrinking has caused the sepic plasmic fabric and the compact nature of the lower horizons. Biotic activity is evident from the prevalence of channels, interconnected vughs and fecal pellets in the Eg horizons, to a depth of about 0.4 m. Clay translocation has been very minor: the large papules in the lowest horizon, and part of the papules in the Bg1 and Bg2 horizons, may have been formed by weathering.

Periodic reduction is indicated by the mainly compound ferric nodules throughout the soil profile and the neoferrans in the Eg horizons. The fine ferric nodules with abrupt boundaries are probably pedorelics. There are indications of clay decomposition in the form of grainy clay illuviation features, and sporadically plasma, in the grey areas mainly in the Bg2 horizon.

Human activity has caused the presence in the Eg horizon of pieces of subsoil material (from ditches) and of matriferrargillans (by winter rains after ploughing).

Grain-size distribution and general chemical data

The sediment in which this profile is developed is quite uniform. A log (grain size)-normal (cumulative percentage) diagram (Fig. 2) indicates that the sediment is bimodal, probably tidal, comprising a uniform, well sorted sand fraction (150-300 μm) and an appreciable proportion of clay (15-40%). The grain-size distribution recalculated to sand + silt total 100 per cent (Fig. 3) indicates very minor variations among the coarser fractions, but a strong trend of clay percentage with depth.

The standard deviation of the sand and silt fractions after recalculation to constant total is about 0.8 per cent, somewhat lower than expected from minor variations in sedimentation conditions plus analytical errors. These data would point to considerable clay translocation or destruction and removal; appreciable synthesis of clay from sand- and

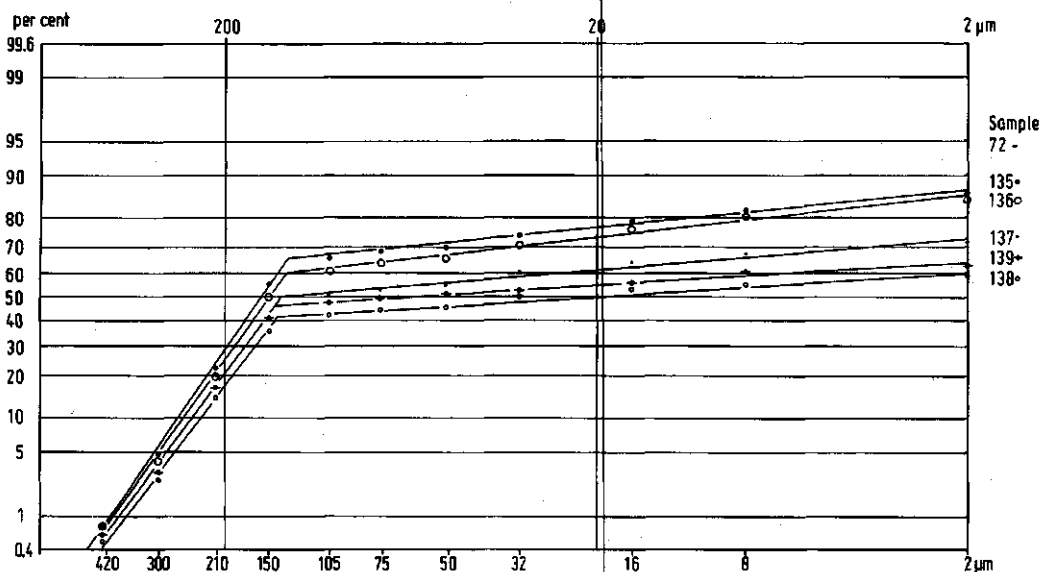


Fig. 2. Grain-size distribution of the Latina profile, recalculated to (sand + silt) fractions total 100 per cent.

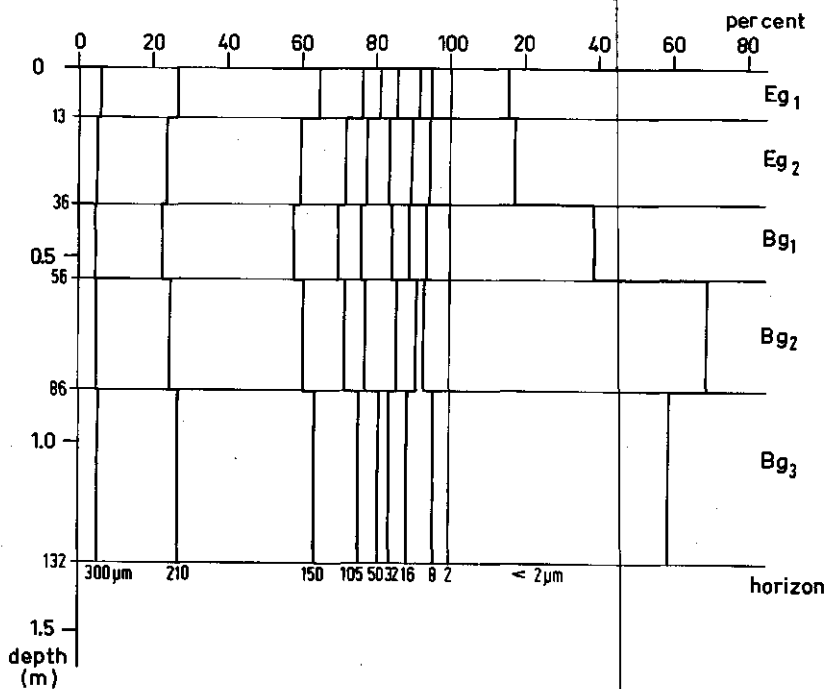


Fig. 3. Cumulative grain-size distribution of the Latina profile. Abscissa: log (grain size), ordinate: transformed to represent a normal (Gauss) distribution as a straight line.

silt-size minerals appears unlikely. The Bg2 horizon may have gained up to about 4 per cent illuviated clay, compared with the Bg3 horizon; however, if bulk densities throughout the profile are assumed constant, the clay loss from the upper horizon is eight times as large as this gain. For this reason, the marginally sufficient (>1%) amount of clay illuviation in one thin section has not been used in isolation to recognize an argillic horizon, in accordance with a statement in USDA, 1975 (p. 20): '... the (argillic) horizon is a mark of the dominance of translocation of silicate clay over processes that destroy clay or remove it ...'.

Rommelzwaal (1978) described two profiles near Latina (Y25 and Y75) that are similar to the Latina profile described here except for their higher subsoil pH and somewhat greater amounts of oriented clay observed in thin sections, mainly between 1.5 and 2 or 3 m depth. C horizons are reported to start at about 3 m or greater depth. He considers that churning in soil materials with more than about 40% clay destroys most of the illuviation features that may have existed at depths less than 1.5 m. On the basis of the high pH (no data on exchangeable cations listed) and the indications for clay translocation, Rommelzwaal classified the two profiles as Natrixeralfic Albaqualf or Albic Natraqualf and Glossaqualfic Natrixeralf, respectively (USDA, 1975). Under the same assumption with respect to clay translocation, the present Latina profile would be an Aeric Albaqualf.

Organic matter contents (Table 1) are low, 0.8-0.2% C, free iron oxides are very low (0-1%), with a slight maximum (0.2%) in the Bg1 horizon. pH (water) is below 5 and pH (CaCl₂) below 4 in the Bg horizons, and 6 and above 5, respectively, in the Eg horizons. This trend, the anomalously high exchangeable Ca content in the Eg and the upper Bg horizons, as well as the presence of water-soluble carbonates in the upper horizons suggest that the soil has been limed. The slightly higher exchangeable K contents in the Eg than in deeper horizons may be due to nutrient cycling or fertilizing.

Total chemical composition and norm mineral calculations

The total chemical composition of total soil (= fine earth) and clay fractions of the Latina profile is listed in Tables 2 and 3. Because the variation in composition of the total soil appears to be correlated with the clay percentage, the chemical composition of the (sand + silt) fraction was calculated by difference (Table 4). Although some of the results are somewhat erratic due to unfavourable error propagation, it is

Table 3. Total chemical composition (%) of clay fractions of the Latina profile.

Sample no. 72-	SiO ₂	Al ₂ O ₃	Fe ₂ O ₃	FeO	MgO	CaO	Na ₂ O	K ₂ O	TiO ₂	Ignition loss	TiO ₂ ¹
135	50.7	24.7	8.3	0.18	0.3	0.11	0.3	1.62	1.31	11.2	0.21
136	50.8	25.0	8.4	0.18	0.3	0.06	0.3	1.58	1.26	10.6	0.21
137	47.0	25.6	10.2	0.13	0.3	0.03	0.2	1.52	1.11	11.2	0.43
138	48.0	26.2	9.0	0.15	0.3	0.03	0.2	1.47	1.07	11.3	0.74
139	50.0	26.7	8.8	0.38	0.3	0.03	0.2	1.46	1.05	11.2	0.62

1. TiO₂ content of the clay fraction recalculated to (sand + silt) total 100%.

Table 4. Total chemical composition (%) of (sand + silt) fractions¹ of the Latina profile.

Sample no. 72-	SiO ₂	Al ₂ O ₃	Fe ₂ O ₃ ²	MgO	CaO	Na ₂ O	K ₂ O	TiO ₂	Ignition loss
135	91.7	4.4	0.4	0.0	0.2	1.0	2.10	0.27	0.0
136	91.8	4.4	0.4	0.0	0.1	1.0	2.03	0.28	0.2
137	93.2	3.9	0.1	0.0	0.1	1.1	2.02	0.29	1.0
138	91.3	4.8	0.4	0.2	0.1	1.2	1.99	0.27	0.9
139	91.5	3.6	-0.4 ³	0.2	0.2	1.5	2.34	0.26	0.3

1. Calculated from composition of fine earth and clay fractions.

2. Total iron as Fe₂O₃.

3. Probably analytical error in Fe₂O₃ (soil).

clear that the (sand + silt) fraction is essentially constant and mainly consists of SiO₂. The calculated epinorm mineral composition comprises 78% quartz, 12% orthoclase, 8% albite, 1% muscovite and 0.27% rutile (titania).

Differences in the clay fractions are minor, but the clay fractions of the Eg horizons tend to contain slightly more SiO₂, TiO₂, FeO, CaO, Na₂O and K₂O, and slightly less Al₂O₃ and Fe₂O₃ than the lower horizons.

Calculation of a goethite norm mineral composition (Table 5) from these data results in slight decreases of norm kaolinite and goethite, and increases of the other norm minerals toward the surface. After recalculation to a constant norm rutile (titania) content in the clay fractions (Table 6), a simpler picture emerges: norm kaolinite and goethite are lost from the Eg horizons, and all other norm minerals remain substantially constant with depth. Probably, this latter table underestimates the total losses from the profile, because titania in the clay fraction appears to be somewhat mobile in seasonally wet, acid conditions (Brinkman, 1977a), and the titania content of the clay fractions, recalculated to a constant (sand + silt) total 100, sharply decreases toward the surface (Table 3).

Not all of this loss need be ascribed to clay decomposition. Part may possibly be due to removal in suspension toward the drainageways during occasional flooding by winter rains.

Table 5. Goethite norm mineral composition (%) of the clay fractions of the Latina profile.

Sample no. 72-	Ru	Go	Ab	I	S	K	Q	W
135	1.31	9.1	2.7	14	8	44	17	3
136	1.26	9.2	2.4	13	7	45	17	2
137	1.11	11.2	1.7	13	6	48	14	2
138	1.07	9.9	1.9	12	6	50	14	2
139	1.05	9.7	1.9	12	9	50	14	2

Abbreviations of norm minerals in this and following tables.

Ab: albite, Ant: antigorite, Go: goethite, Hm: hematite, I: illite (muscovite), K: kaolinite, Ms: muscovite, Or: orthoclase, Q: quartz, Ru: rutile (Ti oxides), S: smectite (Mg- and ferrous iron-substituted montmorillonite), Trem: tremolite, W: excess structural water.

Table 6. Goethite norm mineral composition (%) of the clay fractions of the Latina profile, recalculated on the basis of constant norm rutile.

Sample no. 72-	Go	Ab	I	S	K	Q	W
135	7.3	2.2	11	6	35	14	2
136	7.7	2.0	11	6	38	14	2
137	10.6	1.6	12	6	46	13	2
138	9.7	1.9	12	6	49	13	2
139	9.7	1.9	12	9	50	14	2

Mineralogy

In the heavy fraction of the sand (0.4-0.5%), opaque minerals amount to 21-35% of the transparent grains. The latter comprise 20% garnet, 14% zircon, 12% rutile, 10% epidote, 9% staurolite, 7% picotite, 6% spinel, 6% augite + pyroxenes, 5% tourmaline and minor proportions of several others. Although the proportions of garnet, picotite, zircon, rutile and augite + pyroxenes vary significantly between samples (100-120 transparent grains counted per sample), consistent trends with depth were not observed.

The clay fractions were studied by X-ray diffractometry after Mg-saturation without and with glycerol solvation, and after K-saturation and heating to 100, 200, 300, 400 and 600°C. On the basis of peak heights, kaolinite appears to occur in major proportion, somewhat variable but without a clear trend with depth; quartz increases from traces at depth to clearly evident, but minor proportions, in the upper horizons. Goethite reflections (0.418 nm) are small and decrease to virtually absent in the surface horizon. There are moderate and roughly constant amounts of illite, poorly crystalline or of small crystallite size (broad 001 and 002 reflections). The lowest two horizons contain major amounts of smectite, which may be randomly interstratified with some aluminium-interlayered material, in view of the very wide range of spacings after glycerol solvation. The Bg1 horizon is transitional and the Eg horizons contain much strongly aluminium-interlayered material, presumably derived from the smectite. Most of this has a 1.4 nm spacing after K-saturation which is stable to a temperature between 200 and 300°C; part collapses to a 1.0 nm spacing or a range between 1.0 and 1.4 nm between 100 and 200°C.

These estimates do not coincide with the results of the norm mineral calculation in two respects, probably for the following reasons. The standard goethite norm calculation only considers smectites with octahedral substitution (of magnesium and ferrous iron), whereas the smectite in this profile may have tetrahedral (aluminium) substitution as well. This would entail higher smectite and lower kaolinite contents, depending on the extent of tetrahedral substitution. The substantial amount of aluminium interlayering in the upper horizons, which cannot be considered in norm mineral calculation either, also lowers the kaolinite content, and raises the quartz content compared with the values of the norm calculation.

Recalculation of the cation exchange capacity of the soil per kg clay and graphic

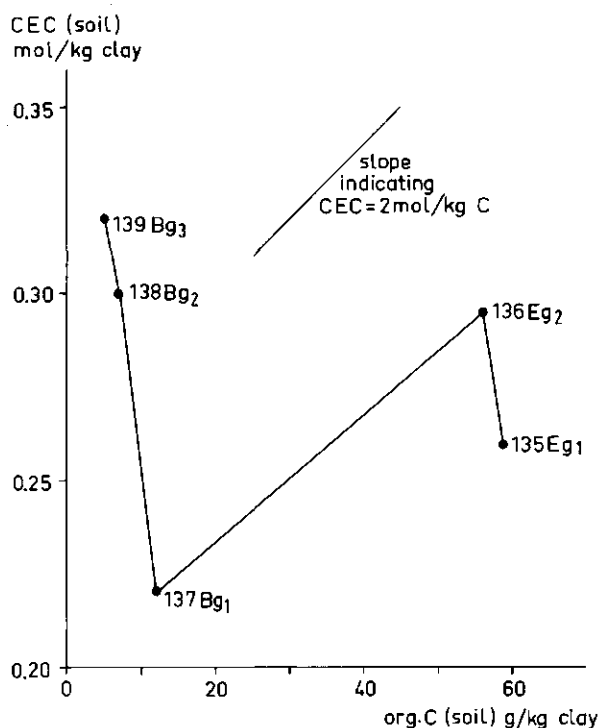


Fig. 4. CEC plot of the Latina profile. Abscissa: organic C in soil, recalculated per kg clay. Ordinate: CEC of soil, recalculated per kg clay.

correction for organic matter (Fig. 4) leads to CEC estimates for the clay fractions in the lower horizons of about 0.3 mol/kg^4 , and in the upper horizons of about 0.2 mol/kg or less, in agreement with the indications for stronger aluminium interlayering in the upper horizons. The trend in CEC of clay fractions determined directly (Table 7) is less clear: a slight decrease toward the surface, but an anomalously low figure for the lowest horizon (possibly an analytical error). All samples show a clear increase in CEC after citrate extraction, so even the lowest horizon appears to contain aluminium interlayers. There is a decrease in FeO content after citrate extraction in the clay fractions of the upper two horizons (Table 7). Ferrollysis presumably has taken place only in the Eg horizons, to a depth of about 0.4 m. The high FeO content in the lowest horizon is not lowered by citrate extraction. This probably represents octahedral ferrous iron within the smectite structure. The reason for the difference with the rest of the profile is not clear.

4. 0.3 mol/kg is 30 meq/100 g in traditional units (Appendix: choice of units and entities).

Table 7. Cation exchange capacities and ferrous iron contents of clay fractions of the Latina profile without and with preliminary citrate extraction.

Sample no. 72-	CEC (mol/kg)		FeO (%)	
	without citrate extraction	with citrate extraction	without citrate extraction	with citrate extraction
135	0.28	0.36	0.18	0.13
136	0.26	0.39	0.18	0.12
137	0.27	0.36	0.13	0.15
138	0.31	0.37	0.15	0.15
139	0.26	0.45	0.38	0.41

HARDTHÄUSER WALD

FAO-Unesco Soil Units (FAO, 1974): Gleyic Podzoluvisol (observation, Fig. 5);

Gleyic Acrisol (according to description⁵)

USDA Soil Taxonomy (Soil Survey Staff, 1975): Fraglössudalf (observation, Fig. 5);

Aquic Fragiudalf (according to description⁵)

Classification by authors of description⁵: Pseudogley - Fahlerde.

The site

Location Site A4⁶, Hardthäuser Wald, Part III, 1 km W. of Neuzweiflingen, South-west Germany. About 49°18' N, 9°16' E. Elevation about 300 m above mean sea level.

Landform and slope: nearly level (1°, about 2% to NW) mid-slope of interfluvium between two small valley heads, each about 100 m from the site.

Vegetation: mature beech-oak forest.

Climate: Humid temperate (Köppen Cfb). Mean annual temperature 8.5°C. Precipitation 750-800 mm/year.

General information on the soil

Parent material deeply decalcified reworked loess, 1.5 m over reworked Keuper clay.

Drainage imperfect. Internal drainage slow because of very slowly permeable lower horizons; external drainage slow owing to nearly level slope. Intermittent, very slow lateral water movement in upper metre.

5. in Blume et al., 1971. Description does not mention clear tonguing (Fig. 5).

6. Excursion site, Conference Pseudogley and Gley, Comm. V and VI, I.S.S.S., Stuttgart, 1971.

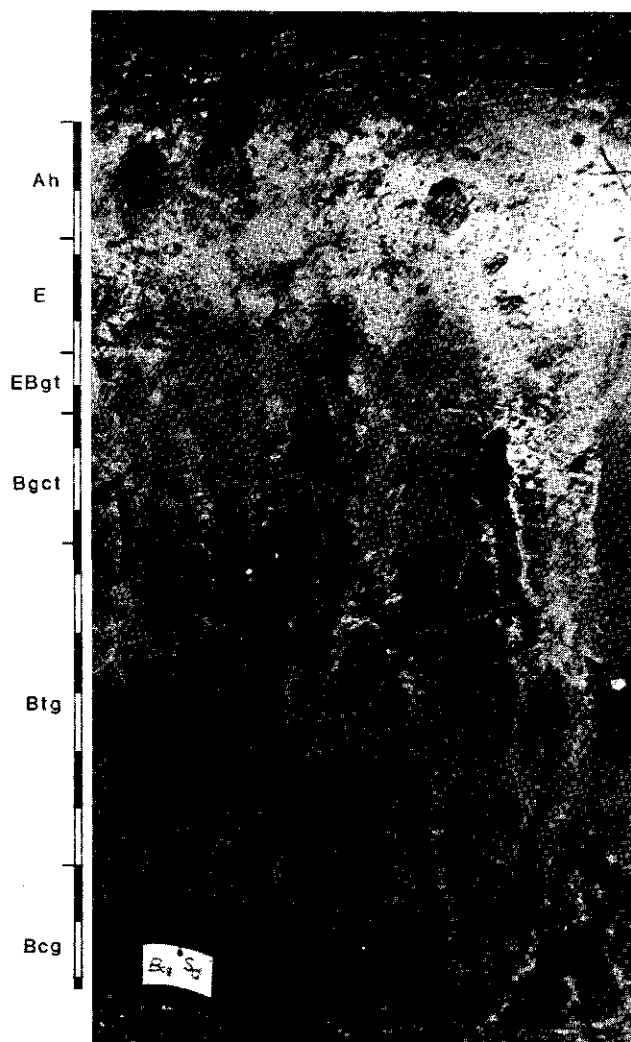


Fig. 5. Soil profile, Hardthäuser Wald. Scale divisions 0.1 m. Ah, E, etc.: soil horizons.

Brief description of the profile

Deep, imperfectly drained, slowly permeable silt loam over silty clay loam. The profile (Fig. 5) consists of a thin, very dark brown A horizon grading into a brownish yellow E over a mottled brown, reddish yellow and white Btg horizon with very dark brown (manganiferous) concretions. This horizon contains a fragipan between 0.65 and 1.2 m depth. Narrow, pale coloured tongues extend deep into the B horizon. Roots are common in the A and E, few in the upper Btg and virtually absent in and below the fragipan.

Descriptions of individual horizons and some physical and chemical data are given in Blume et al. (1971).

Description

Skeleton grains, mainly quartz with some micas and heavy minerals, have a mean size of 20-50 μm ; there are sporadic grains up to 400 μm . The distribution pattern is mainly random, but locally clustered at about 0.4 m depth.

The plasma in the A and E horizons consists of clay minerals with organic matter; in the B horizons of clay minerals with and without ferric oxides in the brown and grey parts, respectively. The proportion of plasma is considerably higher in the B than in the upper horizons, and locally lower in the grey parts than in the brown parts of the B horizon. In grey locations in and below the fragipan the plasma appears to contain secondary silica.

The upper horizons contain mainly biogenic voids but the upper dm has few pores and is dense. The B horizons contain biogenic voids and skew and craze planes. The amounts of the latter two are maximal in the upper B and the fragipan.

Few papules and very few grainy argillans occur in the A and E horizons. The B horizons contain ferriargillans and argillans with continuous and discontinuous orientation in brown and grey areas, respectively, along walls of voids. There are many papules as well, decreasing in amount with depth. Counting data are given in Table 8.

Neoferrans and many neomangans cover ferriargillans in the lowest horizon, 1.2-1.5 m, in which there is also a concentration of iron-manganese nodules (Fig. 5). Throughout the B horizons there are ferric nodules with diffuse to sharp boundaries, part of which cover ferriargillans. Some of the nodules are manganiferous.

Pedotubules occur throughout the profile but are most clearly visible in the EB and upper B horizons. The large pedotubules in the AE and E horizons are aggotubules.

Table 8. Clay illuviation features in the Hardthäuser Wald profile.

Sample no. 710-	Depth (cm)	Horizon	Continuous		Discontinuous		Total (% v/v) ²	Ratio	
			ferri-argillans (points per 800) ¹	papules ¹	grainy argillans (points per 800) ¹	grainy papules ¹		papules /total	grainy /total
73	10-18	AE	0	1	0	0	0.1		
74	18-35	E	0	9	0	3	1.5	1	0.3
75	35-44	EBgt	16	12	4	9	5.1	0.5	0.3
76	44-65	Bgct	20	25	7	8	7.5	0.5	0.3
77	65-120	Btgx	17	12	6	7	5.3	0.5	0.3
78	120-150	Bgc	24	13	5	3	5.6	0.4	0.2

1. 800 points counted per sample, voids not counted.

2. All clay illuviation features, % v/v of total solids.

Interpretation

Part of the ferric nodules (with sharp boundaries) may have been transported. Part of the nodules as well as the neoferrans and neomangans covering ferriargillans must have been formed by periodic reduction and oxidation after clay illuviation. Clay decomposition is indicated by the presence of secondary silica in grey parts of the profile. The occurrence of grainy argillans with discontinuous orientation suggests that clay decomposition has occurred after clay illuviation.

Physical data

The grain-size distribution, recalculated on a clay-free basis (Fig. 6), suggests that the sediment is relatively uniform. The standard deviation of sand and silt fractions on a clay-free basis is about 2.2%, or about 1.7% of contents as determined. The variability between horizons is probably comparable with the errors in determination of grain-size distribution (of the order of 1%).

Clay contents in the upper horizons and the pale-coloured tongues are much lower than in the B horizons. Much of this difference may be ascribed to clay translocation (Fig. 6). A clay balance calculated with the Bgc horizon (1.2-1.5 m) as a standard comes

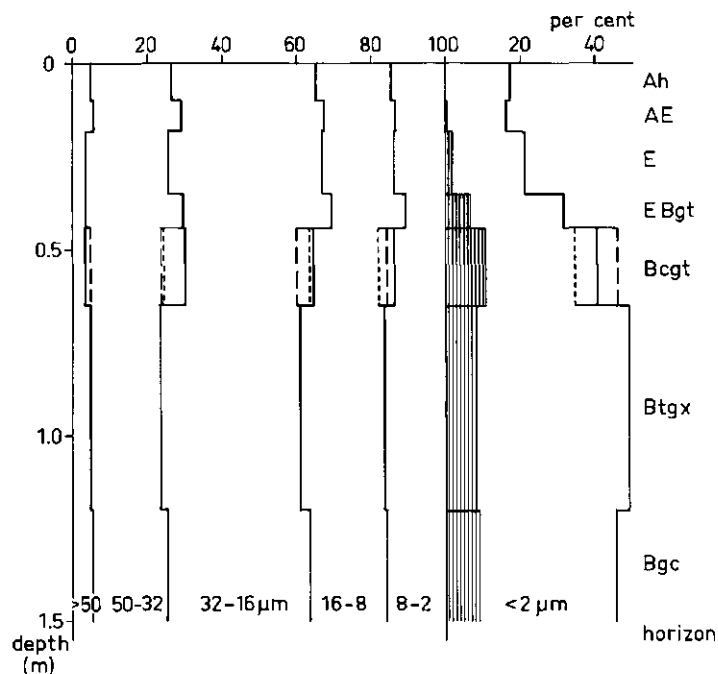


Fig. 6. Grain-size distribution of the Hardthäuser Wald profile, recalculated to (sand + silt) fractions total 100 per cent. Vertical hatching: clay illuviation features in thin sections, volume per cent, similarly recalculated. Dotted lines: pale tongues, dashed lines: ped interiors without tongues.

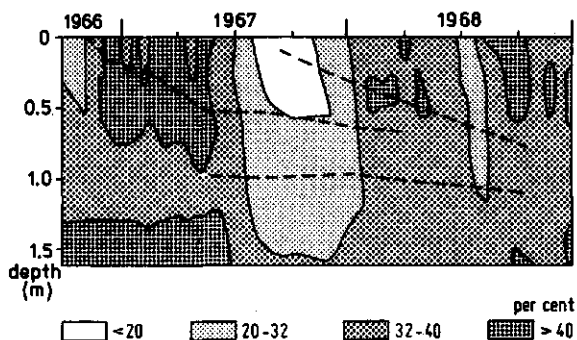


Fig. 7. Moisture contents (volume per cent) and vertical water movements in a Hardthäuser Wald profile under broadleaf forest. Simplified from Blume et al. (1969), p. 108, site 6L. Dashed lines: vertical movements of soil water (positions of HTO tracer maxima as a function of time). Wilting point is at moisture contents of about 20%, water-saturation at about 40%.

out negative by about 40 kg/m^2 . The actual net loss, if any, is probably less, because that horizon still contains illuviated clay. A better standard is not available because a different material (reworked Keuper clay) occurs below 1.5 m depth.

Moisture contents and vertical water movements in the neighbourhood of the profile are illustrated in Fig. 7, simplified from Blume, Münich and Zimmermann (1969). The surface horizons are water-saturated for several weeks in at least the wetter winters; the upper 0.5-1.5 m dries out to about wilting point in most but not all summers (the years illustrated were wetter than normal). Blume et al. (1969) also measured the movement of tritium-labeled water. They report lateral water movements, only during periods when the soil was essentially water-saturated, totalling roughly 0.1 m/year. Vertical water movement in the upper metre was downward (Fig. 7, dashed lines), resulting from precipitation on the surface and extraction by roots throughout that depth. Very little vertical movement occurred below 1 m. Net leaching losses were small, of the order of 40 mm/year, under mature beech-oak forest. Under pine forest and under grass with 8-year-old pines, net leaching losses were greater: roughly 70 and more than 80 mm, respectively. This limited water movement is in agreement with the presumed slow permeability of the dense subsoil and substratum. Bulk densities range from 1 to $1.24 \times 10^3 \text{ kg/m}^3$ in the A and E horizons and are 1.5 and $1.6 \times 10^3 \text{ kg/m}^3$ in the upper B horizon and the fragipan, respectively (Blume et al., 1971, p. 35).

General chemical data

Organic carbon contents are moderate in the upper dm and low throughout the rest of the profile (Table 9); contents of free iron oxides are about 1.5% in the upper horizons and 3.5% in the B horizons. pH (water) ranges from 4 to 5 and pH (CaCl_2) from 3.4 to about 4 in most of the profile; the surface horizon has values of 3.7 and 3.3, respectively.

Exchangeable aluminium is dominant in the upper horizons and exchangeable calcium, with some magnesium and aluminium, at depth.

Table 9. General chemical data of the Hardthäuser Wald profile.

Sample no. 72-	Depth (cm)	Horizon ¹	Org. C (%)	Free Fe ₂ O ₃ (%)	pH		Exchangeable equivalents							
					water	CaCl ₂ (0.01 mol/l)	Ca	Mg	Na	K	Al	H	CEC	
96	0-10	Ah	2.6	1.5	3.7	3.3	9	0	0	4	48	9	60	
97	10-18	AE	1.1	1.6	4.0	3.5	5	2	0	3	47	6	54	
98	18-35	E	0.8	2.1	4.0	3.4	6	8	0	8	63	4	64	
99	35-44	EBgt	0.4	2.6	4.4	3.4	14	5	0	2	74	5	92	
100	44-65	Bgct	0.7	3.5	4.7	3.6	36	25	0	1	51	6	124	
101	44-65	Bgct(i)	0.3	3.5	5.1	4.2	56	33	0	1	35	17	151	
102	44-65	Bgct(t)	0.3	2.9	5.0	2	39	22	0	1	30	30	114	
103	65-120	Btgx	0.1	3.6	5.0	3.8	59	34	0	0	37	7	137	
104	120-150	Bcg	0.9	5.9	5.3	4.1	82	34	0	1	12	4	158	

1. i: interior parts of horizon, without grey tongues. t: grey tongues.

2. Dot indicates not determined.

Exchangeable potassium has a clear maximum in the E horizon and is higher in the upper 0.4 m than in lower horizons. The generally low values for magnesium in the upper horizons are interrupted by a secondary maximum in the E horizon. These maxima may be explained in two steps. Probably, nutrient cycling by the forest vegetation has been very effective, giving rise to relatively high contents of exchangeable K and Mg throughout the upper horizons; acid rain, particularly during the last one or two decades, may have removed part of these ions from the upper 0.2 m but not yet from the E horizon.

Total chemical composition

The main trends in the total chemical composition of this profile (Table 10) appear to be correlated with clay content.

The composition of the clay fractions (Table 11) shows minima for Al₂O₃ and Fe₂O₃ and maximal contents of SiO₂, TiO₂ and FeO in the A horizons and an increasing trend in MgO and K₂O contents from 1.5 m depth toward the A horizons. The presumably residual en-

Table 10. Total chemical composition (%) of the Hardthäuser Wald profile.

Sample no. 72-	SiO ₂	Al ₂ O ₃	Fe ₂ O ₃ ¹	MgO	CaO	Na ₂ O	K ₂ O	TiO ₂	Ignition loss	Clay
96	77.3	8.2	2.8	0.1	0.3	1.0	1.52	0.79	5.9	14.6
97	80.2	8.8	3.0	0.2	0.3	1.0	1.51	0.82	4.0	14.0
98	77.3	10.1	3.7	0.3	0.3	1.0	1.71	0.79	3.7	17.4
99	74.5	11.7	4.7	0.5	0.3	0.9	1.81	0.78	3.8	24.1
100	72.0	12.6	5.5	0.5	0.3	0.8	1.75	0.81	4.2	28.7
101	71.0	13.3	5.6	0.5	0.3	0.8	1.72	0.82	4.6	31.6
102	74.1	11.5	4.8	0.4	0.3	0.8	1.67	0.80	5.0	25.6
103	71.0	13.6	5.4	0.5	0.3	0.8	1.70	0.82	4.6	33.0
104	68.8	12.5	7.3	0.4	0.3	0.6	1.53	0.82	5.1	28.7

1. Total iron as Fe₂O₃.

Table 11. Total chemical composition (%) of clay fractions of the Hardthäuser Wald profile.

Sample no. 72-	SiO ₂	Al ₂ O ₃	Fe ₂ O ₃	FeO	MgO	CaO	Na ₂ O	K ₂ O	TiO ₂	Ignition loss
96	51.2	22.5	7.7	0.8	2.0	0.07	0.34	2.73	1.29	10.1
97	49.6	22.8	8.2	0.9	2.0	0.07	0.33	2.86	1.22	10.8
98	49.0	24.0	9.9	0.4	2.0	0.04	0.27	2.78	1.10	9.4
99	46.5	23.9	11.2	0.4	2.1	0.02	0.21	2.84	0.99	9.7
100	47.6	25.1	10.5	0.3	1.8	0.02	0.22	2.50	0.98	9.6
103	48.9	25.4	9.5	0.3	1.6	0.02	0.22	2.38	1.01	9.5
104	49.9	25.0	8.3	0.2	1.4	0.05	0.20	2.30	0.95	10.8

Table 12. Total chemical composition (%) of (sand + silt) fractions¹ of the Hardthäuser Wald profile.

Sample no. 72-	SiO ₂	Al ₂ O ₃	Fe ₂ O ₃ ²	MgO	CaO	Na ₂ O	K ₂ O	TiO ₂	Ignition loss
96	86.0	6.2	2.0	0.0	0.3	1.1	1.38	0.75	0.1
97	87.0	6.6	2.0	0.0	0.3	1.1	1.32	0.77	0.7
98	84.6	7.2	2.4	0.0	0.3	1.2	1.49	0.74	0.9
99	83.5	7.6	2.5	0.0	0.3	1.2	1.48	0.71	1.9
100	83.2	7.7	3.4	0.0	0.2	1.1	1.47	0.76	0.4
103	82.1	7.7	3.3	0.0	0.2	1.0	1.37	0.73	2.2
104	76.6	7.5	6.8	0.0	0.1	0.7	1.22	0.77	2.8

1. Calculated from composition of total soil and clay fractions.

2. Total iron as Fe₂O₃.

richment of silica and titania combined with the loss of Al₂O₃ and Fe₂O₃ from the upper horizons might be ascribed to cheluviation, leaching by strong acids or ferrolysis; the maximal ferrous iron contents in the upper horizons point to ferrolysis. The contents of MgO and K₂O (as well as CaO and P₂O₅) in clay fractions of the eluvial horizons are higher than in the subsoil, probably owing to nutrient cycling.

The composition of the coarser fractions (Table 12), calculated by difference, shows a slight increase in SiO₂ and decreases in Al₂O₃, Fe₂O₃ and K₂O contents in the surface horizons. TiO₂ contents are somewhat variable without a clear trend. Part of the free iron oxides were probably removed during periodic reduction, as indicated by mottles and nodules in deeper horizons and the high ferric iron and manganese contents in the concretional horizon between 1.2 and 1.5 m depth. The other changes may be ascribed to weathering of a small amount of aluminosilicate and relative accumulation of quartz.

The standard epinorm calculation counts the aluminosilicate as kaolinite, decreasing from about 6% of the (sand + silt) fraction in the lowest horizon to nil in the A and E horizons, and does not yield other information on soil formation beyond that derived from the total chemical composition.

X-ray diffractograms were prepared of oriented aggregates of the clay fractions after Mg-saturation and equilibration at 50% relative humidity, without and with glycerol solvation, and after K saturation without and with heating to 130, 270, 400 and 550°C. The diffraction patterns were also observed in photographs by Guinier - de Wolff camera. Results are briefly summarized below.

The clay fractions contain a major proportion of vermiculite and some interstratified vermiculite-illite. The vermiculite is slightly aluminium-interlayered in the B horizons and strongly interlayered in A and E horizons, as indicated by the stability of the 1.4 nm reflection of the K-saturated samples against heating to different temperatures.

Moderate kaolinite and small quartz contents appear to increase somewhat toward the surface - presumably a relative accumulation. Moderate and approximately constant amounts of illite occur throughout. There is a trace of feldspars.

Cation exchange capacities of clay fractions estimated from CEC (soil) and organic C (soil) and clay contents (Fig. 8) decrease from about 0.5-0.4 mol/kg clay in the B horizons to about 0.35-0.25 mol/kg clay in the eluvial upper horizons, even if the correction for the CEC of organic matter is kept very small, 1 mol/kg C. (The decrease is still greater if the organic matter has a higher CEC). These figures are compatible with the estimate that vermiculite contents are considerable and the conception that aluminium interlayering blocks a large proportion of the cation exchange capacity in the upper horizons. The maximal ferrous iron contents in the clay fractions of the A horizons are probably due to trapping of formerly exchangeable ferrous iron during the formation of the interlayers.

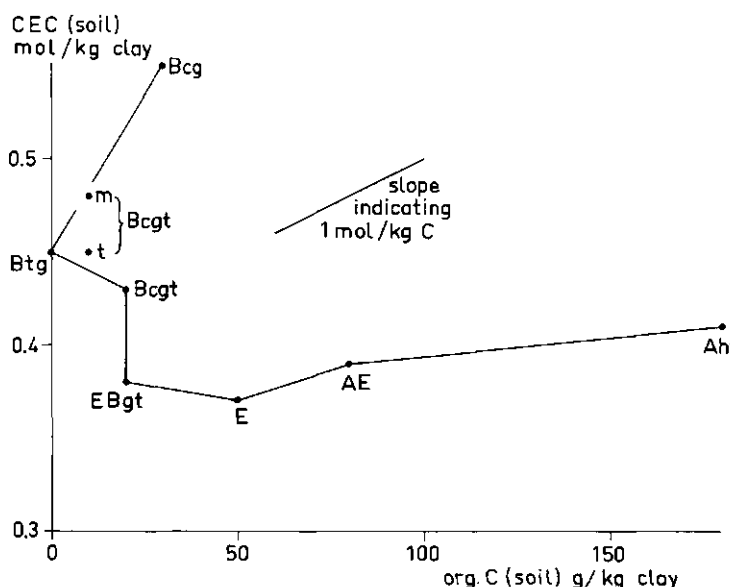


Fig. 8. CEC plot of the Hardthäuser Wald profile. t: pale coloured tongues, m: ped interiors without tongues.

The standard goethite norm calculation does not provide more information on this profile. It ascribes all Mg and Fe (II) to smectite and all K to illite, does not recognize vermiculite except by a variant calculation and cannot deal with variable amounts of aluminium-interlayering, nor with the presence of ferrous iron trapped in these interlayers.

Conventional estimation of vermiculite contents by K fixation according to Alexiades and Jackson (1965) resulted in K fixation figures increasing from 40 through 54 to 80 mmol/kg clay fraction in the E, EBgt and Btg horizons, respectively. This suggests that only a small proportion of the vermiculite is free of aluminium interlayers.

EYNATTEN

FAO/Unesco Soil Units (FAO, 1974): Dystric Planosol

USDA Soil Taxonomy (Soil Survey Staff, 1975): Typic Glossaqualf

Examined 17 Dec. 1972 by R. Brinkman

The site

Location near Eynatten, north-east Belgium. About 3 km ENE of Eynatten village, 8 km SSE of Aachen centre, 500 m SSW of boundary marker 935 Belgium-Germany. $50^{\circ} 42.2'N$, $6^{\circ} 7.2'E$. Elevation about 290 m above mean sea level.

Landform and slope: nearly level part of dissected plateau, general slope about 2 per cent W, local slope 1.7 per cent to SSE, highest part of plateau about 100 m to E.

Vegetation: young beech plantation with many scattered young birches, brambles, locally some grass. Sawn-off stumps of old forest still present. Locally in small slight depressions molinia, ferns. Nearby areas under young fir plantation, old firs, birch seedlings, etc.

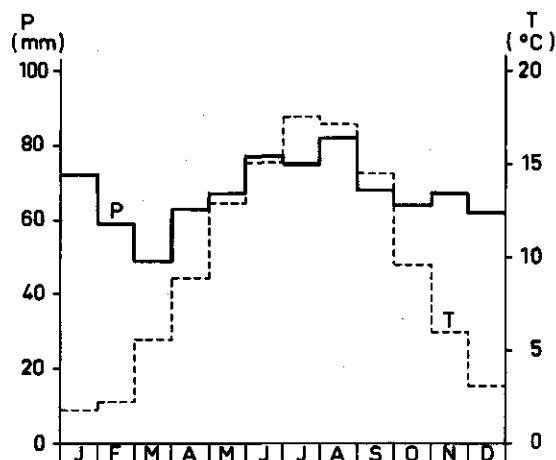


Fig. 9. Temperature and precipitation at Aachen (217 m above mean sea level), about 8 km NNW of the Eynatten profile.

Climate: humid temperate (Köppen Cfb). Data from Aachen: mean annual temperature 9.2°C, coldest month 1.8°C, hottest month 16.6°C. Precipitation 805 mm/year, fairly evenly distributed. Monthly data are given in Fig. 9. The summer rainfall deficit is roughly 180 mm, as estimated from Fig. 9 using the relationships of Fig. 19.

General information on the soil

Parent material reworked loess, silt loam with very few scattered quartzitic sandstone fragments of different sizes up to 1 dm, occurring below about 0.3 m depth. Clayey substratum below 1.6 m is residual material weathered from Carboniferous shales.

Drainage imperfect. Internal drainage slow due to dense deep substratum and low macroporosity in lower B horizon; external drainage slow due to nearly level slope. Moist throughout during description after excavation; ground water observed at 0.75 m depth after 1 day. Intermittently water-saturated up to the mineral surface in rainy periods. No ground water within 1.6 m during dry periods in summer.

No surface stones or rock outcrops, no evidence of erosion, no salinity.

Human influence (logging, planting) has disturbed O, A and E horizons in part of the area.

Brief description of the profile

Deep, imperfectly drained, distinctly mottled silt loam over an impervious silty clay loam deep substratum (Fig. 10). The profile comprises a minipodzol to about 8 cm over a surface-water gley sequum: a pale brown eluvial horizon and a strongly mottled illuvial horizon with deep, narrow tongues of pale material. Roots are concentrated in the O and A horizons; few roots extend into the E and into the tongues of the B horizon.

Description of individual soil horizons

-14 to -10 cm	Litter of leaves and leaf fragments, mainly birch, and twigs; merging,
Ol (litter)	wavy boundary.
-10 to -5 cm	Fine fragments of leaves and twigs with many fine and medium woody roots;
Of (forna)	horizon locally up to 10 cm thick; merging, wavy boundary.
-5 to 0 cm	Black (10YR 1.5/1) moist silty muck; massive breaking into weak fine
Oh (humus)	granular, locally weak coarse platy; friable; common very fine fibrous root remnants, common fine and medium living woody roots; merging, wavy boundary. Sample 73-133; thin section 74068 (-5 to 11 cm).
0-5 cm	Very dark brown (10YR 2/2) moist coarse silt loam; many to common coarse
Ah	faint brown/dark brown areas with indistinct margins; massive, locally very weak platy; friable; very few fine tubes (ex roots); locally fibrous remnants of woody roots, few, locally common, fine and few medium woody roots; very occasional angular quartzite fragments; horizon 3-10 cm thick; clear wavy boundary. Sample 73-134; thin section 74068 (-5 to 11 cm).

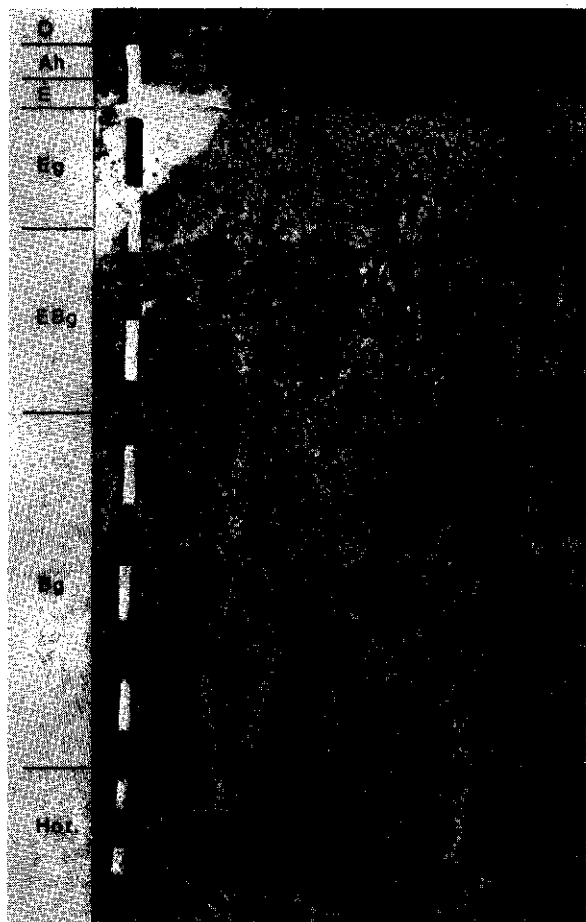


Fig. 10. Soil profile, Eynatten. Scale divisions 0.1 m. O, Ah, etc.: soil horizons (see description). Hor.: horizontal surface at 1.2 m depth, showing polygonal pattern of pale tongues.

5-8 cm	Greyish brown (10YR, locally 2.5Y 5/2) moist silt loam; few medium faint brown and brown/dark brown mottles with indistinct margins, few fine distinct yellowish brown mottles around pores, and few fine black mottles (org. matter, not manganese); massive; friable; few fine and very fine tubular pores; few fine roots and root remnants; horizon discontinuous, 0-7 cm thick; abrupt wavy boundary marked by thin (2 mm) Fe oxide and organic matter accumulation band in places, clear wavy elsewhere. Sample 73-135; thin section 74068 (-5 to 11 cm).
E	
8-27 cm	Pale brown (10YR 6/3) moist silt loam; common fine and medium distinct yellowish brown mottles and few black specks (manganese); weak coarse and medium irregular angular blocky; friable; few fine, common very fine tubular pores; few fine and very fine roots and root remnants, rare medium roots; horizon locally up to 35 cm thick; clear tonguing boundary,
Eg	

	locally broken where remnants of B material occur in this horizon. Sample 73-136; thin section 74069 (11-27 cm).
27-55 cm EBg	Light brownish grey (2.5Y 6/2) silt loam with many coarse distinct light brownish grey, yellowish brown and brown mottles in peds and common fine and medium black (manganese) mottles in peds and on faces; weak medium and coarse angular blocky, with thick to extremely thick light grey, massive silt loam cutans occupying about a quarter of the horizon; friable; few fine random tubular pores; very few medium root remnants, very few fine and medium roots; diffuse boundary. Sample 73-137; thin sections 74070 (27-43 cm), 75 (32-40 cm), 71 (44-60 cm).
55-160 cm Bg	Heavy silt loam coarsely mottled yellowish brown, brown and light brownish grey; moderate coarse prismatic breaking into moderate coarse and weak coarse and medium angular blocky, and weak very coarse prismatic below 90 cm; prism faces have thick to extremely thick, and part of coarse block faces thin, light grey silty cutans; moist friable, firm in place; few fine random tubes, very few medium and coarse open and infilled mainly vertical tubes and locally few cavities, 1-5 cm diameter, coated and largely filled with light grey silty material; very few dead, rotted roots, all in light grey tongues, and no roots below 120 cm; tongues comprise about one seventh of the horizon at 70 and 105 cm, and about one twelfth at 130 cm; abrupt wavy boundary. Samples 73-138 (ped interiors) and 139 (tongues), 55-90 cm; 140 (interiors) and 141 (tongues), 90-120 cm; 142 (total), 143 (interiors) and 144 (tongues), 120-160 cm; thin sections 74072 (60-75 cm), 73 (90-105 cm), 74 (125-140 cm), 76 horizontal (78 cm), 77 vertical (about 160 cm, boundary with 2C horizon).
160-210 cm 2C	Olive brown (2.5Y 4/4) moist silty clay loam; massive, slight indication of platiness in upper few dm; compact, moist firm, very firm in place; very narrow vertical cracks filled with white silty material at about 0.3 m intervals in a polygonal pattern, part of cracks and part of boundary with upper material have many fine and medium distinct black (manganese) mottles, very locally cracks lined by a hard plate of accumulated ferric oxide, several mm thick; scattered stones of hard quartzite; auger observation below 175 cm. Samples 73-145, 160-180 cm; 146, 180-210 cm; thin sections 74078 vertical, 79 horizontal (about 170 cm).

Micromorphology

Description

Skeleton grains throughout the profile are mainly silt-size quartz. There are occasional larger grains, up to 1 mm, some of which are corroded. Mica grains in all stages of weathering increase with depth. Sporadic feldspars and heavy minerals were observed. In the EBg and Btg horizons there are occasional weathered and unweathered glauconite grains as well as angular and rounded lithorelics, mainly bits of heavy clay similar to

the Carboniferous clay occurring below 1.6 m depth. The distribution pattern of the skeleton grains is mainly random. Throughout the profile there are pedotubules and margins of channels and planar voids with mainly skeleton grains and less plasma than the surroundings.

The plasma in the Oh horizon consists of organic matter, dark brown to black welded fecal pellets in a matrix of plant remains at different stages of decomposition. In the Ah horizon, the plasma comprises clay and organic matter, and in the E and Eg horizons mainly clay. A band about 1-2 mm thick between the E and Eg horizons contains amorphous, illuviated organic matter. In the EBg and Btg horizons, the plasma comprises (brown) clay and iron oxides, and mainly clay in grey parts. The grey areas tend to contain less plasma and high proportions of skeleton grains. The plasma in the upper horizons and the grey parts of lower horizons is generally grainy.

Voids throughout the profile mainly comprise channels and vughs, 0.05 to 10 mm in diameter, and occasional craze planes, generally 0.02 to 0.3 mm.

Ferriargillans around channels and vughs, about 0.02 to 0.2 mm thick, and papules with generally continuous orientation occur in the brown parts of the EBg and Btg horizons, and rarely in the grey parts. They are locally covered by ferric nodules and neoferrans. Argillans and papules with discontinuous and continuous orientation occur mainly in the grey parts throughout the lower horizons and occasionally in the Eg horizon. Most are strongly grainy, the continuous ones slightly or not grainy.

The ratio of papules to total clay illuviation features decreases from two thirds in the EBg and upper Btg to about two fifths in the lower Btg horizon. The ratio of grainy to total clay illuviation features gradually decreases from three fifths in the EBg to two fifths in the lower Btg horizon. The two ratios are very strongly correlated (most papules are grainy; most (ferri)argillans have continuous orientation), but this is probably not a causal relationship. Counting data for different clay illuviation features are listed in Table 13.

Neoferrans, about 0.02 to 0.2 mm thick, and some neomangans occur along channels

Table 13. Clay illuviation features in the Eynatten profile.

Sample no. 740-	Depth (cm)	Horizon	Continuous				Discontinuous, grainy, grey		Total (% v/v) ²
			ferri-argillans (points per 800) ¹	brown papules	grey argillans	grey papules	argillans	papules	
69	11- 27	Eg	0	0	0	0	0	0	0.0
70	27- 43	EBg	3	1	0	1	2	8	1.9
75	32- 40	EBg	3	3	0	0	4	3	1.6
71	44- 60	EBg,Btgl	6	3	0	1	1	10	2.6
72	60- 75	Btgl	3	8	4	3	7	17	5.2
76	78 ³	Btgl	12	2	5	0	8	9	4.5
73	90-105	Btg2	9	10	4	1	8	12	5.5
74	125-140	Btg3	8	3	5	1	4	7	3.5

1. 800 points counted per sample, voids not counted.

2. All clay illuviation features, % v/v of total solids.

3. Horizontal thin section; all others vertical.

and vughs in the whole profile except the Ah and E horizons; occasional thin ferrans (0.02 mm) occur in the EBg and the upper part of the Btg horizon. Irregularly shaped ferric nodules with diffuse to abrupt boundaries, 0.05 mm to several cm in size, constitute the brown parts of the EBg and Btg horizons. The proportion of iron oxides within these brown parts is variable. Rounded to irregular fine ferric nodules with abrupt boundaries, 0.05 to a few mm in size, part containing some manganese oxide, are scattered in the Eg and EBg horizons. Some enclose concentrations of amorphous and crystalline iron oxides without other admixtures, some contain vegetative material encrusted with iron oxide.

There are many fungal hyphae in the O and Ah horizons. Aggro- and isotubules, about 0.5 to 1 mm in diameter, occur in low but varying amounts in the upper horizons and in the Eg.

Interpretation

Biotic activity, indicated by channels throughout the profile, papules, pedotubules, and ferric nodules with abrupt boundaries, must have started at an early stage in soil formation because many channels contain (ferri)argillans; it has continued concurrent with and perhaps after clay illuviation because papules exceed (ferri)argillans in the EBg and upper Btg horizon. The few pedotubules indicate a low activity of earthworms. Decomposition of organic matter is slow, as shown by the presence of the O horizons and the many fungal hyphae.

The clay illuviation features observed in the EBg and lower horizons, a few even extending into the underlying Carboniferous clay, are largely deferrated or covered by iron oxides and grainy, particularly in the EBg and upper Btg. This suggests periodic reduction and clay decomposition subsequent to, and possibly concurrent with, clay translocation.

Periodic reduction with translocation of iron is indicated by ferric and ferric-manganese nodules, neoferrans and neomangans, channel ferrans and grey (deferrated) mottles and tongues.

Clay decomposition, particularly in the Eg, EBg and upper Btg horizons and gradually decreasing with depth, is indicated by the graininess of papules and argillans and of the plasma, particularly the deferrated parts.

Physical data

Bulk density

The bulk density of the Eynatten profile is quite uniform: $1.2 \times 10^3 \text{ kg/m}^3$, equivalent to about 45 volume per cent solids, throughout the mineral soil except for some parts of the EBg horizon, about 40 cm depth, with about $1.5 \times 10^3 \text{ kg/m}^3$. The organic horizons range about $0.5 \times 10^3 \text{ kg/m}^3$.

Moisture contents at a matric suction of 0.01 MPa⁷ range about 35 volume per cent in the Bg and Eg horizons (also in the samples with high bulk density), 40 per cent in

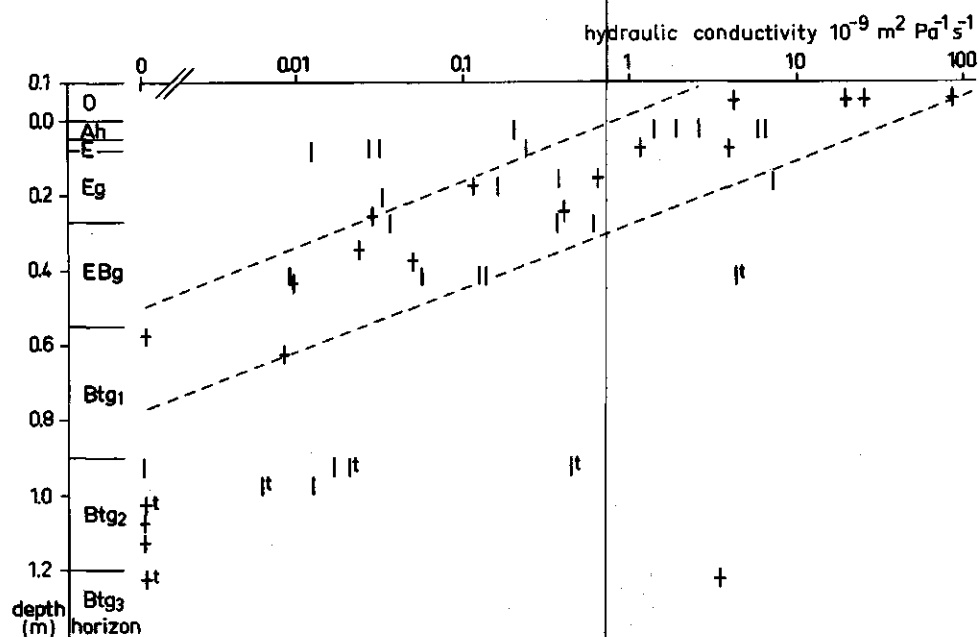


Fig. 11. Hydraulic conductivity of the Eynatten profile. | : vertical. + : horizontal. superscript t: in tongues. Dashed lines indicate range of horizontal hydraulic conductivities.

the E, 40-50 per cent in the A and 60 per cent in the organic horizons. Figures for 0.1 MPa are about 10-12 per cent below those for 0.01 MPa. Moisture contents at 1.5 MPa range about 16 per cent in the mass of the Btg horizons and about 10-13 per cent in the tongues and the Eg and E horizons.

These figures indicate that most of the profile would contain about 20 volume per cent air at 0.01 MPa, so that porosity by itself does not explain its periodic water-saturation. Reasons for this are found in the hydraulic conductivity and the nearly level slope (1.7 to 2 per cent).

Hydraulic conductivity

Vertical hydraulic conductivities⁸ decrease from $1-5 \times 10^{-9} \text{ m}^2 \cdot \text{Pa}^{-1} \cdot \text{s}^{-1}$ in the Ah horizon through $2-50 \times 10^{-11} \text{ m}^2 \cdot \text{Pa}^{-1} \cdot \text{s}^{-1}$ in the E, Eg and EBg horizons to about $10^{-11} \text{ m}^2 \cdot \text{Pa}^{-1} \cdot \text{s}^{-1}$ in the lower Btg. The underlying Carboniferous clay, from about 1.6 m depth, is expected to be impervious. Horizontal conductivities decrease from about $10^{-8} \text{ m}^2 \cdot \text{Pa}^{-1} \cdot \text{s}^{-1}$ in the organic horizons through 10^{-9} in the E and 10^{-10} in the Eg horizon to $10^{-11} \text{ m}^2 \cdot \text{Pa}^{-1} \cdot \text{s}^{-1}$ in the EBg and zero in the lower Btg horizons. Data are listed in Fig. 11.

Excess rainfall on the site and for a distance of roughly 100 m upslope appears to be evacuated laterally through the upper horizons.

7. 1 bar corresponds to 0.1 MPa.

8. The traditional 1 metre per day corresponds to $1.18 \times 10^{-9} \text{ m}^2 \cdot \text{Pa}^{-1} \cdot \text{s}^{-1}$.

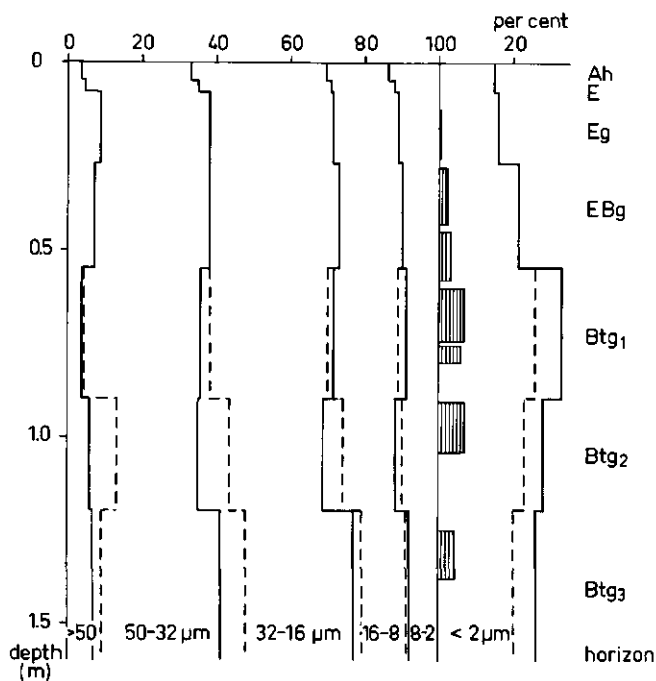


Fig. 12. Grain-size distribution of the Eynatten profile, recalculated to (sand + silt) fractions total 100 per cent. Solid lines: material without tongues, dashed lines: tongues, vertical hatching: clay illuviation features in thin sections, volume per cent. Tongues comprise a quarter of the total at 0.4 m depth, a seventh at 0.7 and 1 m, and a twelfth at 1.3 m depth.

Grain-size distribution

The grain-size distribution (Table 14, Fig. 12) shows an increase in clay contents from the eluvial horizons to a maximum in the upper Btg horizon and a gradual decrease with depth down to 1.6 m. The tongues contain clearly less clay than the intact parts of the Btg horizon. The sand and silt fractions show some variability but no clear trends with depth. The tongues tend to have a higher (coarse silt + sand)/fine silt ratio than the rest of the Btg horizons. Weathering may have affected the fine silt as well as the clay fraction.

General chemical data

Organic carbon contents (Table 14) decrease from about 10 per cent in the Ah horizon of the minipodzol to about 0.2 per cent in the EBg and lower horizons of the surface-water gley sequum. C/N ratios similarly drop from about 40 in the minipodzol to 10 in the lower sequum.

Free iron oxides are low in the minipodzol: 0.7 per cent, rise to a maximum of about 3.5 per cent in the EBg and upper B horizons of the lower sequum and range about 1-2 per cent in lower horizons.

Table 14. Grain-size distribution and general chemical data of the Eynatten profile.

Sample no. 73-	Depth	Horizon ¹	Grain-size distribution (%)							Org. C (%)	N (%)	Free Fe ₂ O ₃ (%)	pH	Exchangeable equivalents																																																																																																																																																																																																																																																																																																																																																																																																																																																																																																																																																																																																																																																																																																																																																																																																																																																																																																																																																																																																																																																																																																																																																																																																																																																																																																																																																																																																																																				
														water																																																																																																																																																																																																																																																																																																																																																																																																																																																																																																																																																																																																																																																																																																																																																																																																																																																																																																																																																																																																																																																																																																																																																																																																																																																																																																																																																																																																																																				
			>2000 ² μm	2000-50 μm	50-32 μm	32-16 μm	16-8 μm	8-2 μm	<2 μm					CaCl ₂ (0.01 mol/l)	Ca	Mg	Na	K	Al	H	Σ																																																																																																																																																																																																																																																																																																																																																																																																																																																																																																																																																																																																																																																																																																																																																																																																																																																																																																																																																																																																																																																																																																																																																																																																																																																																																																																																																																																																																													
																																																																																																																																																																																																																																																																																																																																																																																																																																																																																																																																																																																																																																																																																																																																																																																																																																																																																																																																																																																																																																																																																																																																																																																																																																																																																																																																																																																																																																																		</

1. i: interior parts of horizons, without grey tongues. t: grey tongues.

At 0.4 m depth, grey tongues occupy about a quarter (not sampled separately);

at 0.7 and 1 m depth, about 14%; at 1.3 m, about 8%.

2. % of total soil. All other data refer to fine earth.

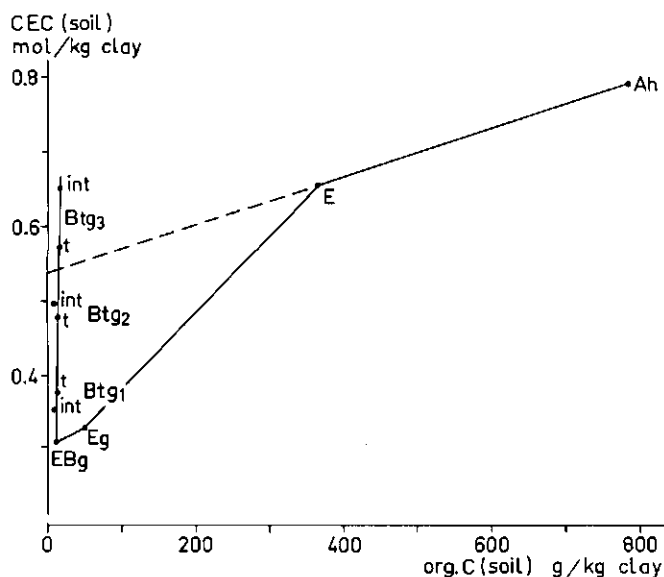


Fig. 13. CEC plot of the Eynatten profile. Ordinate: CEC of the soil (by sum of cations) recalculated per kg clay. Abscissa: organic C, recalculated per kg clay. t: tongues, int: interior, less weathered parts of Btg horizon.

Soil reaction and exchangeable cations similarly show a division into these three zones. pH-water is about 3.8, pH- CaCl_2 3.3 in the minipodzol. This contains about 70 per cent exchangeable aluminium with noticeable proportions of divalent cations and potassium (probably due to nutrient cycling) and hydrogen (probably associated with the high organic matter contents). The Eg, EBg and upper B horizons of the lower sequum have a pH of about 4.2 in water, about 3.6 in CaCl_2 , and about 90 per cent exchangeable aluminium with insignificant proportions of basic cations and hydrogen. The pH of the lower B horizons is about 5 in water, 4 in CaCl_2 , and exchangeable aluminium decreases from about 50 to about 20 per cent with depth. Calcium and magnesium in about equal amounts increase from about 40 to 70 per cent, and potassium and hydrogen each comprise about 5 per cent.

The lowest CEC occurs in the Eg horizon, in qualitative agreement with the low clay and organic matter contents. After recalculation of CEC (soil) per kg clay and graphic correction for organic matter (Fig. 13), however, it is clear that the cation exchange capacities of the clay fractions are much lower in the eluvial horizons and the upper B of the surface-water gley sequum than in the lower B horizons or in the Ah and E horizons of the minipodzol.

Total chemical composition

The total chemical composition of fine earth and clay fractions is listed in Tables 15 and 16. Some of the main changes with depth are indicated by horizontal lines.

The fine earth of the podzol A and E horizons contains less Al_2O_3 , Fe_2O_3 , MgO and K_2O , and has a higher ignition loss (mainly organic matter) than the lower sequum. The

Table 15. Total chemical composition (%) of fine earth fractions of the Eynatten profile.

Sample no. 73-	SiO ₂	Al ₂ O ₃	Fe ₂ O ₃ ¹	MgO	CaO	Na ₂ O	K ₂ O	TiO ₂	Ignition loss ²
134	73.0	6.1	1.2	0.1	0.3	0.7	1.46	0.78	15.4
135	80.3	6.9	1.0	0.1	0.3	0.7	1.68	0.85	6.8
136	79.7	8.1	3.0	0.1	0.3	0.8	1.80	0.85	3.4
137	78.4	9.1	4.2	0.2	0.2	0.8	2.08	0.83	3.0
138	74.1	10.5	5.0	0.7	0.2	0.8	2.21	0.81	3.6
139	78.4	10.0	3.3	0.6	0.3	0.8	2.14	0.82	3.1
140	74.7	10.9	4.4	0.8	0.4	0.9	2.30	0.80	3.4
141	77.8	10.3	2.6	0.6	0.3	0.9	2.22	0.81	3.1
142	76.4	10.2	3.9	0.7	0.4	1.0	2.09	0.77	3.2
143	77.3	9.6	3.8	0.7	0.4	1.0	2.08	0.76	3.0
144	79.3	9.6	2.3	0.6	0.4	0.9	2.02	0.77	2.8
145	72.4	14.2	3.6	0.7	0.2	0.4	2.42	0.84	4.6
146	69.7	14.9	3.6	0.7	0.2	0.2	2.96	0.84	4.8

1. Total iron as Fe₂O₃.

2. Mainly organic matter in upper two samples.

Table 16. Total chemical composition (%) of clay fractions of the Eynatten profile.

Sample no. 73-	SiO ₂	Al ₂ O ₃	Fe ₂ O ₃	FeO	MgO	CaO	Na ₂ O	K ₂ O	TiO ₂	Ignition loss
134	53.4	24.2	5.2	0.14	1.1	0.08	0.31	2.54	1.54	12.1
135	50.8	24.3	5.1	0.19	1.3	0.08	0.31	2.42	1.33	11.3
136	51.2	25.9	6.6	0.32	1.1	0.10	0.32	2.49	1.28	10.0
137	49.7	24.1	10.6	0.32	1.5	0.08	0.29	2.78	1.21	9.4
138	50.8	22.6	11.1	0.35	1.6	0.07	0.22	2.74	0.99	9.0
139	52.0	22.6	9.6	0.28	1.6	0.07	0.24	2.87	1.09	8.7
140	50.6	21.9	9.9	0.21	1.6	0.10	0.22	2.94	1.00	9.4
141	52.5	23.1	10.1	0.18	1.8	0.07	0.24	2.87	1.10	9.6
142	51.0	21.8	10.0	0.18	1.8	0.12	0.25	2.85	0.96	9.6
143	50.7	21.8	10.1	0.18	1.8	0.14	0.25	2.85	0.95	9.6
144	52.1	22.7	7.3 ¹	0.19	1.5	0.13	0.28	2.84	1.05	9.6
145	49.5	27.5	6.6 ¹	.	1.0	0.12	0.32	3.97	0.86	8.7
146	49.7	27.4	6.8 ¹	.	1.3	0.14	0.33	4.32	0.83	7.5

1. Total iron as Fe₂O₃

eluvial horizons and the tongues of the surface-water gley sequum tend to contain less Al₂O₃, Fe₂O₃, MgO and K₂O than the parts of the B horizons without tongues. The bulk chemical composition thus shows but a single broad trend in the two sequa.

The clay fractions of the podzol A and E horizons contain slightly less Al₂O₃, less ferric and ferrous iron, MgO and K₂O, and more Na₂O, TiO₂ and structural water (ignition loss) than the clay of the surface-water gley sequum. The clay fractions of the eluvial horizons of this lower sequum, however, contain more Al₂O₃ and ferrous iron and do not have a higher ignition loss than the clay of the lower horizons. Trends for the other oxides are similar to those in the podzol sequum, but less pronounced.

Recalculation to a goethite norm mineral composition (Table 17) shows similar weathering trends in the clay fractions. The main changes occur between the Eg and EBg, some start in the EBg horizon. Norm illite, smectite and goethite contents are lower and rutile, albite, kaolinite higher in eluvial horizons than in lower ones. Similarly, rutile contents are higher and goethite contents tend to be lower in the clay fractions of bleached tongues than of ped interiors in the Bg horizons. Maximal goethite contents are found in the ped interiors of the upper Bg. Excess structural water increases, and kaolinite decreases in the eluvial horizons of the minipodzol after a maximum in the eluvial horizon of the surface-water gley sequum.

The epinorm mineral composition of the sand + silt fractions and the goethite norm composition of the clay fractions were recalculated on the basis of a constant percentage TiO_2 in the sand + silt fractions, to show weathering changes in the sand + silt fractions and translocation plus weathering in the clay fractions (Table 18). The constant epinorm quartz contents in sand + silt fractions throughout the profile support the assumption that epinorm quartz as well as TiO_2 in those fractions may be used as an index of weathering. Iron oxides (norm hematite) have been lost from the upper horizons and from the tongues; norm muscovite and albite from the upper horizons. The increase upward in the profile of norm orthoclase probably is an artefact of the norm calculation, which assigns K_2O to muscovite and orthoclase in accordance with the availability of Al_2O_3 . If we assume that orthoclase is not weathered (i.e., remains at 4.3%, proportional to TiO_2) and that only muscovite is weathered, a similar weathering trend is still evident (column Ms⁴ in Table 18). This recalculation entails the assumption that there is an alumina-rich phase in the B and Eg horizons equivalent to about 0.5 (0.0 to 0.9) per cent Al_2O_3 , which is essentially absent in the Ah and E horizons.

The low quartz and titania (norm rutile) figures in the clay fractions of the upper horizons and their maximal contents in the interior parts of the Bg horizon reflect clay translocation; the low figures for total clay, norm illite and smectite in the eluvial horizons, translocation and weathering; the figures for kaolinite and albite, the resul-

Table 17. Goethite norm mineral composition (%) of the clay fractions of the Eynatten profile.

Sample no. 73-	Q	Ru	Go	Ab	K	I	S	W
134	15	1.54	5.7	2.6	28	21	20	6
135	11	1.33	5.5	2.6	27	20	24	5
136	10	1.28	7.2	2.7	31	21	23	3
137	8	1.21	11.6	2.4	21	24	30	3
138	10	0.99	12.2	1.9	16	23	32	3
139	12	1.09	10.6	2.0	16	24	30	3
140	11	1.00	10.8	1.9	14	25	30	4
141	10	1.10	11.2	2.0	15	24	34	4
142	10	0.96	10.9	2.1	13	24	33	4
143	10	0.95	11.0	2.1	13	24	34	4
144	12	1.05	8.1	2.4	17	24	29	4

Table 18. Norm mineral composition of the Eynatten profile recalculated on the basis of constant TiO_2 content in the (sand + silt) fractions¹.

Sample no. 73-	Horizon ²	Sand + silt fractions, epinorm						Clay fraction, goethite norm							Clay, total
		Q	Hm	Ab	Or	Ms	Ms ³	Q	Ru	Go	Ab	K	I	S	
134	Ah	55	0.6	5.2	4.1	3.5	3.1	1.6	0.16	0.6	0.28	3.0	2.3	2.2	10.7
135	E	53	0.3	5.0	4.1	3.7	3.4	1.1	0.14	0.6	0.28	2.8	2.1	2.5	10.4
136	Eg	53	1.7	5.1	3.4	5.5	4.1	1.1	0.15	0.9	0.32	3.7	2.5	2.7	11.8
137	EBg	55	2.1	6.1	4.3	6.3	6.3	1.3	0.21	1.9	0.41	3.5	3.9	5.0	16.7
138	Btg1(i)	51	2.1	6.6	4.1	7.3	6.9	2.5	0.25	3.1	0.47	4.1	5.9	8.2	25.5
139	Btg1(t)	54	1.2	6.5	2.9	8.4	6.4	2.4	0.22	2.1	0.41	3.3	4.9	6.1	20.1
140	Btg2(i)	50	2.2	7.4	2.2	10.5	7.4	2.4	0.22	2.3	0.40	3.0	5.4	6.6	21.7
141	Btg2(t)	53	0.6	7.1	2.7	9.6	7.2	1.8	0.20	2.0	0.37	2.8	4.4	6.1	18.0
142	Btg3	54	1.8	7.8	1.9	9.8	6.3	2.2	0.20	2.3	0.44	2.7	5.0	6.8	20.8

1. Fine earth in the Btg3 horizon (sample 74-142) total 100%.

2. i: interior parts of horizons, without grey tongues. t: grey tongues.

3. Muscovite recalculated under the assumption that orthoclase is constant at 4.33%.

This entails the further assumption that an Al-rich phase is present in the B and Eg horizons in amounts equivalent to 0.5 (0.0-0.9)% Al_2O_3 .

tant of translocation plus weathering minus formation out of material from the coarser fractions (albite) or other clay minerals.

Clay mineralogy

Diffractiongrams of glycerol-treated Mg-clay fractions and of K-clay fractions are shown in Fig. 14. Reactions of the 1.4 nm reflection of the K-clay fractions to heat treatment are listed in Table 19. The clay fractions contain kaolinite and some quartz, in proportions roughly constant throughout the profile.

Table 19. 1.4 nm reflections of K-clay fractions of the Eynatten profile after heat treatment.

Sample no. 73-	Heat treatment ¹				
	25°C	200°C	300°C	400°C	500°C
134	t	-	-	-	-
135	c	c	ss	t	t
136	h	c	ss	t	t
137	h	c	s	s	s
138	t	t	-	-	-
139	ss	t	t	-	-
140	ss	t	-	-	-
141	ss	-	-	-	-
143	ss	-	-	-	-
144	t	-	-	-	-

1. Description of reflections, h: high and sharp, c: clear, s: small, ss: small shoulder, t: trace, -: absent.

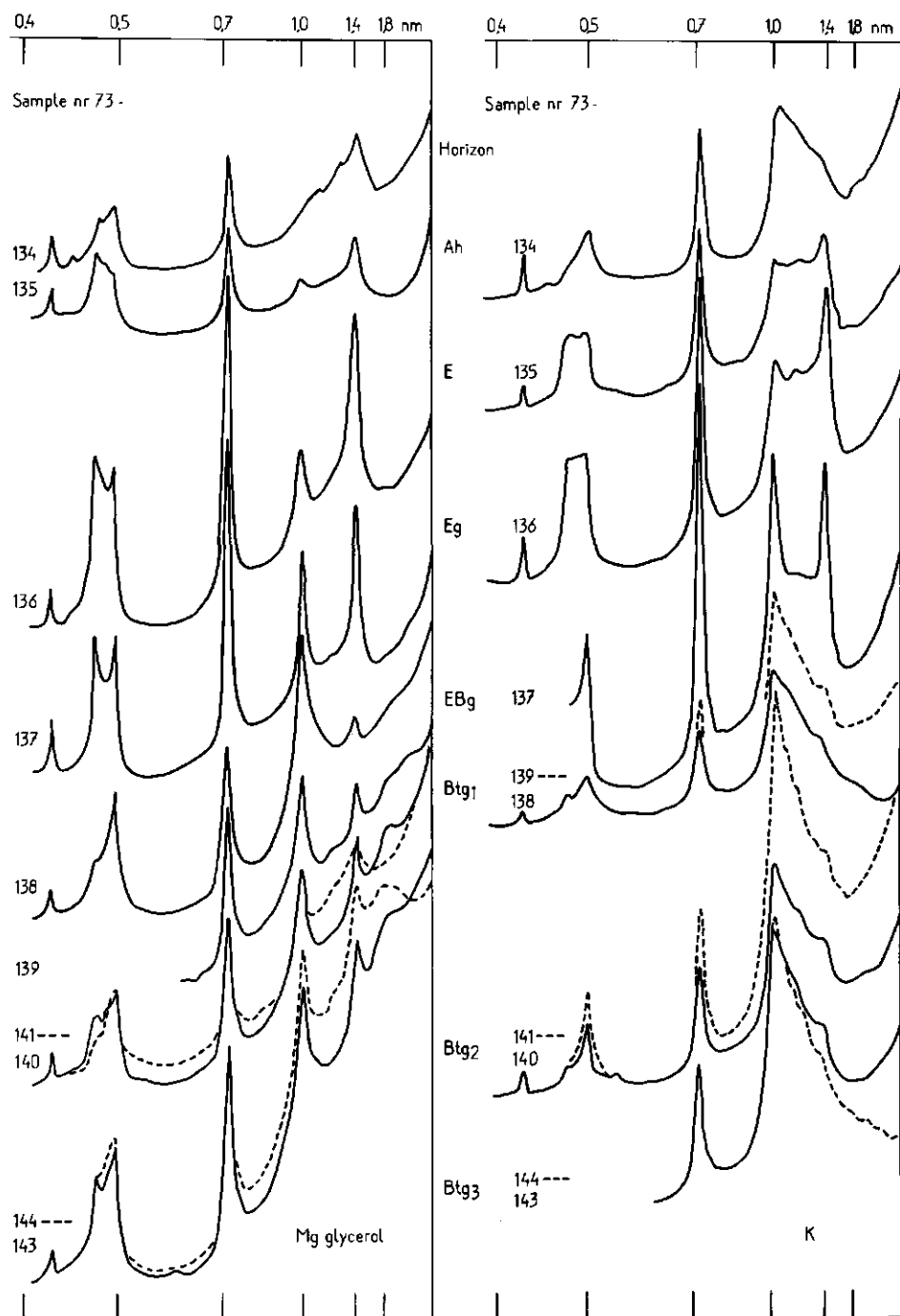


Fig. 14. X-ray diffractograms of clay fractions of the Eynatten profile. Mg-saturated and treated with glycerol; K-saturated. Solid lines: material without tongues, dashed lines: tongues.

Moderate amounts of illite are recognized in the Bg and EBg horizons, less in the Eg, very little in the E and virtually none in the Ah horizon. Some smectite is clearly present in the Bg horizons; no smectite reflections are found in the eluvial horizons. Contents of soil chlorite (aluminium-interlayered material) are very low in the Bg horizon, attain a maximum in the Eg and EBg horizons concurrent with the disappearance of smectite, and are low again in the E and negligible in the Ah horizons of the minipodzol. The latter contains considerable amounts of interstratified illite-vermiculite, possibly with slight aluminium interlayering.

The aluminium-interlayered material in the EBg horizon is heat-stable to 500°C, in the Eg and E horizons to between 200 and 300°C, and in the other horizons to less than 200°C. The proportion as well as the heat stability of the 1.4 nm reflection decrease after citrate extraction (Table 20).

Cation exchange capacities and ferrous iron contents of clay fractions before and after citrate extraction are listed in Table 21. The CEC reaches a minimum and the FeO content a maximum in the eluvial and upper Bg horizons of the surface-water gley sequum; these trends reverse to absolute maxima and minima, respectively, in the Ah horizon of the minipodzol. Citrate treatment increases the CEC by about 0.1 mol/kg clay throughout the surface-water gley sequum, and by much less in the minipodzol. Only the EBg and upper Bg horizons of the surface-water gley sequum contain appreciable (0.1%) ferrous iron that is released by the citrate treatment. This presumably occurs trapped in the interlayers. Not all interlayer material appears to be extracted by three 1-hour extractions with hot Na citrate: even after this treatment, the CEC in the eluvial horizons of the surface-water gley sequum is lower, and the FeO content higher, than in the Bg horizons or in the Ah.

Table 20. 1.4 nm/1.0 nm peak height ratios of K-saturated clay fractions without and with preliminary Na citrate treatment after heating to different temperatures.

Sample no. 73-137, EBg horizon, Eynatten profile

Temperature (°C)	1.4 nm/1.0 nm peak height ratio	
	without citrate	with citrate ¹
25	0.68	0.63
100	0.42	0.37
200	0.42	0.31
300	0.38	0.23
400	0.18	0.2 ²

1. Differences are greater than suggested by this table, because the 1.4 nm/1.0 nm peak height ratio of the citrate-treated sample before treatment was about 1, compared with about 0.7 for the control sample.

2. No peak at 1.4 nm; a diffuse range of reflections between 1.4 and 1.0 nm.

Table 21. Cation exchange capacities and ferrous iron contents of clay fractions of the Eynatten profile without and with preliminary citrate extraction.

Sample no. 73-	CEC (mol/kg)		FeO (%)	
	without citrate extraction	with citrate extraction	without citrate extraction	with citrate extraction
134	0.45	0.44	0.14	0.11
135	0.35	0.39	0.19	0.25
136	0.31	0.38	0.32	0.30
137	0.28	0.41	0.32	0.23
138	0.33	0.41	0.35	0.25
139	0.35	0.45	0.28	0.27
140	0.31	0.48	0.21	0.17
141	0.38	0.48	0.18	0.17
142	0.39	0.44	0.18	0.18
143	0.34	0.46	0.18	0.19
144	0.38	0.48	0.19	0.16

Trends in composition of precipitation and soil solutions

On five occasions during wet periods in 1973 and 1974, soil solutions were extracted from water-saturated horizons at different depths in the Eynatten profile and in the similar Plattebosch profile, situated in southern Limburg, Netherlands, about 10 km WNW of Aachen. As an example, data for Eynatten, Oct.-Nov. 1974, are listed in Table 22. Whenever possible, accumulated or fresh precipitation (rain or hail) was sampled at the same times. The solutions were analysed for pH, Ca, Mg, Na, K, Al, Fe, HCO_3 , Cl, SO_4 , Si and, on two occasions, organic C.

If organic C is calculated as an organic acid with roughly 10 mol acid groups per kg C, electroneutrality is satisfied within 0 to 8 per cent ($0.00\text{--}0.08 \text{ mol/m}^3$) for six samples and within 20 per cent (0.25 mol/m^3) for one sample. The net contribution of NH_4 and NO_3 was not determined, but seems to be generally small if the estimate of organic acidity is valid.

The sampling of precipitation, biased towards wet periods, must have underestimated the input of strong acid (SO_4), because ionic equivalent⁹ sulphate concentrations in the soil solution (0.4 to 1.9 mol/m^3) exceed the corresponding figures in rainfall by about 0.5 to 1 mol/m^3 . Chloride contents generally range between 0.1 and 0.6 mol/m^3 both in precipitation and in the soil solution. Organic carbon decreased from 20 g/m^3 in soil solutions from the upper horizon to 4 g/m^3 in the solution from 1 m depth (assumed to represent 0.2 to $0.04 \text{ mol acid/m}^3$).

Silica, 0.0 mol/m^3 in precipitation, ranges between 0.2 and 0.4 mol/m^3 in soil solutions throughout the profiles, and appears to be dissolved mainly in the surface horizon. Calcium concentrations are more variable but show the same trend. Aluminium is dis-

9. Appendix: choice of units and entities.

Table 22. Composition of precipitation and soil solutions from different depths in the Eynatten profile.

Samples depth	pH	H	Ca	Mg	Na	K	Al	Fe ²	HCO ₃	Cl	SO ₄	H ₄ SiO ₄ ₃ (mol/m ³)	Organic C (g/m ³)
29 October 1974:													
Fresh hail	5.8	0.00	0.20	0.04	0.06	0.08	0.00	0.00	0.26	0.42	0.11	0.00	.
Standing water ³	4.2	0.06	0.39	0.12	0.04	0.07	0.38	0.02	0.00	0.40	0.53	0.19	.
Soil solutions													
0.3 m	4.2	0.06	0.25	0.10	0.04	0.07	0.41	0.02	0.00	0.38	0.45	0.18	18.0
0.5 m	4.2	0.06	0.25	0.10	0.04	0.06	0.40	0.02	0.00	0.40	0.46	0.17	8.0
0.7 m	4.5	0.03	0.39	0.47	0.11	0.04	0.10	0.00	0.00	0.46	0.63	0.20	4.5
16 November 1974:													
Rain water	5.2	0.01	0.12	0.08	0.04	0.17	0.00	0.00	.	0.28	0.31	0.04	.
Soil solutions													
0.3 m	4.1	0.08	0.29	0.10	0.13	0.04	0.43	0.01	.	0.34	0.61	0.25	9.0
0.5 m	4.2	0.06	0.29	0.11	0.13	0.04	0.43	0.01	.	0.34	0.61	0.26	.
0.7 m	4.6	0.03	0.43	0.42	0.24	0.02	0.11	0.00	.	0.38	0.76	0.27	.

1. See Appendix: Choice of units and entities.

2. Calculated as Fe²⁺.

3. Clear puddle from previous rain, in contact with soil and litter.

solved in the upper horizons but disappears from solution in the lower horizons. Magnesium concentrations in soil solutions in the Eynatten profile progressively increase with depth, presumably by ion exchange with aluminium. Trends in the Plattebosch profile are not clear, appreciable Mg concentrations occurring in solutions from all depths. Perhaps the ion exchange effect is masked by the different sulphate concentrations: maximal sulphate contents were found in the surface horizons of the Plattebosch profile. Sodium contents are rather variable without a clear trend: this ion probably passes through the profile with relatively little interaction save some concentration during dry periods.

Potassium is the only ion that appears to be retained in the profiles from the precipitation. Concentrations between 0.01 and 0.17 mol/m³ were measured in rain; between 0.01 and 0.12 in soil solutions from surface horizons; between 0.00 and 0.09 in soil solutions from about 1 metre depth.

Ionic equivalent ferrous iron contents are 0.00 mol/m³ in precipitation and range between 0.00 and 0.04 mol/m³ in soil solutions from surface horizons and between 0.00 and 0.02 mol/m³ in deeper horizons. Iron is presumably mobilized by reduction in water-saturated conditions when the temperature is high enough for microbial activity.

The results of these analyses may be used as qualitative indications for current processes, not quantitative because of low sampling intensity and bias towards wet conditions.

Abrahamsen et al. (1976) report that in southern Norway, strong acid in precipitation totals about 0.02 mol/m² per year. Maps by Eliassen and Saltbones, reproduced in Dovland et al. (1976), indicate sulphate precipitation of the order of 0.1 mol/m² per year in southern Norway and about 4 times that figure in the region of the present profiles. Under the assumptions that about 200-300 mm water per year passes through these soils and that the proportion of acid to sulphate is similar, the ionic equivalent sulphate concentration in the soil solutions should average 2-3 mol/m³ and the concentration of acid plus cations dissolved by acid, 0.5 to 0.7 mol/m³. The present data show about a third to half of these figures for sulphate. Hydrogen (estimated from pH) plus ionic equivalent aluminium total about 0.3 to 0.6 mol/m³ in the surface horizons, of which up to about 0.2 mol/m³ may be ascribed to dissolved organic acids. Because part of the dissolved Ca and Mg are also due to acid dissolution, these different estimations seem to be mutually consistent. Apparently, besides cheluviation and ferrollysis, current soil formation comprises considerable dissolution and leaching by strong acid, of the order of 0.4 mol/m³ or 0.1 mol/m² per year, whereas cheluviation from the surface horizon seems to proceed at (very roughly) half that rate.

SOLLING

FAO/Unesco Soil Units (FAO, 1974): Dystric Planosol

USDA Soil Taxonomy (Soil Survey Staff, 1975): Typic¹⁰ Glossaqualf

¹⁰. most probable: no colour notation available.

Classification according to author of description: Strongly podzolic¹¹, strongly expressed pseudogley.

Examined and described 25 Nov. 1970 by P. Benecke. The field data, below, have been translated and summarized from his description and further information in Van Engelen and Hurkens, 1975.

Samples are from a similar profile with the same classification in the immediate neighbourhood of the described profile.

The site

Location at the margins of a small high moor (Kükenbruch) in Hochsolling, near Silberborn, about 55 km NW of Göttingen, Federal Republic of Germany. Elevation slightly over 500 m above mean sea level.

Landform and slope: nearly level part of high plateau.

Vegetation: young fir, small percentage cover; dense grass undergrowth.

Climate: humid temperate (Köppen Cfb). Mean annual precipitation about 1100 mm, mean annual temperature slightly over 6°C.

General information on the soil

Parent material: solifluction deposit consisting of reworked loess over reworked weathered material from Buntsandstein with variable amount of stones. Loess thickness in the area ranges between 0.3 and 0.9 m.

Drainage imperfect according to profile morphology. Site and adjoining moor drained about 100 years ago by a system of shallow open drains in herringbone pattern.

Some stones in surface horizon, no rock outcrops, no erosion, no salinity.

Human influence has disturbed the normal Of and Oh horizons; remnants of Of material from the previous cycle of fir forest are present. Drainage has presumably reduced the period of seasonal soil saturation.

Brief description of the profile

Shallow, imperfectly drained, strongly mottled, porous silt loam over a very slowly permeable strongly mottled heavy silt loam subsoil with tongues in a very coarse polygonal pattern. The surface horizons have been recognized as podzolic eluvial horizons. Few roots occur throughout the porous upper horizons and extend along the tongues in the subsoil.

Individual horizons of this profile and of an adjacent Brown Earth profile were described by Benecke and reproduced in Van Engelen and Hurkens (1975). Micromorphological observation of thin sections from the pseudogley profile showed several volume per cent

¹¹ defined as having a continuous, grey E horizon less than 3 cm thick and (discontinuous) humus-iron illuvial mottles. The detailed profile description suggests a moderately podzolic designation.

clay illuviation features, mainly ferriargillans, in the mass of the Bg horizon and occasional small ferriargillans in the tongues. The latter are generally grainy and less birefringent. Thin sections from the adjacent Brown Earth profile indicate much stronger biotic homogenization and have no trace of clay illuviation.

Grain-size distribution and general chemical data

The grain-size distribution of the (sand + silt) fractions in this profile is very uniform (Fig. 15). After recalculation to (sand + silt) total 100 per cent, standard deviations for individual fractions range between 0.7 and 1.3 per cent. Proportions of stones vary with depth and from place to place. Clay percentages strongly decrease toward the surface, and are lower in the tongues than in the mass of the subsoil.

Organic carbon contents are high in the surface horizon and decrease rapidly with depth; contents of free iron oxides are highest in the mass of the Bg horizon, and decrease in the tongues and toward the surface to a very low value (0.2%) in the Ah horizon. pH is extremely low in the Ah and rises to about 4.5 (water) and 3.6 (CaCl₂) in the surface-water gley sequum. Exchangeable cations comprise dominantly aluminium throughout the soil, with some hydrogen particularly in the two upper horizons with high organic matter contents, and little Ca and Mg. Data are listed in Table 23.

Total chemical composition

Much of the variation in total chemical composition of the fine earth (Table 24) is correlated with the variation of clay content with depth (last column); part is obscured by the different organic matter contents. Iron and magnesium contents strongly decrease toward the surface; Ca and Na are rather constant; K tends to follow the clay contents.

The total chemical composition of the clay and (sand + silt) fractions (Tables 25 and 26, respectively) shows the effects of weathering after elimination of the possible effects of clay translocation (or congruent dissolution of part of the clay fraction).

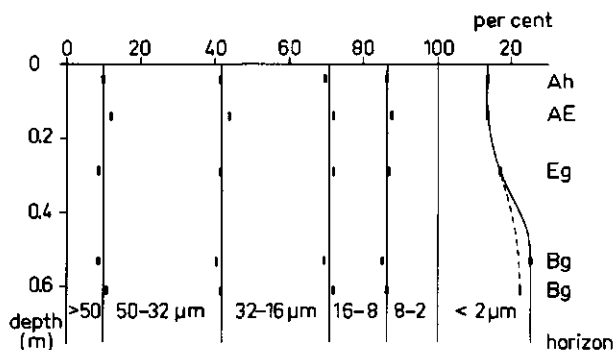


Fig. 15. Grain-size distribution of the Solling profile, recalculated to (sand + silt) fractions total 100 per cent. Solid line: material without tongues, dashed line: tongues.

Table 23. General chemical data for the Solling profile.

Sample no. 74-	Depth (cm)	Horizon	Org. C (%)	Free Fe ₂ O ₃ (%)	pH water	Exchangeable equivalents					
						CaCl ₂ (0.01 mol/l)	Ca	Mg	Na	K	Al H
8	3-5	Ah	14.8	0.2	3.7	2.8	9	1	0	0	56 25
9	13-15	E	4.6	0.8	3.9	3.1	2	10	0	0	63 7
10	28-30	Eg	1.6	0.9	4.5	3.7	2	1	0	0	42 0
11	52-54	Bg (mass)	0.1	1.6	4.4	3.6	0	1	0	0	67 0
12	60-62	Bg (tongue)	0.2	1.1	4.5	3.6	0	10	0	7	57 0

Table 24. Total chemical composition (%) of fine earth fractions of the Solling profile.

Sample no. 74-	SiO ₂	Al ₂ O ₃	Fe ₂ O ₃ ¹	MgO	CaO	Na ₂ O	K ₂ O	TiO ₂	Ignition loss ²	Clay
8	68.5	4.8	0.9	0.1	0.2	0.4	1.28	0.64	24.9	12.3
9	80.8	6.4	1.9	0.2	0.2	0.5	1.64	0.72	8.4	12.1
10	79.0	9.0	2.3	0.4	0.3	0.6	2.08	0.76	5.9	14.6
11	76.4	10.6	3.8	0.6	0.2	0.6	2.44	0.72	3.7	20.1
12	79.2	10.2	2.9	0.6	0.2	0.6	2.46	0.73	3.3	18.5

1. Total iron as Fe₂O₃.

2. Mainly organic matter in upper two horizons.

Table 25. Total chemical composition (%) of the clay fractions of the Solling profile.

Sample no. 74-	SiO ₂	Al ₂ O ₃	Fe ₂ O ₃	FeO	MgO	CaO	Na ₂ O	K ₂ O	TiO ₂	Ignition loss
8	47.0	20.9	2.3	0.08	0.7	0.06	0.16	2.98	1.49	21.9
9	47.2	23.2	3.4	0.17	0.9	0.04	0.16	2.95	1.63	17.3
10	50.7	25.0	7.2	0.46	1.2	0.03	0.14	2.38	1.20	11.4
11	49.9	23.3	8.8	0.21	1.2	0.02	0.12	3.09	1.04	9.1
12	49.5	24.2	8.1	0.25	1.3	0.02	0.12	3.38	1.03	9.2

Table 26. Total chemical composition (%) of the (sand + silt) fractions¹ of the Solling profile.

Sample no. 74-	SiO ₂	Al ₂ O ₃	Fe ₂ O ₃ ²	MgO	CaO	Na ₂ O	K ₂ O	TiO ₂	Ignition loss
8	93.8	3.9	1.0	0.0	0.2	0.6	1.46	0.73	0.9
9	91.6	4.4	1.8	0.1	0.2	0.6	1.58	0.69	0.2
10	87.1	6.4	1.4	0.3	0.3	0.7	2.10	0.71	1.9
11	83.1	7.2	2.5	0.5	0.3	0.7	2.28	0.64	2.3
12	86.0	7.0	1.7	0.4	0.3	0.7	2.23	0.66	2.0

1. Calculated from composition of fine earth and clay fractions after correction for organic matter.

2. Total iron as Fe₂O₃.

Table 27. Total chemical composition (%) of the Solling profile recalculated to constant TiO_2 content in the (sand + silt) fractions¹.

Sample no. 74-	Sand + silt fraction					Clay fraction									
	SiO_2	Al_2O_3	Fe_2O_3	MgO	CaO	Na_2O	K_2O	SiO_2	Al_2O_3	Fe_2O_3	FeO	MgO	K_2O	TiO_2	total
8	72	3.0	0.8	0.00	0.13	0.43	1.13	5.1	2.3	0.2	0.01	0.07	0.33	0.16	11
9	75	3.6	1.4	0.05	0.17	0.47	1.29	5.3	2.6	0.4	0.02	0.10	0.33	0.15	11
10	67	5.0	1.2	0.22	0.24	0.55	1.61	6.7	3.3	0.9	0.06	0.16	0.32	0.16	15
11	66	5.8	2.0	0.40	0.20	0.59	1.82	10.0	4.7	1.8	0.04	0.24	0.62	0.21	20
12	68	5.5	1.3	0.34	0.20	0.58	1.77	8.9	4.3	1.4	0.05	0.22	0.61	0.18	18

1. Fine earth in the mass of the Bg horizon (sample 74-11) total 100%.

2. Total iron as Fe_2O_3 .

The strong increase in TiO_2 content of the clay fractions of the upper two horizons indicates strong weathering, with loss of more than a third of the original clay fraction. The low Al_2O_3 (and MgO) contents of the clay still present suggest that cheluviation may have been active. The relatively high K_2O contents in the upper horizons may be due to nutrient cycling. The changes from the Bg horizon (samples 74-11 and 12) to the Eg horizon (sample 10) are less extreme: the moderate residual increase in TiO_2 without disproportionate loss of Al_2O_3 and the maximal ferrous iron contents are indicative of ferrollysis rather than cheluviation in the Eg horizon.

The bulk of the (sand + silt) fractions probably decreased by about 10 per cent only (under the assumption that SiO_2 or TiO_2 may be used as indexes), due to weathering of mainly the potassium and magnesium minerals. The tongues in the Bg horizon (sample 12) appear to have lost iron oxides, presumably by seasonal reduction, with little further weathering.

As a check on these interpretations all oxides have been recalculated to a constant TiO_2 content in the (sand + silt) fraction (Table 27). Most oxides in the sand + silt fractions show a loss in the upper horizons, but SiO_2 a slight gain. If significant, this might indicate a slight loss even of TiO_2 from this fraction due to cheluviation, and a consequent slight underestimate of the loss of other oxides. All oxides in the clay fraction decrease toward the surface, including TiO_2 and SiO_2 . The changes in TiO_2 may be largely due to clay translocation; all other oxides show greater decreases, which may be ascribed to weathering.

Clay mineralogy

Diffraction patterns of glycerol-treated Mg-clay fractions and of K-clay fractions before and after heat treatment at 550°C are shown in Fig. 16. The Mg-glycerol diffraction patterns indicate a slight increase of kaolinite toward the surface (particularly if a correction for the 002 peak of the 1.4 nm component is taken into account), and roughly the same proportions of illite in the lowest and surface horizons, with a minimum in the Eg horizon. The latter corresponds with a very strong increase in that horizon of the 1.4 nm reflection: presumably due to aluminium-interlayering. The 1.4 nm reflection decreases again to very small in the E and virtually absent in the Ah horizon, with the concurrent appearance of a 1.8 nm reflection in the E, and large 1.8 and smaller 2.8 nm reflections in the Ah horizon. This can be explained by stripping of the Al-interlayers and the formation of a smectite (and interstratified smectite-illite) owing to cheluviation.

The K-diffraction patterns similarly indicate a very strong increase of the 1.4 nm reflection from the Bg to the Eg horizon, and its virtual disappearance with a corresponding increase of the 1.0 nm reflection in the E and Ah horizons, in agreement with the trends in the Mg-glycerol diffraction patterns. A small part of the 1.4 nm material is heat-stable to 550°C . At least part of this is (strongly) interlayered material, not geogenic chlorite, because the small peak at 1.4 nm remaining after heating to 550°C also increases from the Bg to the Eg horizon.

Cation exchange capacities and ferrous iron contents of clay fractions before and after citrate extraction are listed in Table 28. The increase in CEC after citrate ex-

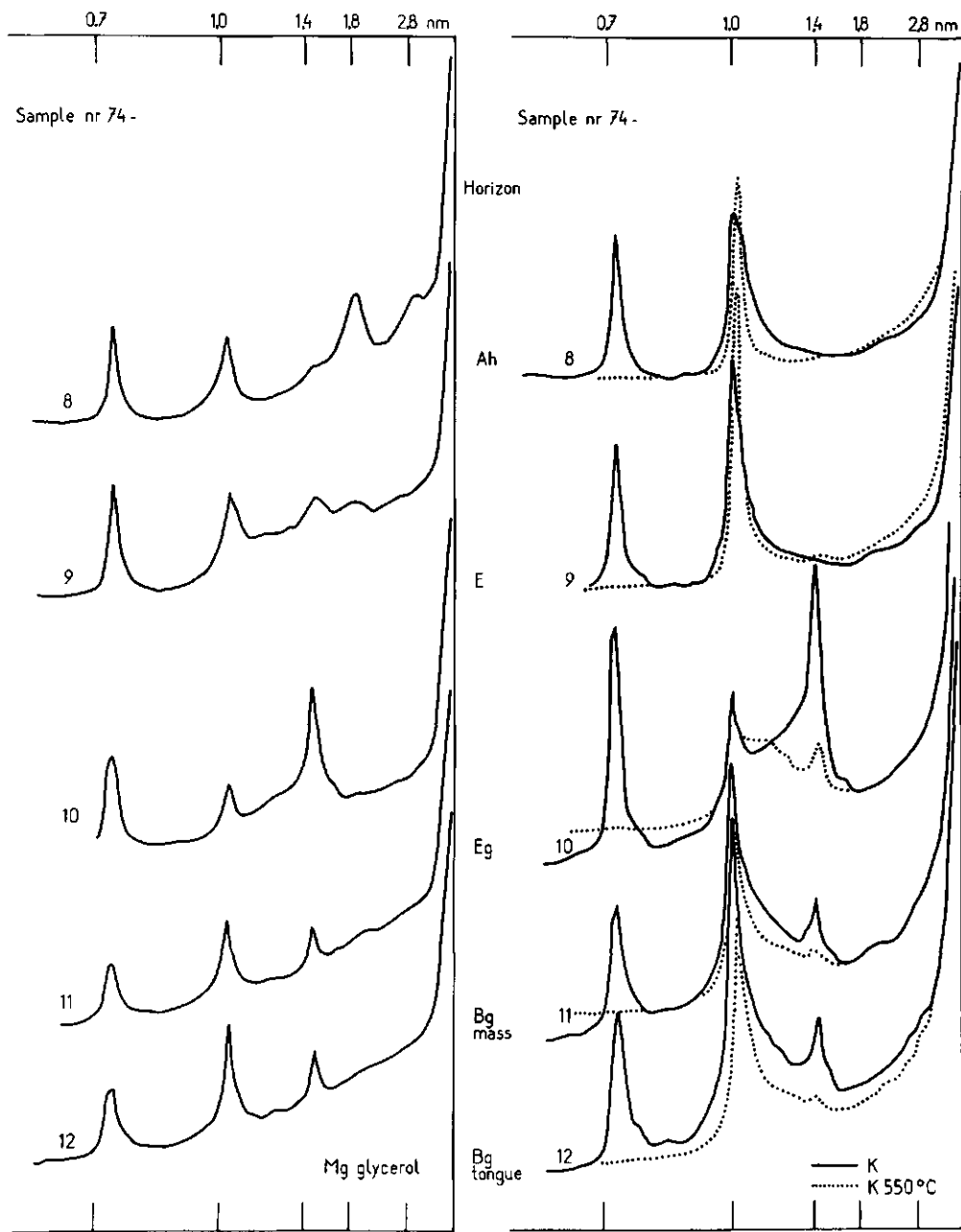


Fig. 16. X-ray diffractograms of clay fractions of the Solling profile. Mg-saturated and treated with glycerol; K-saturated; K-saturated and heated to 550°C.

Table 28. Cation exchange capacities and FeO contents of clay fractions of the Solling profiles without and with preliminary citrate extraction.

Sample no. 74-	CEC (mol/kg)		FeO (%)	
	without citrate extraction	with citrate extraction	without citrate extraction	with citrate extraction
Pseudogley profile				
8	0.41	0.37	0.08	0.06
9	0.25	0.38	0.17	0.16
10	0.25	0.43	0.46	0.40
11	0.28	0.39	0.21	0.25
12	0.29	0.43	0.25	0.28
Brown Earth profile				
1	0.27	0.41	0.18	0.19
2	0.26	0.40	0.16	0.19
3	0.22	0.43	0.22	0.25
4	0.32	.	0.19	.

traction in the clay fractions of the Bg, Eg and E horizons is indicative of aluminium-interlayering; the clay in the Ah horizon is not interlayered. The ferrous iron contents in the clay of the Bg horizon are little affected by citrate extraction, which suggests that ferrous iron is located within the clay structure rather than in the interlayers. The clay in the Eg horizon has a much higher ferrous iron content, the excess presumably consisting of ferrous ions trapped in the interlayers. Part but not all of this excess is removed by the citrate treatment. In contrast, the clay fractions of the E and Ah horizons contain less ferrous iron than even the Bg horizon, and these low percentages are resistant against citrate extraction. These data support the hypothesis that cheluviation has stripped essentially all ferrous iron that may have been trapped in interlayers at an earlier stage, and possibly part of the ferrous iron in octahedral positions within the clay structure.

In the Solling profile, cheluviation superseding ferrolysis is thus indicated in the two upper horizons by the trends in the ferrous iron contents of the clay fractions before and after citrate extraction as well as by the X-ray diffractograms, and in the surface horizon also by the trends in CEC before and after citrate extraction.

In the Solling Brown Earth profile, there is a strong increase in CEC of the clay fractions after citrate extraction whereas FeO contents are fairly constant, with little change after citrate treatment (Table 28), which indicates Al-interlayering but not ferrolysis. The X-ray diffractograms (Fig. 17) indicate strong Al-interlayering in the lower horizons and removal of the interlayers in the surface horizon. This suggests that cheluviation may be active in that horizon, which was not indicated by the FeO contents and CEC of the clay fractions.

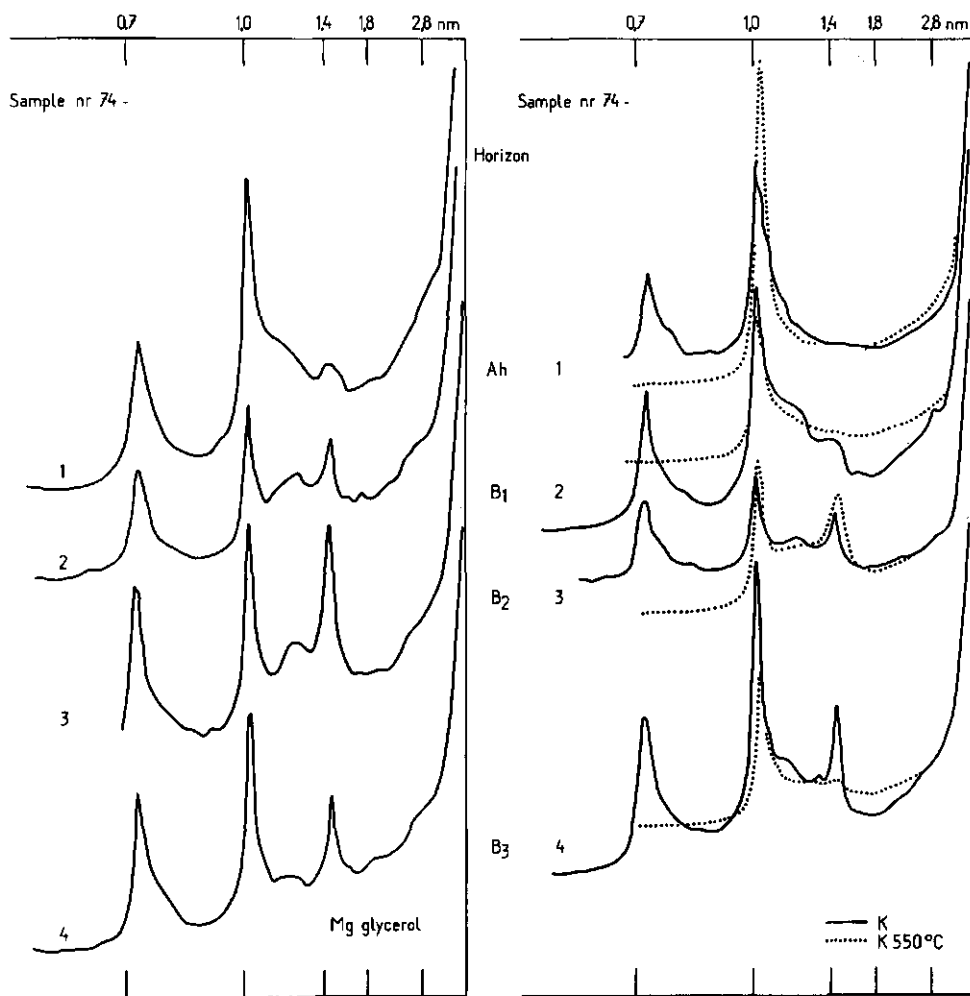


Fig. 17. X-ray diffractograms of clay fractions of the Solling Brown Earth profile. Mg-saturated and treated with glycerol; K-saturated; K-saturated and heated to 550°C.

Norm mineral calculations

Calculation of the epinorm mineral composition of the (sand + silt) fractions from the chemical data leads to substantially the same conclusions as discussed in the previous section, with one addition. Norm calculations suggest that orthoclase is not weathered, its proportion rising toward the surface together with those of norm quartz and rutile, whereas muscovite shows a strong decrease, particularly in the upper two horizons (Table 29).

The goethite norm mineral composition of the clay fractions (Table 30) shows illite and kaolinite contents in qualitative agreement with the X-ray diffraction data, except for the very high norm kaolinite content in the Eg horizon (sample 74-10). This excess

Table 29. Epinorm mineral composition (%) of the (sand + silt) fractions of the Solling profile.

Sample no. 74-	Q	Ru	Hm	Ab	Or	Ms
8	85	0.73	0.4	4.8	5	6
9	82	0.69	1.5	4.9	5	7
10	74	0.71	1.1	6.0	4	12
11	69	0.64	2.3	6.2	4	14
12	72	0.66	1.6	6.2	4	13

Table 30. Goethite norm mineral composition (%) of the clay fractions of the Solling profile.

Sample no. 74-	Ru	Go	Ab	I	S	K	Q	W
8	1.49	2.4	1.4	25	13	21	16	17
9	1.36	3.5	1.4	25	17	24	12	11
10	1.20	7.4	1.2	20	26	29	10	4
11	1.04	9.5	1.0	26	24	20	12	3
12	1.03	8.6	1.0	29	25	20	10	3

Table 31. Goethite norm mineral composition (%) of the Solling profile, recalculated on the basis of constant norm rutile (1.04%).

Sample no. 74-	Go	Ab	I	S	K	Q	W	Total
8	1.7	0.9	18	9	15	11	12	70
9	2.7	1.0	19	13	19	9	9	77
10	6.4	1.0	17	23	25	8	4	87
11	9.5	1.0	26	24	20	12	3	100
12	8.7	1.0	29	25	19	10	3	101

should probably be ascribed to aluminium interlayer material plus norm quartz rather than kaolinite. Random interstratification of smectite layers with different degrees of Al-interlayering may have suppressed most of the evidence for smectite in the diffractograms of the deeper horizons.

Recalculation of the goethite norm mineral composition of the clay fractions on the basis of constant norm rutile (TiO_2) shows considerable losses of goethite and illite from the three upper horizons, of smectite from the two upper horizons and of kaolinite from the surface horizon only (Table 31). Under the assumption that kaolinite has not weathered in the lower horizons (has remained constant at about 20 per cent), the Eg horizon contains about 3 per cent more aluminium interlayer material (calculated as $\text{Al}(\text{OH})_3$) than the lower horizons. The quartz figure would then become 11 per cent, so that norm quartz and albite both are substantially constant compared with the rutile standard.

Ferrollysis thus appears to have attacked mainly illite (and some smectite), with

Table 32. Goethite norm mineral composition (%) of the clay fractions of the Solling Brown Earth profile, recalculated on the basis of constant norm rutile (0.84%).

Sample no. 74-	Depth (cm)	Horizon	Go	Ab	I	S	K	Q	W	Total
1	2-7	Ah	4.9	0.4	18	11	14	4	2	58
2	15-20	B1	8.1	0.9	27	17	24	5	2	88
3	45-50	B2	7.8	0.8	27	21	24	3	2	90
4	65-70	B3	9.6	0.7	28	24	27	3	3	100

most of the aluminium involved reappearing in the form of interlayers, whereas subsequent cheluviation in the upper horizons has stripped the interlayers again, with concurrent dissolution of part of the smectite and hydration at dissolution defects of the smectite structure and, only in the surface horizon, some dissolution of kaolinite after removal of all interlayer material.

The clay fractions of a nearby well drained Brown Earth, recalculated in the same way (Table 32), show no trace of ferrolysis but only desilication (loss of smectite, one of the silica-rich phases) in most of the profile. In the surface horizon, there is much stronger evidence of cheluviation than in the upper horizon of the pseudogley profile. This comprises loss of mainly norm kaolinite and illite, some smectite and goethite.

BIEBOSCH VALKENBURG

FAO/Unesco Soil Units (FAO, 1974): Orthic Luvisol

USDA Soil Taxonomy (Soil Survey Staff, 1975): Typic Hapludalf

Examined 11 June 1975 by N. van Breemen, R. Brinkman and W. van Wijngaarden.

The site

Location near Valkenburg, Limburg, Netherlands.

Topographic map sheet 62A, scale 1:25 000, 4th ed. (1968), coordinates 318.5 km N, 186.7 km E. About 50°51.3'N, 5°50.3'E. Elevation 120 metres above mean sea level.

Landform and slope: mid-slope from plateau surface about 147 m to dry valley about 85 m above mean sea level. Hilly. Moderately steep, constant slope 20 per cent to NNW.

Vegetation/land use: mixed deciduous forest (Querco-carpinetum). Trees: Fraxinus, Alnus, Quercus petraea, Betula, Acer; shrubs: Corylus, Sorbus, Sambucus; undergrowth: Rubus, Galeobdolon, Polystichum filix-mas, few Hedera, Acer seedlings, Moehringia.

Climate: humid temperate (Köppen Cfb). Mean annual temperature 9.4°C, coldest month 1.6, warmest month 17.2°C; mean annual rainfall 745 mm, fairly evenly distributed; evaporation from a free water surface (Penman calculation) 724 mm/year, ranging from 6 mm in December to 125 mm in June. Monthly data are given in Fig. 18. There is a considerable excess of winter rainfall; in summer, potential evapotranspiration exceeds rainfall by about 200 mm. Because few data exist for evapotranspiration and temperature data are com-

monly available for more locations, the two were plotted against each other (Fig. 19) to allow an estimate of rainfall deficit in summer for the Eynatten profile.

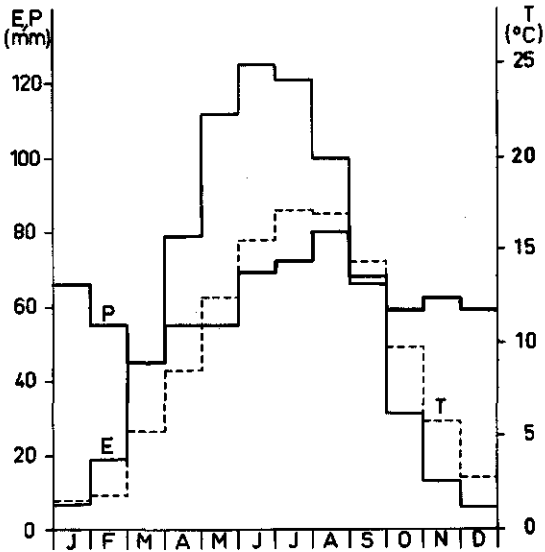


Fig. 18. Temperature, precipitation and evaporation from an open water surface (Penman calculation) in Southern Limburg, Netherlands. Normals 1931-1960; station Beek (temperature and evaporation); mean of stations Beek, Echt, Epen, Maastricht (rainfall). Source: Royal Netherlands Meteorological Institute, De Bilt.

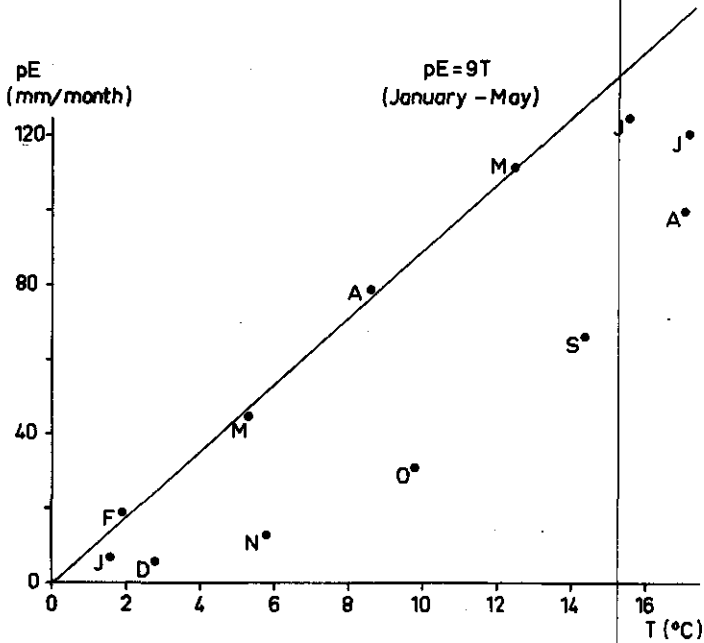


Fig. 19. Relation between monthly evaporation from a free water surface and mean temperature in Limburg, Netherlands.

General information on the soil

Parent material: loess with a thin (0.45 m) mantle of colluvium mainly from loess; older mixed colluvial or solifluction deposit from terrace material, limestone and possibly loess below 1.7 m depth.

Well drained. Moist throughout. Ground water not observed, presumed deeper than 20 metres.

Very few stones, occasional gravel and no rock outcrops at the surface. No evidence of accelerated erosion. Upper 45 cm of profile probably contain colluvial admixture of Old Pleistocene Meuse terrace material from upper slope.

No salt or sodicity present.

Human influence: None evident. Probably many centuries of extensive forest exploitation with occasional light grazing and without clear cutting. Presently nature reserve.

Brief description of the profile

Deep, well drained yellowish brown silt loam, deeply perforated and rooted.

Description of individual soil horizons

0-12 cm Ah	Dark greyish brown (10YR 3.5-4/2) moist silt loam; moderate medium and fine granular and weak medium and fine subangular blocky; very friable; few fine and very fine tubes; many fine and very fine and common medium roots; occasional gravel; clear smooth boundary. Sample 76/159; thin section 78138 (0-15 cm).
12-45 cm AB	Yellowish brown (10YR 4.5/4) moist silt loam; weak coarse and medium subangular blocky and moderate fine and medium granular; very friable; common fine and many very fine tubes; common fine and very fine and few medium roots; occasional gravel throughout, and faint stone line near bottom; clear smooth boundary. Sample 76/160; thin sections 78139 (17-32 cm), 78140 (32-45 cm).
45-62 cm B1	Yellowish brown (10YR 5/4) moist silt loam; weak medium and fine subangular blocky with thin patchy cutans slightly redder than soil mass on vertical and horizontal faces; friable; common fine and common, locally many very fine tubes; few coarse vertical tubes; common fine and very few medium roots; clear smooth boundary. Sample 76/161; thin section 78141 (49-64 cm).
62-95 cm Bt2	Yellowish brown (10YR 5/4) moist silt loam locally with laminar light grey-white (2.5Y 7-8/2) infillings and reworked patches of infillings and strong brown cutans; moderate very coarse prismatic and weak very coarse and coarse angular blocky with medium continuous cutans on vertical and some horizontal faces, and thin discontinuous cutans on many horizontal faces; friable, but firm in place; common fine and very fine, few medium tubes; few fine and very fine, very few medium roots; very little gravel; diffuse boundary. Sample 76/162; thin sections 78142 (65-80 cm), 78143 (80-95 cm).

Table 33. Number of tubular pores per dm² at several depths in the Biebosch Valkenburg profile.

Depth (cm)	Pore diameter					
	horizontal face					vertical face
	0.5-1 mm	1-2 mm	2-3 mm	3-5 mm	5-10 mm	0.5-1 mm 1-2 mm
50 ₁	100	5	1.5	1	0.5 ²	60 ₁
60 ₁	80	20	1	0	0.3	80 ₁
90	70	2.5	0.5	0.5	0.2	not determined
1. Plus infilled animal burrow 5-cm diameter with very many tubes, all < 2 mm. 2. All coated with dark grey material. In addition: 0.2 pedotubules. 3. Plus very many < 0.5 mm.						

95-160 cm B3 Yellowish brown (10YR 5/4) moist silt loam; weak very coarse prismatic and very weak coarse and medium angular blocky with cutans of the same colour; friable; common fine and very fine tubes; very few fine and very fine, occasional medium roots; clear boundary. Samples 76/163 (95-115 cm), 164 (115-140 cm), 165 (140-160 cm); thin sections 78144 (96-111 cm), 78145 (112-127 cm).

160-190+ cm 2C Yellowish brown variable silt loam-silty clay, locally fine sandy (auger observation); moist friable, clayey part plastic, nonsticky; gravel and chalk fragments; moderate to strong reaction to HCl.

Some data on porosity are given in Table 33.

Micromorphology, summary observations

0-15 cm Strong porosity, pores up to 5-8 mm; moderate amount of plasma; some coarse silt and fine sand grains; moderate amount of fine ferric nodules with diffuse and abrupt boundaries; remnants of roots; no ferriargillans.

17-32 cm Moderate porosity; regions with little plasma; occasional large sand grains; ferric nodules with diffuse boundaries, ferric nodules with sharp boundaries enclosing a coarser silty matrix than the rest of the material; very few very thin ferriargillans; moderate amount of new clay.

32-45 cm Moderate to low porosity; regions with little plasma; few thin ferriargillans; moderate amount of new clay.

49-64 cm Many pores of all sizes up to several mm, most not coated with ferriargillans; regions with little plasma; few, thin ferriargillans; moderate amount of new clay.

65-80 cm Transition to deeper thin sections.

80-95, Very low porosity, several (about 5) per cent clay illuviation features,

96-111 and mainly ferriargillans; much new clay, mainly from micas.

112-127 cm

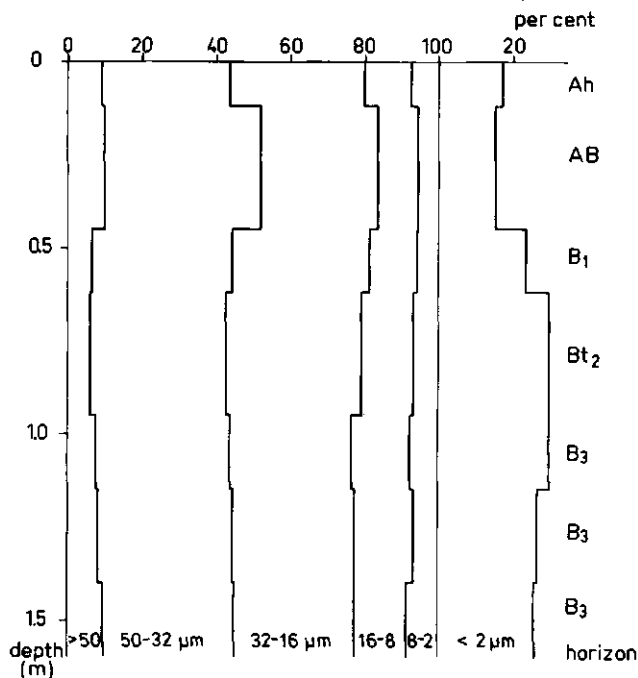


Fig. 20. Grain-size distribution of the Biebosch profile, recalculated to (sand + silt) fractions total 100 per cent.

Grain-size distribution

The grain-size distribution (Fig. 20) indicates that the parent material of the profile is not uniform: the ratios of the sand and silt fractions among themselves are variable with depth. The clay increase toward the B horizon may not be due to clay illuviation. The data were set out in a rectangular graph (Fig. 21) as described by Doeglas (1955), in order to see whether the grain-size distribution could be explained by a simple mixture of sediments. The figure shows that the B₂ and B₃ horizons are rather uniform, and that the AB, Ah and B₁ horizons contain less of a material consisting of 60% clay, 30% fine silt (2-16 μ m) and 10% coarse silt. If it is assumed that the sand fraction has been retained in the profile (as well as most of the coarsest silt) and that the material was originally uniform, the loss amounts to about 15-20 per cent of the original soil material. The clay and fine silt may have been gradually removed by erosion from the rather steep slope, and the coarser materials concurrently mixed in the upper horizons by biotic activity.

Chemical and mineralogical data on the whole soil or the (sand + silt) fractions therefore should be considered with caution; possible clay illuviation cannot be argued on the basis of texture data alone; but chemical and mineralogical changes of the clay fractions with depth probably are valid indications for weathering.

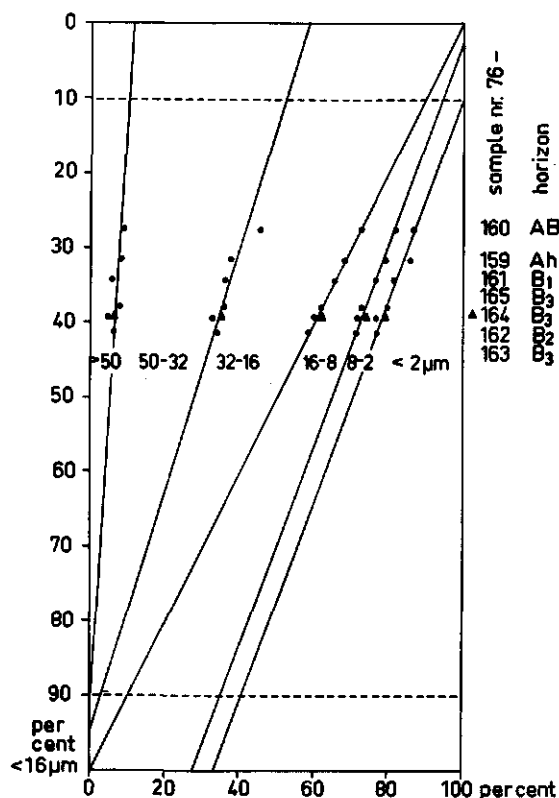


Fig. 21. Rectangular graph according to Doeglas (1955) of the grain-size distribution of the Biebosch profile.

General chemical data and total chemical composition

Organic matter contents are low in the Ah and very low in the rest of the profile (Table 34). The three upper horizons have a pH (water) below 4.5 and pH (CaCl_2) of 4 or less, with a base saturation below 50 per cent; pH (water) and pH (CaCl_2) exceed about 5

Table 34. General chemical data on the Biebosch Valkenburg profile.

Sample no. 76-	Depth (cm)	Horizon	Clay (%)	Org. C (%)	pH		Exchangeable equivalents					
					water	CaCl_2 (0.01 mol/l)	Ca	Mg	Na	K	CEC	
159	0-12	Ah	15	2.6	4.4	4.0	22	6	0	0	80	
160	12-45	AB	13	0.5	4.4	3.9	0	7	0	0	50	
161	45-62	B1	19	0.1	4.2	4.0	22	5	0	0	63	
162	62-95	Bt2	23	0.2	4.6	4.3	57	12	0	0	103	
163	95-115	B3	23	0.1	4.9	4.6	79	8	0	0	107	
164	115-140	B3	21	0.1	5.2	4.8	85	6	0	0	93	
165	140-160	B3	20	0.1	5.6	5.2	86	5	0	0	97	

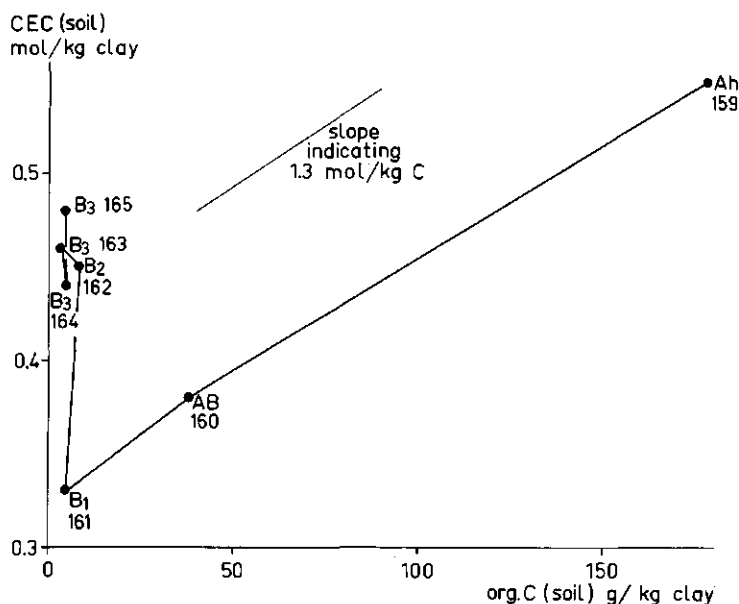


Fig. 22. CEC plot of the Biebosch profile.

Table 35. Total chemical composition (%) of the fine earth fractions of the Biebosch Valkenburg profile.

Sample no. 76-	SiO ₂	Al ₂ O ₃	Fe ₂ O ₃	FeO	MgO	CaO	Na ₂ O	K ₂ O	TiO ₂	Ignition loss
159	78.8	7.4	1.9	0.23	0.39	0.52	0.58	1.92	0.76	7.5 ¹
160	83.8	7.7	2.1	0.19	0.42	0.45	0.61	1.98	0.78	2.9
161	81.0	8.5	2.6	0.20	0.54	0.50	0.62	2.17	0.81	2.7
162	77.3	9.9	3.7	0.24	0.75	0.62	0.61	2.35	0.83	3.4
163	77.7	10.2	3.9	0.28	0.80	0.71	0.62	2.42	0.81	3.5
164	78.0	9.8	3.7	0.24	0.80	0.76	0.65	2.35	0.81	3.3
165	78.6	9.8	3.6	0.22	0.81	0.80	0.65	2.30	0.80	3.3

1. About 4.5% organic matter included in ignition loss: after correction, no differences in bulk composition between Ah and AB (samples 76-159 and 160) except slightly higher FeO and CaO contents.

Table 36. Total chemical composition (%) of the clay fractions of the Biebosch Valkenburg profile.

Sample no. 76-	SiO ₂	Al ₂ O ₃	Fe ₂ O ₃	FeO	MgO	CaO	Na ₂ O	K ₂ O	TiO ₂	Ignition loss
159	47.1	22.6	11.2	0.42	1.87	0.14	0.22	2.67	1.08	10.1
160	46.9	23.1	11.4	0.34	1.87	0.12	0.24	2.61	1.07	9.4
161	47.3	22.7	11.8	0.29	1.93	0.12	0.22	2.81	1.00	9.4
162	48.1	21.9	12.4	0.24	1.98	0.10	0.23	2.99	0.94	9.2
163	48.1	21.4	12.6	0.29	2.03	0.11	0.23	3.06	0.93	8.9
164	48.2	21.1	12.7	0.29	1.93	0.14	0.22	3.10	0.92	9.2
165	48.7	20.9	12.4	0.26	1.94	0.13	0.23	3.17	0.90	9.1

and 4.5, respectively, and the base saturation exceeds 90 per cent below about 1 m depth.

A CEC plot (Fig. 22) indicates cation exchange capacities of about 1.3 mol/kg organic C, about 0.33 mol/kg clay fraction in the upper three horizons, and about 0.45 mol/kg clay in the B2 and B3 horizons. The decrease in CEC/clay toward the surface suggests that the clay in the upper horizons may be aluminium-interlayered.

The total chemical composition of the fine earth (Table 35) mainly reflects the differences in clay content.

The composition of the clay fraction (Table 36) is indicative of weathering changes. In comparison with the lowest horizons, titania increases by about 20 per cent, mainly in the two upper horizons; K_2O and Fe_2O_3 contents decrease in the upper three horizons. There are slight but steady increases in Al_2O_3 and decreases in SiO_2 content toward the surface, but these trends reverse in the surface horizon. These changes, except for the decrease in ferric iron, are indicative of weathering by desilication (hydrolysis by water containing carbon dioxide) in most of the profile, and of slight cheluviation in the surface horizon. FeO contents increase somewhat toward the surface, for reasons unknown. Citrate extraction did not lower the FeO contents. Therefore, the ferrous iron does not appear to be located in interlayers.

Norm mineral calculations

The standard epinorm mineral composition of the (sand + silt) fractions, calculated from chemical data obtained by difference from total fine earth and clay fractions after correction for organic matter, is listed in Table 37. The figures show an increase of norm quartz toward the surface; a slight decrease of rutile, possibly not significant; decreases in hematite, albite, tremolite and muscovite. The erratic figures for orthoclase may be an artefact of the norm calculation, due to the presence of small amounts of an Al-rich phase in the (sand + silt) fraction. If orthoclase is assumed constant at 7.2 per cent, norm muscovite figures range from about 8 per cent in the lowest four horizons to about 6 per cent in the surface horizon, and amounts of an Al-rich phase, perhaps a weathering skin on the weatherable minerals, are equivalent to about 1 (0.0-1.5) per cent Al_2O_3 . All these changes with depth may be due to weathering, differential removal

Table 37. Epinorm mineral composition (%) of the sand + silt fractions of the Biebosch Valkenburg profile.

Sample no. 76-	Q	Ru	Hm	Ab	Or	Tr	Ms	W	Ms ¹	Al_2O_3 ¹
159	77	0.75	0.4	5.7	5.9	0.6	7.6	1.5	5.7	0.5
160	78	0.74	0.7	5.7	5.4	0.8	8.3	0.4	5.7	0.7
161	76	0.77	0.5	6.0	7.2	0.8	6.8	0.7	6.8	0.0
162	72	0.80	1.1	6.1	5.4	1.4	10.6	1.0	8.0	0.7
163	72	0.77	1.3	6.2	4.5	1.7	12.4	1.2	8.5	1.0
164	72	0.78	1.2	6.5	3.9	2.0	12.5	1.0	7.8	1.2
165	72	0.78	1.4	6.4	3.0	2.1	13.3	1.0	7.3	1.5

1. Muscovite and an Al-rich phase under the assumption that orthoclase is constant at 7.2%.

Table 38. Goethite norm mineral composition (%) of the clay fractions of the Biebosch Valkenburg profile.

Sample no. 76-	Q	Ru	Go	Ab	K	I	S	W
159	3.8	1.08	11.6	1.8	14.0	22.6	37.6	3.7
160	3.4	1.07	11.9	2.0	16.3	22.1	36.3	2.8
161	4.3	1.00	12.7	1.8	13.5	23.7	36.8	3.1
162	5.6	0.94	13.3	1.9	9.3	25.3	37.7	3.3
163	5.6	0.93	13.5	1.9	6.9	25.9	39.0	3.2
164	7.1	0.92	13.6	1.8	7.4	26.2	36.2	3.5
165	7.9	0.90	13.2	1.9	6.2	26.8	36.2	3.7

Table 39. Goethite norm mineral composition (%) of the clay fractions of the Biebosch Valkenburg profile, recalculated on the basis of constant norm rutile (0.90%); variant with aluminium interlayer material.
A. assuming quartz constant (7.9%)
B. assuming kaolinite constant (6.2%)

Sample no. 76-	Go	Ab	I	S	W	A		B	
						K	Al(OH) ₃ ¹	Q	Al(OH) ₃ ¹
159	9.7	1.5	18.8	31.3	3.1	1.5	5.5	5.8	3.0
160	10.0	1.7	18.6	30.5	2.3	2.9	5.8	6.4	4.0
161	11.4	1.6	21.4	33.1	2.8	3.3	4.7	6.6	3.2
162	12.7	1.8	24.2	36.1	3.2	4.0	2.6	6.9	1.5
163	13.1	1.9	25.0	37.8	3.1	1.2	2.9	5.6	0.2
164	13.3	1.8	25.7	35.4	3.5	5.3	1.0	7.5	0.6
165	13.2	1.9	26.8	36.2	3.7	6.2	0.0	7.9	0.0

1. Al(OH)₃ represents Al interlayer material in 2:1 clay minerals.

of fine silt, or both.

The standard goethite norm mineral composition of the clay fractions (Table 38) indicates an increase in norm rutile (Ti minerals), a doubling of kaolinite contents, and decreases in norm quartz, goethite and illite toward the surface. Norm smectite and albite remain constant. This unlikely-looking combination of trends is probably due to the limitations of the standard goethite norm, which tends to hide aluminium interlayers in the form of excess norm kaolinite, with a corresponding shortage of norm quartz.

Recalculation of the norm on the basis of constant rutile contents, under the assumption that quartz remains proportional to rutile during weathering and with representation of Al interlayers in 2:1 type clay minerals by Al(OH)₃ (Table 39, A), leads to more reasonable results. About half of the decrease in 2:1 clay minerals is compensated by aluminium interlayer material; the other half comprises loss of mainly silica and some structural K and Mg. Calculated interlayer material amounts to 1-1.5 mol Al per kg smectite + illite in the upper three horizons. However, the strong decrease in kaolinite toward the surface now is unrealistic. Probably, the assumption that clay-sized quartz is completely unaffected by desilication is not justified. Recalculation on the assumption that kaolinite rather than quartz is not affected by weathering (Table 39 B) shows some loss of

quartz and somewhat lower contents of calculated Al-interlayer material: rising toward the surface up to 4 per cent in the AB horizon, and dropping back to about 3 per cent in the surface horizon. These amounts represent about 1 and 0.75 mol Al interlayer material per kg 2:1 type clay present.

These trends are compatible with moderate desilication throughout the profile, increasing toward the surface, superseded by slight cheluviation in the surface horizon only.

Clay mineralogy

X-ray diffractograms of the clay fractions were prepared after K saturation, Mg saturation with and without glycerol treatment, and after heating to temperatures between 100 and 600°C. The following summary interpretation is based on comparisons of peak heights between samples and between treatments.

The dominant clay mineral present in the profile is an interstratified vermiculite-smectite. Toward the surface this appears to contain gradually increasing amounts of aluminium-interlayer material, but the clay fraction of the Ah contains less interlayer material than the underlying horizon. Other minerals comprise moderate amounts of kaolinite, slightly increasing toward the surface; some illite and little smectite, both decreasing to about half in the surface horizons; little quartz, virtually constant with depth; traces of geogenic chlorite.

The clay mineral data thus support the hypotheses that this soil has been subject to moderate desilication throughout, with the strongest effects in the upper horizons, and that cheluviation has started to undo some of the resultant interlayering only in the surface horizon.

NUTH

FAO/Unesco Soil Units (FAO, 1974): Orthic Luvisol

USDA Soil Taxonomy (Soil Survey Staff, 1975): Typic Hapludalf

Examined and described 9 October 1972 by A.G. Jongmans and R. Miedema.

The field data, below, have been summarized from their description.

Macromorphological descriptions of individual soil horizons and micromorphological data are given in Slager et al. (1978).

The site

Location near Nuth, Limburg, Netherlands. Topographic map sheet 60C, scale 1:25 000, ed. 1968, coordinates 326.57 km N, 188.67 km E. About 50°55.75' N, 5°52.02' E. Elevation 117.5 metres above mean sea level.

Landform and slope: nearly level plateau surface, slope 0-2%.

Land use: intensive arable cultivation (sugarbeets) in adjacent land; profile taken from side of deep excavation.

Climate: humid temperate (Köppen Cfb), the same data as for the Biebosch (Valkenburg) profile in this chapter.

General information on the soil

Parent material: deep loess deposit, 4.8 m over sandy and gravelly Meuse river terrace material.

Well drained. Moist throughout. Groundwater not observed, presumably very deep.

No stones, no gravel, no rock outcrops. No evidence of accelerated erosion. No salt or sodicity.

Human influence: ploughing, presence of charcoal and brick fragments to 25 cm.

Brief description of the profile

Deep, well drained, yellowish brown to yellowish red silt loam, porous throughout and with common roots to about 0.4 m.

Soil horizons and micromorphology are described in Slager et al. (1978).

General physical data

The grain-size distribution (Table 40), recalculated on a clay-free basis (Fig. 23), is reasonably constant throughout the profile. The sedimentary break indicated at 1.9 m depth by Slager et al. (1978) on the basis of macro- and microstructure is not visible in this figure, or in a graph (not shown) of cumulative percentages transformed to a normal (Gauss) distribution against log grain size. A sedimentary break at about 2.2 m is suggested by norm mineral calculations, as discussed under Profile balance, below.

Clay percentages are maximal in the Bt3 horizon. The volume percentages oriented clay obtained by counting (800 data points per thin section over a 15-cm depth range) show a similar trend with depth as the total clay contents (Fig. 23), although there appears to be more oriented clay (vol %) than the difference in clay content (weight %) between B and C horizons.

Hydraulic conductivities (Table 41) range between 5 and $0.1 \times 10^{-9} \text{ m}^2 \cdot \text{Pa}^{-1} \cdot \text{s}^{-1}$; the Bt2 and Bt3 horizons have the lowest conductivity, but there is no evidence of any impeded drainage. Bulk densities range from $1.4 \times 10^3 \text{ kg/m}^3$ in the Ap to 1.5-1.6 in the lower part of the Bt horizon, and are about $1.5 \times 10^3 \text{ kg/m}^3$ in the C horizons.

Table 40. Grain-size distribution (%) of the Nuth profile.

Sample no. 73-	Depth (cm)	Horizon	2000-100 μm	100-50 μm	50-32 μm	32-16 μm	16-8 μm	8-2 μm	<2 μm
102	0- 25	Ap	4	6	34	32	9	5	11
103	25- 41	Bt1	1	6	31	32	10	5	15
104	41- 80	Bt2	0	4	30	31	11	4	20
105	80-130	Bt3	0	6	27	29	10	6	21
106	130-180	Bt3	0	7	28	28	10	6	20
107	180-223	C1	0	5	28	30	11	7	19
108	223-270	C2	0	6	30	30	13	5	16

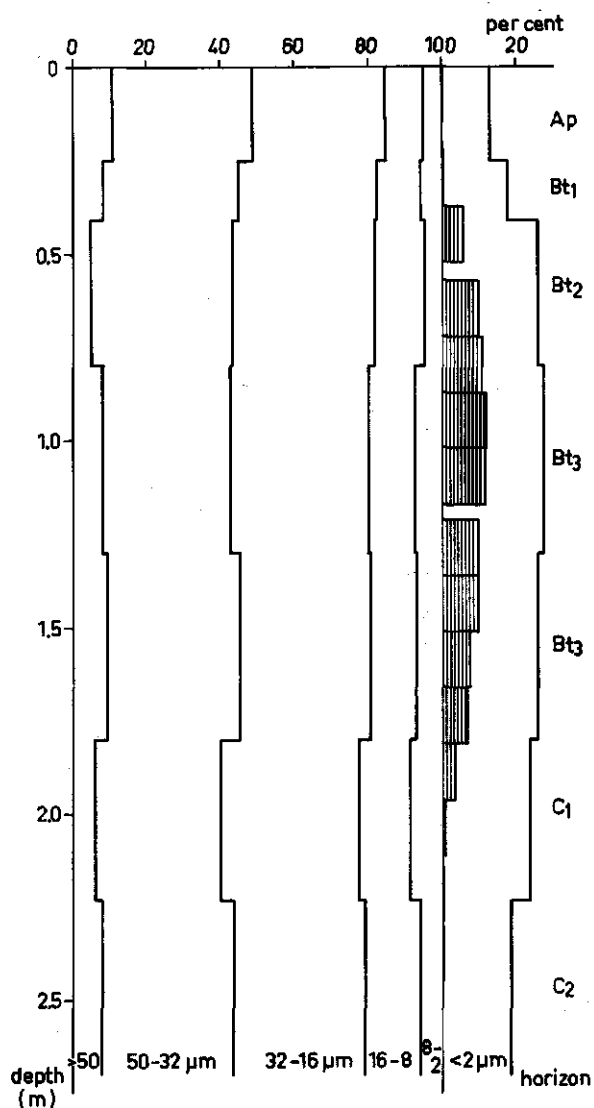


Fig. 23. Grain-size distribution of the Nuth profile, recalculated to (sand + silt) fractions total 100 per cent. Vertical hatching: clay illuviation features in thin sections, volume per cent, similarly recalculated.

General chemical data

Organic matter contents (Table 42) are low throughout the profile. Free iron contents are low but maximal between the calcium carbonate boundary (2.2 m) and about 0.8 m depth. pH (water) ranges between about 5.5 and 6 to 2.2 m, and rises above 7 in the calcareous substratum; pH (CaCl_2) ranges between 5 and 5.7, and is 6.5 in the calcareous

Table 41. Hydraulic conductivity and bulk density of the Nuth profile.

Depth (m)	Hydraulic conductivity ¹	Bulk density ²
	($10^{-9} \text{ m}^2 \text{ Pa}^{-1} \text{ s}^{-1}$)	(10^3 kg/m^3)
0.1	.	1.40
0.3	0.4	1.44
0.5	4.9	1.44
0.7	3.5	1.50
0.9	0.5	1.60
1.1	0.1	1.54
1.3	0.2	1.53
1.5	0.1	1.57
1.7	0.1	1.60
1.9	0.2	1.54
2.1	0.3	1.39
2.3	0.3	1.51
2.5	0.2	1.48

1. The traditional metre per day corresponds to $1.18 \times 10^{-9} \text{ m}^2 \text{ Pa}^{-1} \text{ s}^{-1}$.
2. Duplicate determinations, standard deviation of means 0.023.

Table 42. General chemical data of the Nuth profile.

Sample no. 73-	Organic C (%)	Free Fe ₂ O ₃ (%)	CaCO ₃ (%)	pH		exchangeable equivalents				
				water	CaCl ₂ (0.01 mol/l)	Ca	Mg	Na	K	CEC
102	1.31	1.03	0.0	5.9	5.6	61	8	1	3	65
103	0.61	1.24	0.0	5.3	4.8	63	10	1	4	87
104	0.24	1.84	0.0	5.6	5.3	92	14	1	2	115
105	0.26	2.00	0.0	6.0	5.6	99	13	2	1	115
106	0.29	1.91	0.0	6.1	5.7	103	13	2	3	130
107	0.39	1.90	0.0	6.2	5.7	103	13	2	3	144
108	0.46	0.96	17.1	7.2	6.5	97	9	1	1	101

material. Exchangeable cations are dominantly Ca and some Mg; exchange acidity is virtually zero.

Total chemical composition

The chemical compositions of the total soil (= fine earth) and of the clay fractions of the Nuth profile are listed in Tables 43 and 44. Differences of total composition with depth appear to be minor, and may be due to the different clay contents (Table 43, last column). The composition of the clay fractions, too, changes little with depth, except for a 10 per cent relative increase in TiO₂ content in the upper 0.4 m. FeO contents decrease slightly toward the surface.

Table 43. Total chemical composition (%) of the Nuth profile.

Sample no. 73-	SiO ₂	Al ₂ O ₃	Fe ₂ O ₃ ¹	MgO	CaO	Na ₂ O	K ₂ O	TiO ₂	Ignition loss	clay
102	81.6	7.4	2.5	0.4	0.6	0.9	1.85	0.75	3.6	11.1
103	81.5	8.1	2.9	0.4	0.5	0.9	1.99	0.77	2.7	14.8
104	77.5	9.4	3.9	0.6	0.6	0.9	2.17	0.74	2.9	20.3
105	77.8	9.5	4.1	0.7	0.6	0.9	2.15	0.75	2.8	21.3
106	77.9	9.5	4.0	0.7	0.7	1.0	2.13	0.74	2.6	20.4
107	76.5	9.9	4.0	0.8	0.8 ₂	1.0	2.32	0.74	2.6 ₂	18.9
108	65.7	7.6	3.1	1.0	8.7 ₂	0.9	1.76	0.59	9.4 ₂	15.7

1. Total iron as Fe₂O₃.2. Including CaO and CO₂, respectively, from CaCO₃.

Table 44. Total chemical composition (%) of clay fractions of the Nuth profile.

Sample no. 73-	SiO ₂	Al ₂ O ₃	Fe ₂ O ₃	FeO	MgO	CaO	Na ₂ O	K ₂ O	TiO ₂	Ignition loss
102	48.1	21.7	11.6	0.27	1.7	0.1	0.2	3.06	0.95	9.4
103	48.4	22.0	11.8	0.21	1.8	0.1	0.3	3.00	0.96	9.3
104	48.6	21.7	11.8	0.21	1.4	0.1	0.2	2.99	0.86	9.1
105	49.3	20.8	12.2	0.29	1.5	0.1	0.2	2.95	0.85	8.8
106	50.6	20.6	11.9	0.22	1.4	0.1	0.2	3.07	0.85	8.6
107	49.7	20.5	11.8	0.29	1.8	0.2	0.3	3.30	0.87	8.5
108	50.5	19.4	11.7	0.44	2.2	0.2	0.3	3.37	0.81	8.8

Table 45. Goethite norm mineral composition (%) of the clay fractions of the Nuth profile.

Sample no. 73-	Q	Ru	Go	Ab	I	S	K	W
102	8	0.95	13	2	26	33	11	3
103	7	0.96	13	2	25	33	12	3
104	11	0.86	13	2	25	27	15	3
105	12	0.85	14	2	25	29	12	3
106	14	0.85	14	2	26	28	11	3
107	10	0.87	13	2	28	35	5	3
108	11	0.81	13	2	28	38	0	4

Norm mineral calculations

Recalculation of the chemical data to a goethite norm mineral composition of the clay fractions (Table 45) results in about 32% norm smectite, 26% illite, 13% goethite, about 10% each kaolinite and quartz, 2% albite and 0.9% norm rutile (titania). Titania increases and norm quartz tends to decrease toward the surface, norm smectite contents show a minimum and kaolinite contents a maximum in the B2 and B3 horizons.

The epinorm mineral composition of the sand + silt fractions (Table 46) does not show great differences with depth: about 70% quartz, 10% muscovite, 9% albite, 4% ortho-

Table 46. Epinorm mineral composition (%) of the sand + silt fractions of the Nuth profile.

Sample no. 73-	Q	Ru	Hm	Ab	Or	Ms	W	Trem	Ant ²
102	75	0.74	1	9	4	9	0	1	0
103	74	0.75	1	9	5	8	0	1	0
104	70	0.71	2	9	5	9	1	2	0
105	71	0.72	2	9	5	10	1	2	0
106	70	0.71	2	10	4	11	0	2	0
107	66	0.71	2	10	4	12	0	2	0
108 ²	70	0.69	1	11	4	10	1	0	2

1. Chemical composition calculated by difference from clay percentage and compositions of total soil and clay fractions.
2. Lowest horizon recalculated without CaCO₃. The antigorite instead of tremolite in the lowest horizon is an artefact of the norm calculation, due to the arbitrary assumption that the CaCO₃ in this horizon is pure rather than with some Mg substitution (Slager, pers. commun. 1978).

Table 47. Norm mineral compositions of sand + silt and clay fractions of the Nuth profile, recalculated on the basis of constant TiO₂ content in the (sand + silt) fractions¹.

Sample no. 73-	Sand + silt fractions, epinorm							Clay fraction, goethite norm								
	Q	Hm	Ab	Or	Ms	Trem	W	Q	Ru	Co	Ab	I	S	K	W	total
102	58	1.0	6.9	3.4	6.6	0.7	0.0	0.8	0.10	1.2	0.2	2.5	3.2	1.1	0.3	9.8
103	57	0.9	7.0	3.9	6.3	0.5	0.0	1.0	0.13	1.7	0.3	3.4	4.5	1.6	0.5	13.4
104	55	1.3	7.0	4.0	7.2	1.2	0.7	2.1	0.17	2.7	0.4	5.0	5.4	2.9	0.6	20.0
105	57	1.3	7.4	3.6	7.9	1.3	0.5	2.5	0.18	3.0	0.4	5.4	6.3	2.6	0.7	21.7
106	56	1.3	8.1	3.0	8.5	1.7	0.4	2.8	0.17	2.8	0.4	5.4	5.8	2.3	0.6	20.8
107	54	1.5	8.2	2.9	10.1	1.7	0.5	1.8	0.16	2.5	0.4	5.3	6.6	0.9	0.6	18.9
108	60	1.3	9.5	3.2	8.5	1.9 ²	0.0	2.1	0.16	2.7	0.5	5.6	7.5	0.0	0.8	19.8

1. Fine earth in the C1 horizon (sample 73-107) total 100%.
2. Antigorite (see Footnote 2 of Table 46).

Table 48. Balance calculation for the Nuth profile.

Sample no. 73-	Depth (cm)	Estimated bulk density (10 ³ kg/m ³)	Weight of horizon (kg/m ²)	Original weight of horizon ¹ (kg/m ²)	Loss(-) or gain(+)	
					total (kg/m ²)	clay (kg/m ²)
102	0- 25	1.40	3.50	3.98	-0.48	-0.36
103	25- 41	1.44	2.30	2.54	-0.24	-0.16
104	41- 80	1.47	5.73	5.63	+0.10	+0.06
105	80-130	1.56	7.80	7.67	+0.13	+0.21
106	130-180	1.57	7.85	7.71	+0.14	+0.15
107	180-223	1.47	6.32	6.32	0	0

1. Assuming constant TiO₂ in sand + silt fraction, as in Table 47.

clase, 2% hematite, 2% tremolite. Rutile and quartz tend to increase toward the surface; hematite, muscovite and tremolite decrease slightly.

Recalculation of the norm mineral compositions to a constant rutile content of the sand + silt fraction (0.58% of fine earth in the C1 horizon) results in somewhat clearer trends (Table 47). Norm quartz and orthoclase in the sand + silt fractions remain roughly constant, contents of all other sand + silt minerals decrease by about a quarter to two thirds toward the surface. Compared with the C1 horizon, the clay fraction increases by about one seventh (3%) to the B horizon and decreases by half (10%) toward the surface.

Profile balance

A gross balance was calculated for the Nuth profile (Table 48) on the basis of constant TiO_2 in the sand + silt fractions. The C1 horizon was used as a standard, because the apparent loss of about 4% mineral material from the C2 to the C1 horizon (apart from 17% CaCO_3) may not be due to weathering. The norm mineral compositions recalculated on the same basis (Table 47) show that this difference is essentially due to norm quartz in the sand + silt fractions; this, combined with the reverse trend in muscovite content, indicates a probable sedimentary difference between the C2 and C1 horizons.

The gross balance with the C1 as a standard horizon is negative by about 0.35 kg/m^2 , comprising a loss of 0.72 kg/m^2 from the upper two horizons and a gain of 0.37 kg/m^2 in the horizons between 0.4 and 1.8 m depth. The latter amounts to 2 relative per cent, about the lower limit of significance for this calculation, and equivalent to a 0.01% difference in TiO_2 content measured in the fine earth fraction of sample 107. Loss and gain of the clay fraction (-0.52 and $+0.42 \text{ kg/m}^2$) are roughly in balance; most of the loss from the profile should be ascribed to the (sand + silt) fractions.

Clay mineralogy

X-ray diffractograms were prepared of oriented aggregates on ceramic tiles after Mg saturation without and with glycerol solvation and after K saturation without and with heating to 400 and 600°C. Semiquantitative interpretation on the basis of peak height ratios resulted in the following estimates.

Kaolinite and illite are present in roughly equal and major proportions throughout the profile. Illite contents remain constant, kaolinite increases slightly toward the surface. There is a small and constant percentage of quartz. The amount of aluminium-interlayered material is about half that of illite; some vermiculite is included in this estimate. The proportion of smectite to illite decreases from roughly equal in the lowest horizons to about half or less in the surface horizon.

Norm illite percentages and mineralogical estimates are in reasonable agreement; norm smectite percentages are similar to estimates for Al-interlayered material plus smectite. Agreement for kaolinite is very poor. Possibly, this is overestimated in the diffractograms because of a high degree of stacking order.

Calculation from the goethite norm composition would result in a CEC of about 0.35

mol/kg clay, and calculation from the estimates on the basis of X-ray diffractograms, about 0.35 mol/kg clay in lower horizons and 0.25 in the surface horizon. On the basis of CEC (soil) or sum of exchangeable cations and organic C and clay percentages, cation exchange capacities of the clay fractions were estimated to range from about 0.6 mol/kg in lower horizons to about 0.5 in the upper horizons.

A reason for this discrepancy is possibly the cation exchange capacity of minerals in the coarser fractions, but more likely our underestimate of the amounts of vermiculite present. The standard goethite norm calculation cannot take this mineral into account; the presence of randomly interstratified illite-vermiculite or vermiculite-smectite would not contribute to clear X-ray reflections at 1.0 or 1.4 nm, which were used for estimation. The aluminium interlayers in the clay apparently interfere with conventional estimation of vermiculite contents by the method of Alexiades and Jackson (1965) : K fixation of the clay fractions in the B horizons amounts to about 0.02 to 0.05 mol/kg, increasing from the Bt1 to the Bt3.

Multiple soil-forming processes in single profiles

THE PROCESSES LISTED BY SOIL PROFILE

Several soil profiles were studied with a view to elucidate the ferrolysis process and its effects. Results for soils in Bangladesh and Thailand were reported in separate papers (reprints in a separate volume); data on several soils in Western Europe are given in the previous chapter.

Besides ferrolysis, several other processes were identified by their effects on the soils (Table 49). In all six of the surface-water gley soils studied there is evidence of at least some clay translocation; one (Chhiata, Bangladesh) has traces of a former Vertisol stage. The profiles show various degrees of activity of soil fauna, but none have strong biotic perforation.

In two profiles (Solling and Eynatten), cheluviation has succeeded ferrolysis in the upper horizons; in the next section, the features illustrating this transition are discussed and compared with work by the Coninck on similar soils.

Processes other than cheluviation have also left traces in the upper horizons. Superficial erosion (natural or man-made) of fractions up to coarse silt or fine sand size was recognized in two profiles. The forest vegetation on one soil apparently has been effective in cycling nutrient cations to the upper horizons. Three other processes were identified, each in one profile: accumulation of soluble acid aluminium and iron salts, calcium carbonate addition and leaching by strong acid (the last two as a result of human activities).

The three well-drained soils, in materials comparable with those of nearby surface-water gley soils, show evidence of desilication but not of ferrolysis. Clay translocation and perforation were important in two of these; in one, the surface horizons are affected by erosion and slight cheluviation. Cheluviation of the surface horizons is the only important process identified besides desilication in the third well-drained soil.

Not all processes acting on a soil necessarily leave clear traces. For example, leaching by strong acid, which takes place over large parts of Western Europe, has left traces in the proportions of exchangeable cations in the Hardthäuser Wald profile but not in the Eynatten profile. In the latter soil, only the composition of the soil solution at different depths indicates that leaching by strong acid has taken place.

In general, the effects of a current or past process can only be identified if they exceed the natural variations in the data, if another process has not produced more comprehensive, though similar, changes and if different processes have not obliterated the effects.

Table 49. Main soil-forming processes recognized in different soil profiles.

Processes	Profiles ¹							
	Chhiata	Roi Et	Latina	Hardthäuser Wald	Eynatten	Solling	Solling Brown Earth	Biebosch Valkenburg
								Nuth
Mainly in surface horizons								
calcium carbonate addition			+					
nutrient cycling				+				
erosion	+			+				+
acid salt accumulation		+ ²						
leaching by strong acid				+	+ ³			
cheluviation					+	+	+	
In major part of profile								
perforation by soil fauna		+					+	+
ferrolysis	+	+	+	+	+	+		
desilication							+	+
clay translocation	+ ⁴	+ ⁵	+	+	+	+		+
churning ⁶	+							

1. Chhiata and Roi Et described in Brinkman, 1977 a and b, respectively; other profiles in previous chapter (Solling Brown Earth summarized under the Solling profile).

2. Related profiles (Brinkman & Dieleman, 1977).

3. Only recognized by the composition of the soil solution.

4. Indirect evidence.

5. Minor amounts of translocated clay only.

6. Slickensiding and gilgai formation as shown by features in deep horizons.

EXAMPLES OF BOTH CHELUVIATION AND FERROLYSIS IN SINGLE PROFILES

Evidence for cheluviation as well as ferrolysis in single soil profiles was found in a 'strongly podzolic pseudogley soil' in Solling, near Göttingen, Federal Republic of Germany, and in a surface-water gley soil near Eynatten in N.E. Belgium, just south of Aachen. Both profiles are described more extensively in the previous chapter.

The Solling profile is bisequal. The upper sequum comprises an eluvial (podzolic) Ah horizon and an eluvial horizon described as transitional between that of a podzol and that of a surface-water gley soil. The lower is a surface-water gley sequum consisting of an eluvial (Eg) and an illuvial (Bg) horizon. The clay fractions throughout the profile contain illite, kaolinite and a little quartz. In addition, the Bg horizon contains

some aluminium-interlayered material, probably vermiculite, and interstratified illite-vermiculite. In the eluvial horizon of the surface-water gley sequum, there is a strong increase in aluminium-interlayered material compared with the Bg horizon.

In the transitional eluvial horizon and in the podzolic surface horizon, all mineralogical evidence for aluminium interlayering has disappeared again. The clay fraction of the podzolic Ah horizon contains smectite, some regularly interstratified smectite-illite and a little vermiculite, and the transitional horizon some vermiculite and a little smectite.

The strong aluminium interlayering combined with the maximum in ferrous iron content of the clay fraction of the Eg horizon (sample 74-10 in Table 28) is in accordance with the hypothesis that ferrolysis has formed this horizon. The removal of the interlayers with the ferrous iron trapped in them combined with the formation of swelling clays in the transitional and podzolic eluvial horizons indicate that the clay mineralogy in these horizons is determined by cheluviation.

Analysis of the clay fractions after citrate extraction (Table 28) has shown considerable increases in cation exchange capacity in the Eg and lower horizons, confirming interlayering. A decrease in ferrous iron content after citrate extraction was found only in the Eg horizon, supporting the indications of ferrolysis.

In contrast, the cation exchange capacity of the clay fraction from the podzolic surface horizon decreases after citrate treatment, with an insignificant change in ferrous iron content. These trends confirm that cheluviation is the latest dominant process in this horizon. By the same criteria, the transitional horizon shows interlayering but no trapped ferrous iron. Presumably, cheluviation has succeeded ferrolysis in this horizon, but its effects are less pronounced than in the surface horizon.

The Eynatten profile (Fig. 10) is also bisequal and comprises a minipodzol over a surface-water gley sequum, abruptly overlying Carboniferous clay at 1.6 m depth. The mineral part of the minipodzol, about 8 cm thick, consists of eluvial Ah and E horizons underlain by a very thin (2 mm) discontinuous sesquioxide and organic matter accumulation band. The lower sequum comprises eluvial Eg and EBg horizons, both with strong evidence of periodic reduction, and a thick Btg horizon, with tongues of bleached material extending to the underlying clay.

The clay fractions from different depths in the Btg horizon contain little quartz, moderate amounts of kaolinite, illite and smectite, and little vermiculite or smectite with some aluminium interlayering. Smectite is absent in the EBg and the overlying eluvial horizons; illite reflections are very much smaller in the eluvial horizons than in the lower part of the profile. The amount and stability of aluminium-interlayered material abruptly increase to a maximum in the EBg, decrease again in the Eg and podzolic E horizons, and are essentially zero in the Ah horizon. The latter contains considerable amounts of randomly interstratified illite-vermiculite, possibly with slight aluminium interlayering.

These data suggest that the strongest effects of ferrolysis occur in the EBg, which is now an eluvial horizon but was formerly the upper part of the thick textural B horizon. The decrease in interlayering observed particularly in the Ah horizon indicates cheluvi-

ation in that horizon.

Cation exchange capacities and ferrous iron contents of clay fractions before and after citrate extraction (Table 21) confirm these interpretations. The CEC of the clay fractions is lowest in the EBg and highest in the Ah horizon; citrate extraction considerably increases the CEC in the EBg and Btg horizons, whereas the increase is progressively less in the Eg and E and essentially zero in the Ah horizon. Maximal ferrous iron contents occur in the Eg, EBg and the uppermost part of the Btg horizon. Citrate extraction removes a significant percentage of the ferrous iron from the latter two horizons. The presence of trapped ferrous iron in the upper part of the Btg horizon suggests that ferrolysis has invaded horizons that were previously illuvial. The virtual absence of trapped ferrous iron in the Eg, as well as the evidence for a decrease in aluminium interlayering in that horizon, indicate that cheluviation, in its turn, has invaded this horizon which was previously influenced by ferrolysis.

In an extensive study mainly on similar bisequal, seasonally wet soils, de Coninck (1967) distinguished three stages of development. After a first stage comprising clay formation and translocation in the stratified sediment, de Coninck recognized a second stage, which he labelled homogenization. Under this stage he included bleaching of the homogenized zone with segregation of iron oxides, secondary migration of bleached clay, and destruction in situ of argillans and plasma, all under conditions of seasonal wetness. In extreme cases, a planosol is formed. The third stage is the formation of a podzol sequum in the upper part of the bleached, homogenized zone. The eluvial horizons of the two latter stages are distinguished as A'2 and A2, respectively. Compared with the parent material, clay minerals in this bleached zone (A'2 and secondary Bt) are more aluminium-interlayered; aluminium interlayering in the A2 of the podzol sequum tends to be less than in the A'2 and Bt horizons. The mean cation exchange capacities of the clay fractions from the A'2 and Bt horizons of the lower sequum range between about 0.5 and 0.7 mol/kg with occasional figures much higher as well as lower; the cation exchange capacities of clay fractions from A2 horizons of the podzol sequum (few data) are about twice as high. Ferrous iron contents were not determined.

The development under seasonally wet conditions as described by de Coninck under the second stage corresponds to the ferrolysis process; the third stage corresponds to the process of cheluviation. Although the driving force and the mechanism of the second stage are not identified, imperfect drainage is recognized as an accelerating factor, and autolysis of expanded illite with subsequent Al-interlayering are described as important component processes. In the third stage, the central importance of chelating organic acids in the removal of aluminium is clearly identified.

Processes taking place in surface-water gley soils, podzols and podzolic soils, and criteria for distinguishing their effects

There is some general agreement in the literature of soil science about what constitutes a podzol. This agreement is not universal; neither does it apply to several cases studied in detail. About the nature of podzolic soils and surface-water gley soils the literature is less clear. Still less agreement exists about the processes giving rise to these different soils. The use of the same basic term, both for the soils themselves and for the main process postulated to explain their nature, has contributed to the persistent confusion about the genesis of podzols, podzolic and podzolized soils.

This chapter starts with some descriptive and genetic terms for podzols and surface-water gley soils. Two main processes that may take place in them, cheluviation and ferrolysis, are described in tabular form; their respective consequences for the clay mineralogy and chemistry of the eluvial horizons are discussed. Criteria are proposed to distinguish the effects of ferrolysis from those of clay translocation and desilication and to discriminate between cheluviation and ferrolysis.

EXISTING SOIL TERMINOLOGY, CLASSIFICATION AND GENETIC CONCEPTS

Because the science of soils and much of its terminology originated in Russia and because there is an ongoing discussion in Russian literature on genetic processes in seasonally wet soils, some Russian concepts will be dealt with before touching on work in other countries.

The term podzolic horizon in the Russian literature is used for any bleached eluvial surface or subsurface horizon, except when the underlying material contains appreciable exchangeable sodium. Then the bleached horizon is designated as a solodic horizon. Soils are identified as podzol, sod-podzolic¹² or podzolized if they contain a podzolic horizon, and as solod or solodized if they contain a solodic horizon. No clearly defined distinction is made between podzolic and solodic horizons by themselves; they are distinguished by their underlying horizons.

Originally, these terms appear to have had a morphological meaning only. Later, however, different authors used podzolization and solodization as terms for postulated soil-forming processes. At that time, confusion set in, since it was never certain that all podzolic horizons were formed by the same process or that solodic horizons were not formed by the same or a similar process as certain podzolic horizons.

Liverovskiy et al. (1973) recognized the danger of this confusion and recommended

12. sod (Russ. dern) denotes a dark coloured mineral surface horizon with well humified organic matter normally occurring under grass but not under forest.

that terminology for processes be strictly separated from soil and horizon nomenclature. Process and soil terms based on the same roots have been and still are in general use, however. Probably as a result of this confusion in terminology, there is an ongoing debate in the Russian literature on whether or not podzolization necessarily comprises seasonal waterlogging.

The term *podzol* (ashy soil; Russian *zola* means ash) in farmers' usage denotes a soil with a bleached grey or white horizon (Glinka, 1914). The grey or white material is almost always found under a darker surface horizon such as an O, Ah or Ap; this observation explains the prefix *pod* (under) according to Ponomareva (1964, p.4). Already in the description of podzol soils by Georgiewski in 1888 (quoted by Glinka, 1914) a clear distinction is made between the sandy podzols and the clayey and silty, loessic podzols. The eluvial horizon of the sandy podzol is described as snowy white or ashy white, fine quartz sand; that of the clayey podzol as an almost white, floury powder with brown concretions. The B horizon of the sandy podzol is a brown or black, partly hard, partly coherent mass; that of the clayey podzol is a dense, clayey mass, mottled whitish, reddish and yellowish, with many dark and brown concretions. The silty podzol is similar to the clayey one, but with few concretions in the eluvial horizon, and brown and whitish mottles and few concretions in the B horizon.

Glinka's wide definition of a podzol, comprising the sandy as well as the clayey kinds, is based on the presence of a clear and completely developed whitish horizon without or with mottles and concretions, and with or without an underlying humus illuvial horizon. Podzolic soils are defined as soils with whitish flecks and streaks in an A horizon but lacking a clear and complete whitish horizon.

The two kinds of eluvial horizons may also occur in a single soil profile, but in different sequa. As an example, a summary from a description by Glinka (1914, p. 74-75): an eluvial horizon without mottles or concretions overlies a more coherent, brown, not dense horizon (a humus illuvial horizon, R.B.), and below this sequum a second eluvial horizon with brown mottles overlies a thin (1 dm) dense, slightly green horizon over a slightly green horizon with many yellowish red mottles of ferric oxides.

Under the single term *ortstein*, Glinka included the hard humus illuvial material of the sandy podzols, containing more than 10% humus, about 0.2 to 4% Al_2O_3 and Fe_2O_3 and very little MnO, as well as the sesquioxide-cemented nodules of the clayey podzols with, e.g., 10 to 15 per cent each of Al_2O_3 , Fe_2O_3 and MnO and at the most a few per cent humus.

In the discussion on soil genesis, Glinka dealt with the sandy and clayey podzols as a whole, and ascribed the evident loss of elements from the eluvial horizons mainly to dissolution and removal by organic acids. The formation of *ortstein* concretions or continuous horizons, as opposed to the formation of illuvial horizons that are not hard, was explained by periodic reduction of iron and manganese to mobile forms. The difference between *ortstein* dominated by humus, i.e., in the sandy podzols, and the *ortstein* with low humus contents occurring in the clayey podzols was ascribed to the different iron contents of the soils.

Gerasimov (1959) used the term *gleyey pseudopodzols*, indicating his belief that the seasonally wet soils which he dealt with were not 'real' podzols.

The similarity of Russian sod-podzolic soils and grey forest soils on the one hand and west European soils lessivés on the other in hydrology, morphology, grain-size distribution and chemical characteristics, was demonstrated by Kundler (1959). These soils are characterized by a periodically wet and reduced pale brown (10YR 6/3) eluvial horizon containing fine very dark brown (schwarzbraune) concretions, with weak platy structure, medium and fine pores and some earthworm tunnels. This horizon overlies a mottled transitional horizon containing white powder on part of the blocky ped faces, over a very firm, blocky to prismatic B horizon containing much more clay than the upper horizons.

Kornblum & Zimovets (1961) recognized 'bleached meadow soils' or 'variable-gleyey eluvial soils', the equivalent of the Chinese *beidzhan-tu*, soils as white as milk, in the Amur region. They considered the eluvial processes occurring in these soils to be different from podzolization and solodization, and to comprise: a) the differential removal of clay minerals under the protection of humic substances; b) the removal of the decomposition products of minerals and 'ash elements' in the ionic or colloidal form; c) the segregation of iron and manganese concretions within the whitish horizon, possibly with a certain addition of these elements from the outside and, correspondingly, d) profound changes in the proportions of adsorbed cations, viz. loss of Ca and Mg, stability or accumulation of Na, and the appearance of large quantities of exchangeable Al.

Rode (1964) thought that a pseudogley profile described and analysed by Schuylenborgh (1962, 1963, profile XI) does not differ noticeably from ordinary sod-podzolic soils in the distribution of clay, silica and sesquioxides over the soil horizons.

In defense of the concept that both sandy and clayey podzols would result from weathering by organic acids, Ponomareva (1964) proposed the theory that the soil solution leaching through clayey podzols passes through pores of the order of 100 to 10 nm; that passage through these capillaries depolymerizes the fulvic acids to crenic acids of very low molecular weight, which remain in solution even after saturation with aluminium or iron; and that the acids saturated with aluminium and iron are thus removed to the ground water instead of being precipitated in an illuvial horizon as in sandy podzols. This theory fails to take into account that virtually all the water draining through a clayey soil passes through macropores, i.e. biopores or cracks, rather than through micropores in the soil mass. Less than 40 mm of water per year can move by gravity through pores of 100 nm diameter even at 40% porosity and under the unrealistic assumption that all pores would be straight tubes with uncharged walls.

Zaydelman (1965) argued for inclusion of the pseudopodzolic or pseudogley soils with the hydromorphic sod-podzolic soils, on the basis of his belief that partial return of iron and aluminium compounds by capillarity toward the eluvial horizon would explain the differences between their profile characteristics and those of podzolic soils without hydromorphic characteristics.

According to Kanivets (1975), the main source of exchangeable aluminium in 'acid gleyed soils' is the breakdown of Fe and Mn hydroxides by reduction, with release of the Al fixed in them, rather than breakdown of aluminosilicates. This conclusion was based on laboratory experiments with hydrogen sulphide as the reducing agent on concretions and samples without concretions. The origin of the aluminium in the concretions was not discussed.

Zonn (1973) briefly described three processes, formerly taken together under podzolization: podzolization *sensu stricto*, i.e. cheluviation; lessivage or clay translocation; pseudopodzolization, involving reduction and leaching of iron compounds and clay translocation.

Zonn et al. (1975) convincingly distinguished pseudopodzolic soils of the Soviet Far East from podzolic soils using data on iron forms and listed the characteristic trends in ferrous iron contents of soil and clay fractions. Similar FeO determinations and related data seem not to be available for sod-podzolic soils of the European USSR.

The subtropical podzols of western Georgia, described and analysed by Zyrin et al. (1976), also fit in with the descriptions of Glinka's clayey podzols and with the characteristics and analyses of western European pseudogley soils rather than with Glinka's sandy podzols, or podzols *sensu stricto*.

In the United States, surface-water gley soils with strong texture differentiation were first included under the claypan soils, later under the Planosols. Brown et al. (1933) indicated that seasonal reduction and lateral removal of dissolved material has played a part in the strongly developed claypan soils. They used the term podzolized for whitish material that has lost clay and iron, but suggested that there is a definite distinction between these soils and the podzols of the cold and humid areas. In other parts of the paper, the authors referred to fractionation of the colloids, avoiding the term podzolization, and in conclusion mentioned the pseudopodzolic character of a claypan soil profile.

In the older U.S. soil classification (Baldwin et al., 1938), Planosols denote soils in generally nearly level locations with dense, slowly or very slowly permeable, clayey B horizons overlain by a generally pale eluvial horizon with much less clay. Most of these are acid and imperfectly drained, with a perched water-table after periods of heavy rainfall. This concept, representing a strongly expressed surface-water gley soil, has proved useful in other parts of the world, and planosols have been recognized and mapped in southern Europe and parts of Africa, for example. The term, with appropriate definition, now appears in the Legend of the FAO-Unesco Soil map of the World (FAO, 1974). In this Legend, surface-water gley soils with less extreme texture differentiation are classed among the Dystric Gleysols and the Gleyic Acrisols.

In the current U.S. Soil Taxonomy (Soil Survey Staff, 1975), the Planosol designation has disappeared, the soils being scattered over various Great Groups. The move away from the planosol concept seems to have been made at least partly because seasonal wetness and low subsoil permeability were considered less important than clay illuviation features, base saturation and thermal regime.

Several characteristics of the surface-water gley soils appear at different levels in the Soil Taxonomy. Periodic wetness is indicated at Suborder level (e.g., Aqualfs) if it is expressed by defined colours, mottling or nodules. A clearly expressed, pale-coloured eluvial horizon (within a defined range of colours) or clear tonguing of the eluvial into the underlying horizon are identified at Great Group level (e.g., Albaqualfs or Glossaqualfs, respectively). A dense, slowly permeable subsoil horizon can be traced only indirectly, by the characteristics mentioned above or by a high exchangeable sodium percentage, or not at all.

In Britain, large areas of seasonally wet, acid soils, part on medium-textured material, part on heavy clays and shales, have been identified as Stagnogley soils on the Soil map of England and Wales (Avery et al., 1975). Although all of these are subject to alternating wet and dry conditions, there are differences in the extent of soil formation and in the kinds of processes that have operated in them. Processes recognized include solution and redeposition of carbonates, pyrite oxidation, apparent accumulation of clay attributable to weathering of silt-sized or sand-sized material, clay transformation causing higher proportions of expansible and/or chloritized layers as well as clay translocation, obscured in part by turbation (shrink-swell) effects (Avery, pers. commun. 1978).

Surface-water gley soils in, for example, the Netherlands are intrazonal soils, formed under the influence of level topography and low permeability of parent material or substratum: the latter factors peculiar to the soils themselves. In France, for example on the Rhone terraces of recent to Villafranchian age, the degree of clay illuviation and compaction of the B horizon increases with the age of the terrace; the oldest two levels have hydromorphic, 'degraded' upper horizons 'due to the acidification and the water-saturation' (Bornand, 1973). Because these terrace levels have been subject to the climatic alternation of several glacials and interglacials, it would be rash to interpret the surface-water gley soils occurring on them as zonal with respect to the present environment. In spite of their seasonally deficient drainage, similar soils may be zonal in other climates.

Glinka (1914) described the Russian clayey podzols (surface-water gley soils) among the zonal¹³ soils. Smith (1941) and Smith et al. (1950, p. 188-192) described an increasing proportion of Planosols with increasing age of landform in the Prairie soil landscape of Illinois and Iowa, formed in originally well-drained parent material on low to moderate relief, and implied that the transition from Prairie soils to Planosols is a zonal trend. This inference should be viewed with caution, however, in view of the widespread occurrence of paleosols with planosol characteristics exhumed by later erosion on slopes in presumably similar materials further west in Iowa (Ruhe et al., 1967). Surface-water gley soils also appear to be zonal in humid monsoon climates, as in Bangladesh or North-east Thailand and adjoining regions.

TWO MODELS FOR THE GENESIS OF BLEACHED ELUVIAL HORIZONS

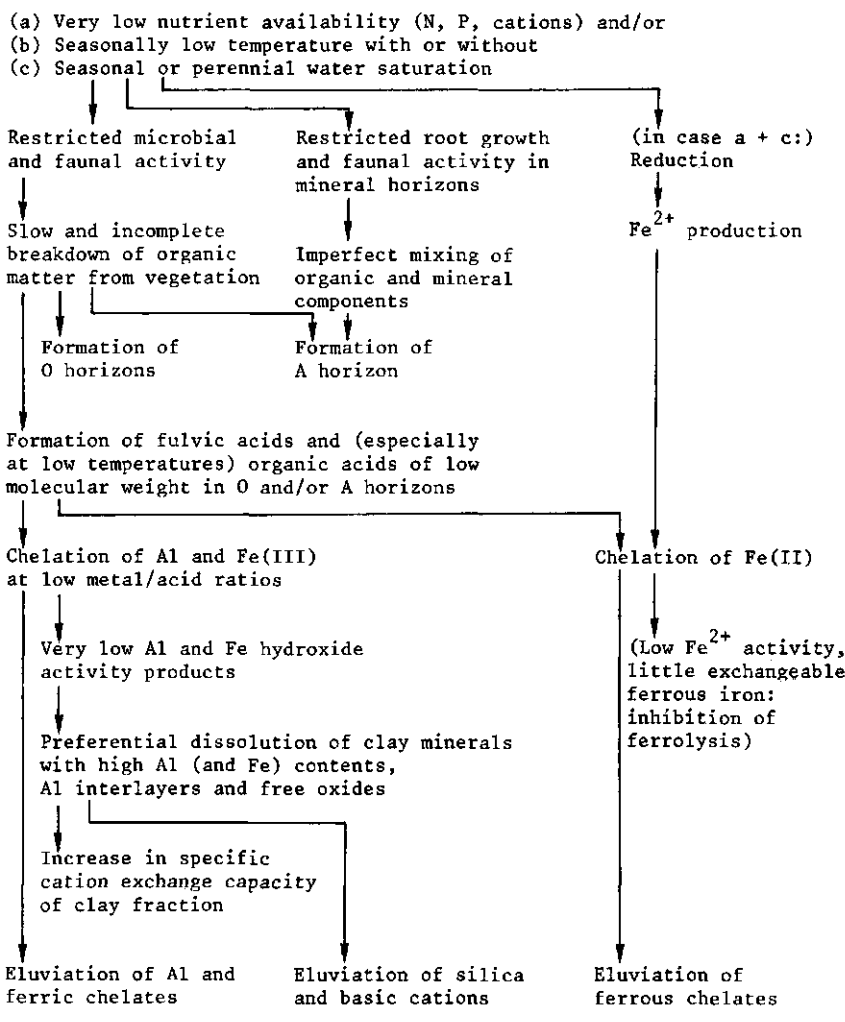
Schematic models for the genesis of bleached eluvial horizons in podzols, *cheluviation*¹⁴ and in surface-water gley soils, *ferrolysis*¹⁵, are shown in Tables 50 and 51, respectively.

13. Glinka used the Greek terms *ekto-* and *endodynamomorphous*, meaning formed by external forces and by forces within the soils themselves, for zonal and intrazonal, respectively. In this original sense, the recognition of zonal soils seems to be allowed on level land, in contrast to the later requirement of a moderate relief.

14. term coined by Swindale & Jackson, 1956. The general concept of aluminium and iron removal by organic acids is much older - see, e.g., Glinka (1914), p. 83-84 - but has become increasingly specific and quantitative with time, for example by the work of Bloomfield (1957), Schnitzer et al. (1963, 1964, 1968), Schuylenborgh & Bruggenwert (1965), Bruckert & Jacquin (1969), Petersen (1976); review by, e.g., Davies (1971).

15. Brinkman (1970) and summary in this book.

Table 50. Schematic model of the genesis of eluvial horizons in podzols: cheluviation.

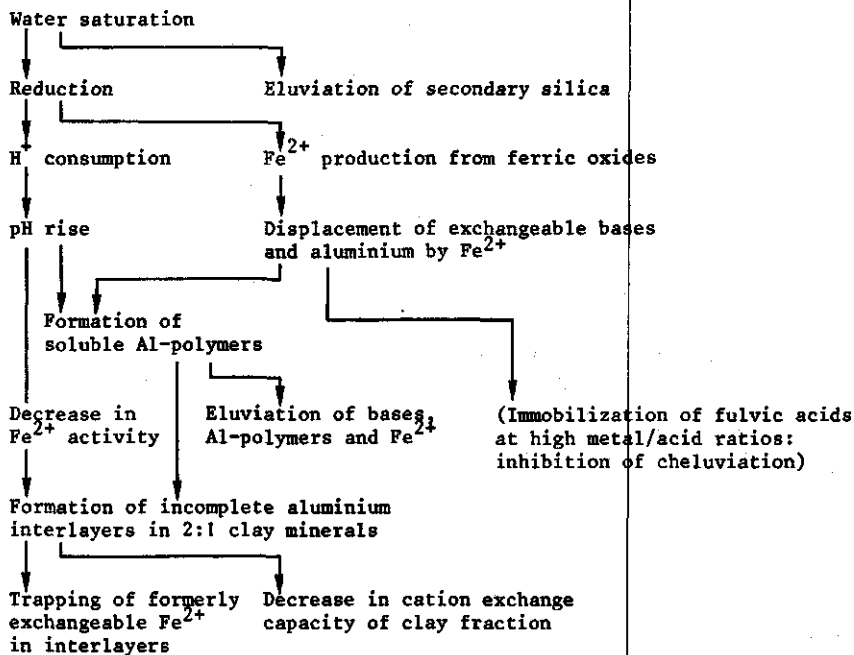


The cheluviation model was worked out in order to list the implications of the concept that chelation of Al (and Fe) from minerals and oxides and removal from the eluvial horizon in the form of soluble chelates is the main process of podzol formation. The ferrolysis model lists the consequences of alternate reduction and oxidation of iron compounds under periodically water-saturated conditions with some leaching. These include alteration and decomposition of clay minerals besides the translocation of iron and its segregation into mot-tles or nodules.

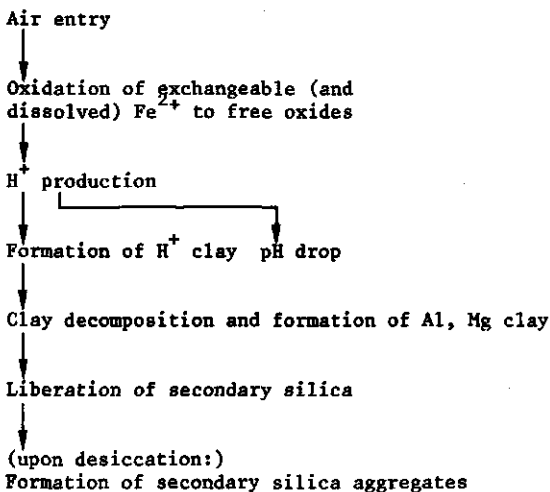
The models for both soil-forming processes provide for the decomposition of weather-able minerals and the relative accumulation of silica in the upper horizons of the soil profile under acid conditions. Both models explain the formation of bleached eluvial hori-zons by removal of grain coatings of ferric oxides, albeit in different ways. In both, the

Table 51. Schematic model of the genesis of eluvial horizons in seasonally wet, acid soils: ferrolysis.

WET SEASON



DRY SEASON



bleaching may be masked by incorporated organic matter. Both processes cause loss of clay by decomposition from the upper horizons, but this may be counterbalanced by the breakdown of sand-sized and silt-sized minerals to clay, or masked by sedimentary heterogeneity. Seasonal reduction occurs in many podzols and is a necessary factor in the formation of surface-water gley soils. In other respects the models of the two processes differ considerably.

In cheluviation, the presence in the upper horizons of an excess of chelating acids causes a very low concentration of uncomplexed dissolved Al^{3+} . This results in the preferential removal of Al-interlayers from soil chlorites and preferential dissolution of Al-rich minerals, and a relative immunity of a silica-rich, montmorillonite-type smectite. Eventually, even this becomes unstable, ultimately leaving a pure quartz sand or a quartz-anatase mixture. For thermodynamic reasons, a high silica activity in the leaching solution would be expected during the dissolution of clay minerals under near-equilibrium conditions at a very low $Al(OH)_3$ activity product, even though total concentrations of soluble Al may be high (Brinkman, 1979). The high silica activities are corroborated by experimental results with organic acids (Huang & Keller, 1971).

Liberation of aluminium by microbial decomposition of the chelates would cause a high $Al(OH)_3$ activity product in an underlying illuvial horizon. This may have three results: precipitation of an aluminium hydroxide; aluminium interlayering with a consequent decrease in CEC of the 2:1-type clay minerals; synthesis of clay with a high Al content and low CEC by combination with silica from the soil solution.

The trend to be expected in podzols *sensu stricto*, soils subject to cheluviation, thus is a higher CEC of the clay fractions from the A and E horizons compared with the underlying B or C horizons, at least if the eluvial horizons contain clay minerals. The clay fractions of the eluvial horizons would contain more smectite and less chlorite, kaolinite and free oxides compared with the lower horizons.

In ferrolysis, the rate of decomposition of the clay minerals in the eluvial horizons is dependent on their CEC since exchangeable hydrogen produced by oxidation of exchangeable ferrous iron is the agent of destruction. Hence, smectites and vermiculites are decomposed more rapidly than the more aluminous chlorites and kaolinite with their lower CEC.

During the reduced phase, aluminium interlayers are formed in the 2:1-type clay minerals, which raises their Al content and lowers their CEC. Exchangeable ferrous iron may be trapped during interlayer formation, which raises the ferrous iron content of the clay fraction.

The trends to be expected in surface-water gley soils subject to ferrolysis thus comprise a lower content of smectite and vermiculite, relatively more aluminium-interlayered material, a lower CEC and a higher ferrous iron content in the clay fractions of the A and/or E horizons than in those of lower horizons.

These contrasting trends may be used to distinguish between eluvial horizons formed by cheluviation and by ferrolysis, as discussed and illustrated in the last section of this chapter.

Simultaneous cheluviation and ferrollysis appear to be impossible. On the one hand, the presence of an excess of fulvic acids during cheluviation causes very low ferrous iron and aluminium activities. This inhibits displacement of exchangeable cations by ferrous iron and formation of aluminium interlayers, two component processes of ferrollysis. On the other hand, the relatively large quantities of aluminium readily available during ferrollysis immobilize fulvic acids and thus inhibit cheluviation. Ferrollysis following cheluviation appears unlikely, but cheluviation may take place subsequent to ferrollysis. This may happen in surface horizons when the rate of fulvic acid production exceeds the supply of divalent and trivalent cations, e.g., in the terminal stage of ferrollysis, once the intensity of this process has decreased owing to the very low CEC of the soil chlorite formed. In such cases, cheluviation inhibits the further progress of ferrollysis.

A humus illuvial horizon, i.e. ortstein with high organic matter contents and relatively low Fe and Al contents as described by Glinka (1914) in sandy podzols, is evidence for mobility of organic matter present in excess over iron and aluminium available in the associated eluvial horizon and hence for present or past cheluviation. The ferric and manganese nodules in the eluvial and illuvial horizons, i.e. the ortstein with low organic matter contents described by Glinka in clayey podzols, are evidence for the presence and mobility of iron and manganese and, by inference, for the lack of mobility of organic matter in these soils.

CHOICE OF CRITERIA FROM ELUVIAL OR ILLUVIAL HORIZONS FOR DIAGNOSIS AND CLASSIFICATION

In morphometric classification systems, easily recognizable features, even if fossil, tend to be given preference over the marks of current processes that so far have had less evident influence on soil development.

Several current systems of soil classification define the soils with translocation of material, such as organic matter and sesquioxides or clay, by secondary evidence: the presence of immobilized material in an accumulation horizon. As a result, relatively little attention appears to have been given to the description and characterization of eluvial A and E horizons. A change in this practice may be desirable for several reasons, as outlined below.

- The nature of the upper horizons, rather than that of the underlying accumulation horizons, is normally of direct interest at least for the growth of annual plants and short grasses.
- If the recognition of accumulation phenomena is accurate, this is a sufficient criterion for the present or past occurrence of mobilization and translocation. These two processes are not necessarily accompanied by accumulation phenomena, however. They may well have taken place with removal of part or all of the products from the sequum.
- In cases where more than one main process has been active, only one of which has led to accumulation phenomena, the effects of the others tend to be neglected or ascribed to the process most easily recognized.
- By its very nature, an accumulation horizon represents an integral of intensity of the accumulation process over time. Thus, there is a possible bias towards fossil processes and a possible neglect of currently active processes in soil classification.

These imbalances may be corrected by the use of criteria derived from eluvial horizons, albic as well as less clearly expressed E or Eg horizons, and from the upper part of illuvial horizons subject to 'degradation'.

The material accumulated in illuvial horizons usually has been lost from, or transported through, eluvial horizons. In principle, therefore, the latter would also be indicators of an integral of soil-forming processes over time as are the illuvial horizons. In eluvial horizons, however, the traces left by earlier processes of decomposition or transformation and removal may be modified or obliterated by clear indications of more recent or current processes more easily than in an accumulation horizon. This lack of emphasis on accumulated 'old' evidence tends to make eluvial horizons particularly suitable for the study of recent or present trends in soil formation.

The genetic significance of the different kinds of bleached eluvial horizons has not been generally recognized. In the Russian soil science literature, for example, the bleached eluvial horizons have been taken together under the single term podzolic horizon. The Albic horizon of the Soil Taxonomy (Soil Survey Staff, 1975) has not been subdivided either.

Present analytical techniques, however, make it possible to distinguish the effects of the two different processes, cheluviation and ferrollysis, in eluvial horizons. There are also some morphological characteristics associated with these processes that generally enable their distinction in the field.

The distinction of ferrollysis from clay translocation and desilication is discussed in the next section. In the last section, the analytical criteria and field characteristics of cheluviation and ferrollysis are listed in tabular form.

THE DISTINCTION OF FERROLYSIS FROM CLAY TRANSLOCATION AND DESILICATION

Evidence for ferrollysis in a profile containing translocated clay is based on a combination of criteria.

A clay balance for a soil profile in homogeneous material subject to clay translocation without decomposition or interlayering normally would be near zero or positive. The latter may be due to erosion of part of the eluvial horizons, or to clay synthesis from weatherable sand-sized or silt-sized minerals, or both. Where clay decomposition or interlayering have taken place, the clay balance is often negative, but this is not a sufficient criterion for ferrollysis.

In the case of clay translocation without decomposition or interlayering, the cation exchange capacity of the clay fractions may be constant throughout the profile or show a maximum in the illuvial horizons if fine clay with a high CEC has been transported preferentially. Decomposition or interlayering may be suggested by a low CEC of the clay fractions in the upper horizons, in some soils with a minimum near their lower boundary, combined with a higher CEC of the clay in the lower horizons that is constant or continually increasing with depth, i.e., without a maximum in an illuvial horizon. Examples from some planosols in Iowa, recalculated from data in Cain & Riecken (1958), are shown in Fig. 24 and 25.

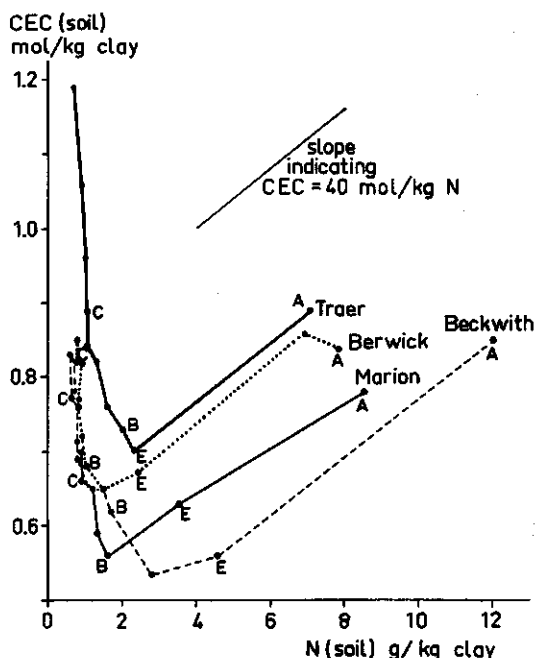


Fig. 24. CEC plots of four planosol profiles in Iowa, U.S.A. Source: sum of exchangeable cations, N and clay contents in Cain and Riecken (1958).

Besides ferrollysis, a moderate degree of hydrolysis by water containing carbonic acid, desilication, may also give rise to aluminium-interlayered clay fractions with a relatively low CEC in upper horizons.

Desilication causes lower silica and higher aluminium contents in clay fractions of the upper, weathered horizons, whereas these tend to remain similar during ferrollysis. Secondary silica may accumulate as a result of ferrollysis and periodic dehydration, in contrast to the preferential removal of silica during hydrolysis by water and carbonic acid. Ferrollysis produces graininess, low birefringence and opalescent reflection of incident light in oriented clay observed in thin sections (owing to clay-sized quartz or secondary silica), features not found in well-drained soils subject to desilication. The most specific characteristic for the distinction of ferrollysis from desilication is probably the trapped ferrous iron in the clay fractions of the eluvial horizons.

DIAGNOSTIC CHARACTERISTICS FOR CHELUVIATION AND FERROLLYSIS; CONSEQUENCES FOR SOIL CLASSIFICATION

Diagnostic characteristics of the clay fractions from eluvial horizons that can be used to distinguish between the effects of cheluviation and ferrollysis are listed in Table 52. Table 53 comprises field characteristics of eluvial horizons of the corresponding kinds of soils associated with these two processes, podzols and surface-water gley soils, respectively. The different trends of ferrous iron contents and CEC of clay frac-

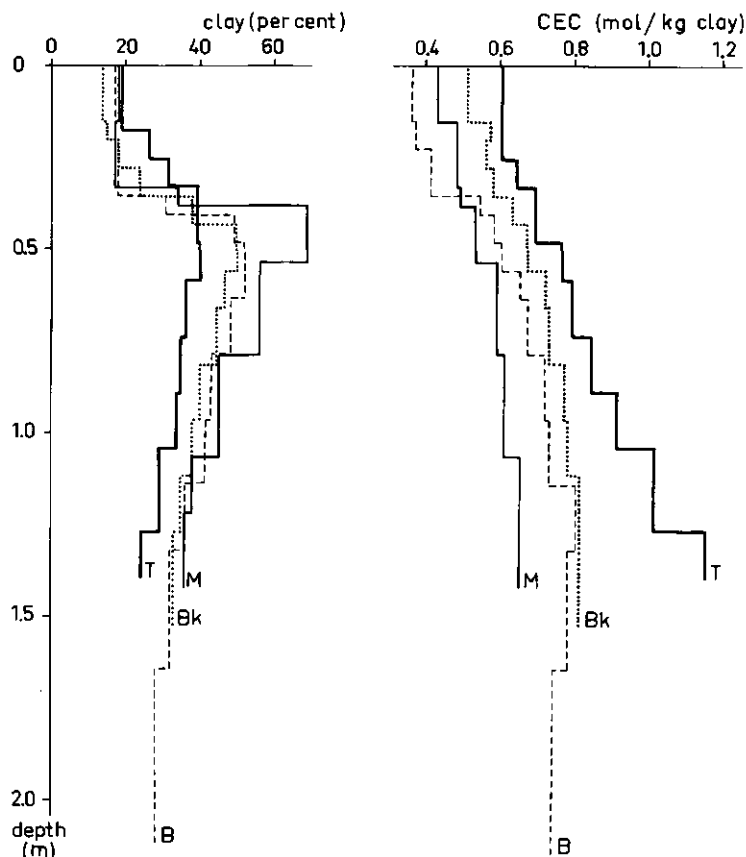


Fig. 25. Clay percentages and CEC of clay fractions as functions of depth in four planosol profiles in Iowa, U.S.A. CEC/clay recalculated from sum of cations and clay percentage after deduction of 40 mol/kg N (see Fig. 24).

tions before and after citrate extraction are illustrated in Fig. 26. Surface-water gley and podzol sequa in single soil profiles are compared in the previous chapter.

The present very wide group of podzolic soils as used in the Russian soil classification could be reduced to more manageable proportions by the use of criteria derived from Tables 52 and 53, particularly the contrasting trends in ferrous iron contents, mineralogy and CEC of the clay fractions with depth. Seasonally wet soils that are clearly formed by processes other than cheluviation, now included in the sod-podzolic soils or termed pseudopodzols or subtropical podzols, could then be placed in a separate group, comparable with the surface-water gley or pseudogley soils and planosols rather than in the podzols.

In the context of the two processes discussed, no changes would be needed in the group of podzols with a clearly identifiable humus illuvial horizon, such as the Spodic horizon (Soil Survey Staff, 1975), the Spodic B horizon (FAO, 1974) or the clear humus podzol B in the Netherlands classification (Bakker & Schelling, 1966).

The identification of marks of cheluviation in an eluvial horizon, for example through

Table 52. Diagnostic characteristics¹ for distinguishing between cheluviation and ferrolysis in clay fractions of eluvial horizons.

Characteristics in clay fractions ² of eluvial (E or A) horizons compared with the clay in lower horizons	Diagnostic for cheluviation	Diagnostic for ferrolysis
content of ferrous iron trapped in interlayers ³	equal or lower or insignificant difference	significantly higher (about 0.05% FeO or more)
increase in cation exchange capacity after citrate extraction ⁴	less (often near zero or negative)	greater or similar
total ferrous iron content ⁵	equal or lower	higher
content and stability under heat treatment of aluminium-interlayered material ⁶	lower	higher or similar
content of smectite or swelling component of interstratified material	higher	lower
cation exchange capacity ⁷	higher	lower
total iron content	much lower	similar or lower
aluminium content	lower	similar
clay mineralogy in extreme cases	resistant minerals, e.g. quartz and anatase only	kaolinite, quartz, with little aluminium-interlayered material

1. The characteristics taken individually do not necessarily distinguish between these two processes and others. For example, a well-drained, acid soil subject to desilication may also have higher or similar contents of aluminium-interlayered material in the eluvial horizon, compared with lower horizons. The characteristics are less generally applicable or tend to be less sharply diagnostic toward the bottom of the list.

2. Clay fractions should only be pretreated with H₂O₂ -Na acetate buffer at pH 5. Other pretreatments, including unbuffered H₂O₂, acid or dithionite-citrate, may destroy or impair the characteristics diagnostic for ferrolysis by extraction of interlayer material and liberation of trapped ferrous iron.

3. Trapped ferrous iron calculated by difference of total ferrous iron contents before and after citrate extraction.

4. Procedure for citrate extraction in Appendix: Methods. This treatment removes all or part of Al-interlayer material, depending on its degree of organization or completeness, tends to increase the CEC of Al-interlayered clay fractions and removes ferrous iron trapped in interlayers.

5. Total ferrous iron determination according to Begheyn (1979). Procedure summarized in Appendix: Methods.

6. By X-ray diffraction peak height or peak area at 1.4 nm after K saturation and heating to a range of temperatures between 100 and 550° C. Heat treatment to a given temperature should preferably be simultaneous for the clay samples from a whole profile.

7. Conventional CEC at pH 7 or 8.4. We used Ba saturation at pH 7, Ba-MgSO₄ exchange, calculation of exchangeable Mg by difference between A.A.S. determinations on standard and solution after exchange (Appendix: Methods).

Table 53. Field characteristics¹ of eluvial horizons associated with cheluviation and ferrollysis.

Field characteristics of eluvial (A or E) horizons	Associated with cheluviation	Associated with ferrollysis
texture	sand to silt loam	silty clay to sandy loam, occasionally to sand
colour	neutral, or chroma 1	chroma at least 2, e.g. 10YR hue
mottling	none or faint, or distinct dark grey to dark or very dark brown (organic matter)	distinct yellowish brown, strong brown or reddish yellow (iron oxides)
nodules	normally none	fine black (manganiferous), occasionally brown (ferric), or none
structure	normally single grain, without medium or fine tubes (earthworm tunnels)	weak platy, massive (coherent), occasionally single grain. Normally with medium and fine earthworm tunnels and pedotubules
clay content	lower, equal or higher than in deeper horizons	normally lower than in deeper horizons
transition to next deeper horizon	abrupt to clear, smooth to wavy or convoluted with or without intact parts of lower horizons isolated in (lower part of) eluvial horizon (may or may not overlie a clearly expressed humus illuvial horizon)	abrupt to gradual, smooth to tonguing or interfingering, or broken with cores of lower horizon material at different stages of transition in lowest part of eluvial horizon (does not overlie a humus illuvial horizon)
pH (water)	< 5.5 ²	> 4 ³
pH (CaCl ₂ 0.01 mol/l)	< 3.5	> 3.5

1. None of these characteristics are necessarily present; they are associated with the processes but not essential to them.

2. Or higher due to, for example, occasional addition of windblown material (Bouma & Van der Plas, 1971).

3. Or lower if saline (Brinkman & Dieleman, 1977).

higher CEC, higher smectite contents and less aluminium interlayering than in clay fractions of deeper horizons, would make it feasible to define podzols even in the absence of a Spodic horizon. Presumably, such a definition would move some of the sandy Humaquepts (Soil Survey Staff, 1975) into the Spodosols and most of the Gooreerd soils (Bakker & Schelling, 1966) into the Podzol soils, in spite of the removal of much of the cheluviated material in the ground water.

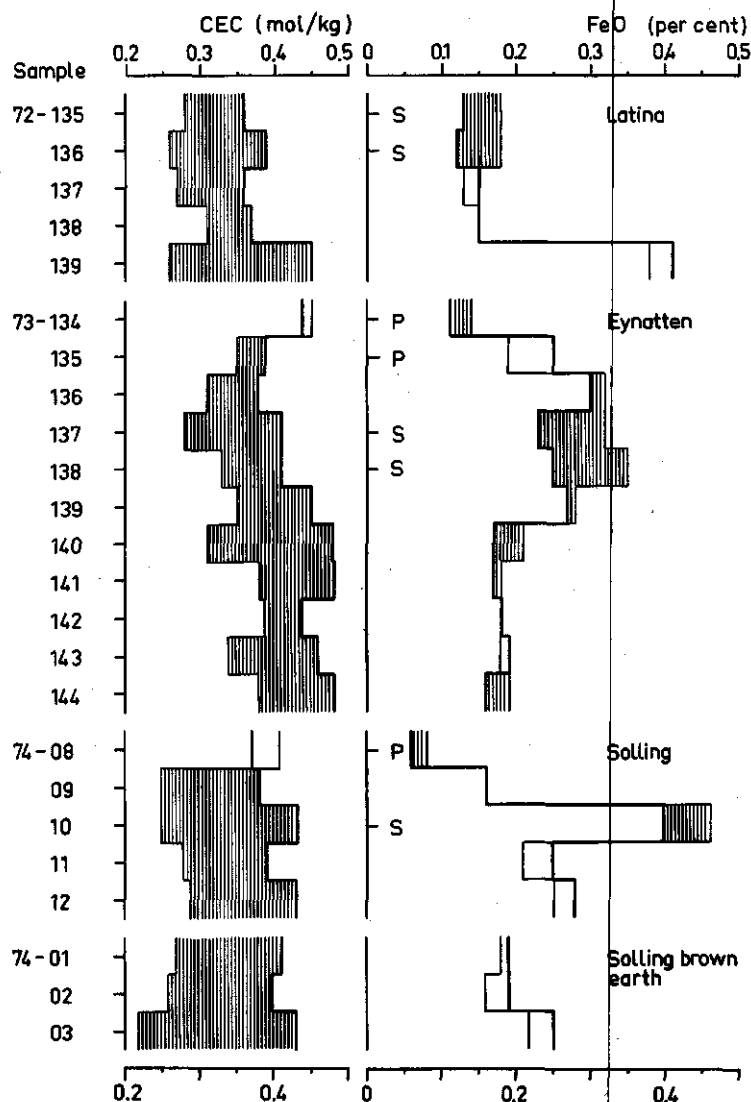


Fig. 26. FeO contents and CEC of clay fractions from four soil profiles before and after citrate extraction. Thin lines: without, heavy lines: with preliminary citrate extraction. Samples are from soil horizons in sequence of depth. P: eluvial horizons of a podzol sequum, S: eluvial horizons of a surface-water gley sequum, blank: transitional or lower horizons. Latina is a surface-water gley soil; Eynatten and Solling are surface-water gley soils with the Ah and E horizons of a minipodzol in the upper dm; Solling Brown Earth is a well drained, acid brown earth. Descriptions and analytical data of these soils are given in the first Chapter.

Appendix

METHODS

Most methods are summarized or quoted in Brinkman (1977a), p. 112-115 and (1977b), p. 171; X-ray transmission stereo radiography in Brinkman, Jongmans and Miedema (1977), p. 109; electron microprobe analysis in Brinkman et al. (1973), p. 260-261. Reprints of these papers are bound in a separate volume, available from the author.

Procedures for pretreatment and clay separation, citrate extraction and related analyses (ferrous iron, CEC, etc.) are discussed and summarized below.

Pretreatment and separation of clay fractions

Clay fractions used for the determinations discussed below and for total chemical analysis may contain free oxides, but should have at most low contents of reactive organic matter (not all carbon need be removed). Any aluminium interlayers in the clay should be preserved intact. Pretreatment should therefore avoid strong acids and unbuffered H_2O_2 , which may also cause strongly acid conditions during the oxidation of organic matter, as well as complexing agents such as (dithionite-)citrate. Reagents should not contain phosphate, which would be taken up by the clay fraction.

Procedure. Pretreat 20 or more g soil (containing at least about 5 g clay) with Na acetate - acetic acid buffer at pH 5 and centrifuge-wash to remove exchangeable calcium and carbonate if present. Oxidize (most of the) organic matter by H_2O_2 10% after adding acetate buffer to keep the pH about 5; first cold, then on hot waterbath. (H_2O_2 anal. grade; technical grade contains phosphate as stabilizer.) Centrifuge-wash (add NaCl solution in case clay remains in suspension) to remove most of the acetate and any oxalate formed. Disperse by addition of water and NaOH to pH between 7 and 8 and syphon off twice; calculate standing time from temperature and intended syphoning depth to collect fraction smaller than $2\mu m$ equivalent sedimentation diameter.

Reserve an aliquot from this suspension for X-ray diffractometry and coagulate remainder with Ba acetate 0.5 mol/l at pH 7, (decant clear supernatant and) centrifuge, repeat Ba treatment. Remove soluble salt by washing with water and centrifuging twice: check decanted second supernatant with sulphate solution for absence of Ba. Freeze-dry the Ba-clay.

Citrate extraction of clay fractions

A conventional procedure, citrate extraction according to Tamura (1958), is used to estimate the degree of aluminium-interlayering of 2:1-type clay minerals and of the amounts of ferrous iron trapped in the interlayers.

The method allows identification by X-ray diffractometry of the general types of clay minerals that were aluminium-interlayered (Tamura, 1958) and estimation of the extent of aluminium-interlayering. It appears to discriminate well between ferrous iron trapped in the interlayers and originally present within the clay minerals, and to allow good estimates of the increase in cation exchange capacity upon removal of interlayers. The most well-ordered and complete interlayers are apparently not extracted completely by only three 1-hour treatments.

The amount of aluminium (and total iron) extracted is sensitive to the temperature of extraction (about 85 and 100°C tested) and to citrate concentration (0.33 and 1 mol/l tested). This method probably causes slow dissolution of structural aluminium besides rapid removal of aluminium interlayers. Other methods of interlayer removal do not seem to be better in this regard and work with more aggressive extractants, such as fluoride, HCl, NaOH or KOH, or at higher temperatures.

Procedure. Extract 100 to 500 mg Ba-saturated, freeze-dried clay fraction in a 100 ml (short type) polypropylene centrifuge tube for 1 hour in a boiling, shaking water bath with 20 ml Na citrate solution (0.33 mol/l) per 100 mg clay. After cooling, centrifuge 10 min. at 3000 r.p.m. and decant clear supernatant into a 100 to 500 ml volumetric flask. Repeat extraction twice with citrate solution and once with water. Bring volumetric flask to volume with water, mix. Suspend extracted sample of clay fraction (now Na-saturated) in water if it is to be studied by X-ray diffraction; or saturate with Ba by three times shaking one hour with 20 ml Ba acetate solution (0.5 mol/l) and centrifuging (discard clear supernatants) and twice with water; check decanted second supernatant with sulphate solution for absence of Ba. Freeze-dry for further chemical analysis.

Estimates of ferrous iron, magnesium and aluminium in interlayers

The amount of ferrous iron trapped in aluminium interlayers is estimated by difference of total contents in clay samples without and with preliminary citrate extraction. The procedure for rapid HF decomposition and ferrous iron determination according to Begheijn (1979) is summarized below. Magnesium can also be determined, by atomic absorption, in the solution obtained after decomposition. Ferrous iron determination in the citrate extract would be meaningless because citrate tends to reduce ferric iron.

Procedure for HF decomposition. Weigh 100 mg freeze-dried, powdered clay fraction in Pt crucible. Add 1 ml H_2SO_4 96%, mix; add 3 ml HF 48% (caution: use gloves, work in fume cupboard from HF addition up to the filtering step). Swirl 10 seconds (temperature rises to 60–65°C by heat of mixing); transfer to quartz beaker containing 10 ml H_3BO_3 4% and 3 ml HCl 4 mol/l. Boil gently 2 minutes. Cool, transfer to 100 ml polypropylene volumetric flask containing 40 ml H_3BO_3 4%, dilute to mark and mix. Filter through folded filter in polypropylene funnel into dry 100 ml polypropylene bottle (discard first filtrate). Run a complete blank determination with each batch of samples.

Procedure for ferrous iron determination. Pipet 2.00 ml of the filtrate from HF decomposition into 50 ml volumetric flask, dilute to about 30 ml; add 10.0 ml potassium hydrogen phthalate buffer solution 0.5 mol/l (10% w/V) and mix well; add 4.0 ml 1.10-orthophenanthroline solution 0.25%, dilute to mark and mix. Measure absorbance at 510 nm against

water within 15 minutes. Add 2.00 ml of blank solution to standard series. (If the filtrate is coloured by organic matter, measure and correct for its absorbance after dilution of 2.00 ml to 50 ml.)

Procedure for Mg determination. Pipet 2.00 ml of the filtrate from HF decomposition into plastic 50 ml volumetric flask. Add 25 ml HCl 2 mol/l (sufficient to prevent precipitation of La fluoride) and 10 ml LaCl_3 solution 5%. Make up to volume and measure on atomic absorption spectrophotometer.

If desired, the amount of aluminium and magnesium extracted can be estimated in the extract, Al colorimetrically with pyrocatechol violet (Wilson and Sergeant, 1963) and Mg by atomic absorption, after destruction of the citrate with $\text{Se-H}_2\text{SO}_4$. The procedure, from Begheijn and van Schuylenborgh (1971), p. 54-55, is summarized below. The high citrate concentration would entail hazards of clogging and explosion in an atomic absorption spectrophotometer and the citrate complex would prevent proper colour development of aluminium-pyrocatechol violet. Aqua regia seems to be ineffective and H_2O_2 tends to cause explosions during attempts at citrate destruction. Estimation of extracted aluminium by difference would be less accurate than in the case of ferrous iron and magnesium because a much smaller proportion is extracted.

Procedure for destruction of citrate in extract. Pipet 2.00 ml of the citrate extract into a 25 ml borosilicate beaker. Add 1.0 ml $\text{Se-H}_2\text{SO}_4$ solution (1 g Se dissolved in 100 ml H_2SO_4 96% by heating to about 150°C) to the beaker and place it on the hotplate, the temperature of which is adjusted to 150°C beforehand. Evaporate to constant volume. Cover the beaker with a watch glass and adjust the temperature of the plate to 250°C and after 30 minutes to 360°C . Continue heating for another hour after the liquid has become clear. Remove the watch glass from the beaker and evaporate the sulphuric acid. Remove the beaker from the plate and adjust the temperature of the plate to 150°C . Add 1.0 ml NaCl solution (1 mol/l) and 1 ml aqua regia to the contents of the beaker. Cover the beaker with a watch glass and transfer to the plate. After gas development has ceased remove the watch glass from the beaker and evaporate to dryness. Remove the beaker from the plate, add 1.0 ml HCl (1 mol/l) and about 10 ml water. Cover the beaker with the watch glass, transfer to the plate and dissolve the residue (dilute if necessary). Transfer quantitatively into a 100 ml volumetric flask, dilute with water to the mark and mix.

Cation exchange capacity blocked by Al-interlayers

The difference between conventional CEC values determined with and without preliminary citrate extraction can be used as an estimate for the extent of aluminium interlayering. If the total chemical composition of clay samples is determined by X-ray fluorescence spectrophotometry as in this laboratory (Halma, 1973), Ba measured in this routine procedure allows a rapid and economical estimate of CEC. Alternatively, Ba may be exchanged (and precipitated) completely in one operation by addition of MgSO_4 solution and the CEC derived from the difference in Mg concentration in solution before and after addition to the sample. (Other conventional methods of CEC determination presumably would be satisfactory as well for the present purpose).

Procedure. Weigh at least 300 mg Ba-saturated, freeze-dried clay into a 15 ml plastic centrifuge tube, add 10.0 ml MgSO_4 solution 0.025 mol/l, shake at least 1 hour. Centrifuge 15 min. at 3000 r.p.m. Pipet 0.5 ml of the clear supernatant into a 100 ml volumetric flask, add 5 ml HCl 0.1 mol/l and 10 ml LaCl_3 solution 5%. Make up to volume and measure on atomic absorption spectrophotometer.

CHOICE OF UNITS AND ENTITIES

The units used in this book conform to SI, the *Système International d'Unités* (BIPM, 1977). In the sections on clay mineralogy, the nm (10^{-9} m) was used throughout, rather than the traditional Ångström unit (10^{-10} m), for which recognition is being withdrawn in the European Economic Community in December 1979.

Matric suction is expressed in MPa. 1 bar corresponds to 0.1 MPa; 1 cm water head to 98.0665 Pa. In practice, the conversion factor is 100, because the relative error in soil physics data is generally large owing to the variability between samples (see, for example, Fig. 11). Traditional pF values should be increased by 1.9915 (in practice, by 2) to convert them to log (matric suction in Pa).

Hydraulic conductivity is expressed in $\text{m}^2 \text{Pa}^{-1} \text{s}^{-1}$. Values in the traditional unit metres per day (under the pressure gradient due to gravity) should be multiplied by 1.18022×10^{-9} (in practice, by 10^{-9}) to convert them to $\text{m}^2 \text{Pa}^{-1} \text{s}^{-1}$.

The traditional milliequivalent (meq) is not recognized in SI, which has the coulomb (C) as unit of charge and the mole (mol) as unit of amount of substance, n . The latter is proportional to the numbers of elementary entities such as atoms, molecules, ions, electrons or groupings of such entities. The kind of entity (e.g. Ca^{2+} , Na^+) must always be specified (BIPM, 1977). An expression fulfilling the function of the traditional milliequivalent is needed wherever ions of different valencies and ion exchange capacities are considered as a category, as in ionic reactions or in reporting compositions of soil solutions or cation exchange data.

As long as no suitable entity has been defined, an expression such as the sum of positive ions $\sum n(\text{B}^{z+})$, in mol, is proportional to the total numbers of these ions, not to their total charge as needed for a check on electroneutrality in solutions or in calculations involving ion-exchange capacity. If charge rather than amount of substance is used for this purpose, inconvenient conversion factors are encountered (1 mmol of a monovalent ion carries a charge of 96.5 C).

One inelegant solution would be to specify that for all ions, CEC, etc., the unit mol referred to the amount of substance of the charge carried in terms of electron as elementary entity. Amounts for positive ions would then carry a minus sign, since 1 mol Ca^{2+} , for example, carries the same charge as -2 mol electrons. Another solution would be to state for every ion, in text and table headings, that the unit mol referred to an entity defined as that fraction of the given ion that would carry one elementary charge, for example $\frac{1}{3}\text{Al}^{3+}$. This can be expressed for any ion as $\frac{1}{z}\text{M}^{z+}$ or $\frac{1}{z}\text{A}^{z-}$. There would need to be a further statement that expressions such as \sum^+ (the traditional total equivalents of positive ions) or CEC would imply the same entity $\frac{1}{z}\text{M}^{z+}$ but without indication of a

specific ion. Thus, there did not seem to be a convenient, clear and simply designated alternative for the milliequivalent in SI.

Since the International Union of Pure and Applied Chemistry has recently redefined the equivalent as a class of entities in keeping with the requirements of SI (IUPAC, 1978), a good alternative for the old unit milliequivalent is now available.

The class of entities *ionic equivalent* of M^{z+} (or A^{z-}) can be defined, in accordance with IUPAC (1978), as those entities which, in an ionic reaction, would combine with, or substitute for, 1 entity of hydrogen ions. Then, the expressions ionic equivalents Mg, Al, Σ^+ , in mol/m³, for example, have the same meaning as the old expressions Mg, Al, Σ^+ , meq/l. For convenience, particularly in table headings, the term *exchangeable (or exchange) equivalent* of M^{z+} (or A^{z-}) can be defined as a subclass of the class ionic equivalents, referring to exchange reactions or used for reporting exchangeable ions or exchange capacities. In accordance with operational rules for SI, these should be reported in units with as denominator the base unit of mass, kg - for example mol/kg or mmol/kg (not mmol/g, nor mmol/100 g).

Summary

The formation of surface-water gley soils has been explained in various ways. About 1900, these soils were described in Russia and included among the (loamy and clayey) podzols, though it was recognized that they differed from the sandy podzols in several characteristics besides soil texture. The 'loamy and clayey podzols' contain nodules of iron and manganese oxides in the bleached horizon as well as in the mottled underlying horizon, which has a low organic matter content. The 'sandy podzols' have a bleached eluvial horizon without nodules or iron or manganese oxides underlain by a brown to black horizon with a higher organic matter content.

Until recently, the surface-water gley soils were still considered 'podzolic'. The ill-defined term podzolization was used to explain the genesis of the different kinds of 'podzols' as well as of some other soils. In the last decades there has been a tendency to restrict the meaning of the term podzolization to cheluviation, i.e. removal in chelated form, for example of aluminium. In Russian literature, the term pseudopodzolization has come into use for the formation of surface-water gley soils.

The bleached eluvial horizons of sandy podzols are formed by cheluviation of aluminium and iron by organic acids, often with formation of smectites. During cheluviation, aluminium activities in the eluvial horizon necessarily remain very low. Only in an underlying accumulation horizon do aluminium-interlayered clays or aluminium hydroxides commonly occur. Eluvial horizons of surface-water gley soils, however, contain aluminium-interlayered rather than swelling clay minerals. This observation constitutes clear evidence for a relatively high aluminium hydroxide activity product at some time during their formation and indicates that cheluviation cannot have dominated soil formation.

Translocated clay is recognized in many surface-water gley soils. Clay translocation can explain textural differences between surface horizons and subsoil, but not the apparent net clay loss calculated for some profiles. The seasonally fluctuating pH and the bleached and mottled nature of the eluvial horizons in surface-water gley soils can be accounted for by periodic reduction with some leaching. Secondary silica commonly occurs in eluvial horizons of surface-water gley soils. The aluminium interlayers in the clay fractions from these horizons contain trapped ferrous iron. These features as well as the interlayering and the apparent clay loss may be due to a soil-forming process under hydromorphic conditions.

The following sections of this summary first deal with separate papers and then with the chapters and appendix of this book.

In this paper, a hypothesis was formulated describing such a hydromorphic soil-forming process, and a term for it was coined: ferrolysis, i.e., clay decomposition by a process based on the alternate reduction and oxidation of iron (Brinkman, 1970). Data by other authors were used to show the existence in soils, clay suspensions or soil columns of most of the processes which together constitute ferrolysis.

The process is illustrated in the frontispiece figure. In brief, iron oxides are reduced to Fe^{2+} during continued microbial decomposition of organic matter after water-saturation of the eluvial horizons. The Fe^{2+} displaces exchangeable cations, which are removed by leaching together with part of the ferrous ions. Hydrogen ions consumed during reduction are replaced by the partial neutralization and polymerization of aluminium ions. Next, the pH rises from about 4-5 to 6-7. Part of the aluminium polymers is leached, part is fixed as octahedral fragments or incomplete interlayers between the layers of swelling clay minerals; some Fe^{2+} is trapped and becomes non-exchangeable; the cation exchange capacity of the clay fraction is decreased. Upon the re-entry of oxygen into the eluvial horizons, exchangeable ferrous ions are oxidized again to ferric oxides. The hydrogen ions produced during oxidation become exchangeable. The hydrogen clay is rapidly altered to an aluminium-magnesium clay by partial dissolution of cations from the clay minerals. Silica from unsupported tetrahedral sheets is partially dissolved and may reprecipitate in amorphous form when the eluvial horizons dry out. Part of the silica is removed in solution during the next period of water-saturation.

EVIDENCE FOR CLAY DECOMPOSITION FROM INDIVIDUAL ARGILLANS

Thin sections of eluvial horizons in many acid, seasonally wet soils have plasma and clay illuviation cutans that differ from those in underlying horizons in their grainy character, isotropic nature or low birefringence, lower content of iron oxides and strong opalescent reflection in incident light. The nature of these differences, which can be seen most clearly in oriented clay, was studied in individual argillans by microscope, electron microprobe and X-ray diffraction microcamera (Brinkman, Jongmans, Miedema & Maaskant, 1973).

The X-ray diffraction photographs of isotropic, grainy argillans indicated the presence of more, extremely fine-grained, quartz and less clay minerals than in intact, birefringent argillans. These data suggested that quartz was newly formed during decomposition of clay minerals. Later observations by electron microscope indicated, however, that at least the quartz of coarse-clay size largely consisted of detrital grains. At least part of the quartz increase during decomposition of clay minerals therefore must be due to relative accumulation rather than synthesis.

Electron microprobe analyses of grainy and birefringent argillans indicated lower contents of Fe, Mg, K, slightly lower Al and higher Si and Ti contents in the isotropic, grainy parts than in birefringent ones. Those with the highest Si contents have the brightest opalescent reflection in incident light, probably due to finely distributed secondary silica. X-ray diffractograms of clay fractions from the E horizon, which con-

tains mainly grainy clay, indicated much less smectite, more quartz and more interlayered clay than the B horizon, which contains mainly birefringent clay.

SURFACE-WATER CLEY SOILS IN BANGLADESH

During field work throughout Bangladesh, large areas of acid, seasonally wet soils were identified. After a description of their characteristics and relationships with climate and physiography (Brammer & Brinkman, 1977), a detailed study was made of the genesis of a representative example (Brinkman, 1977a) to find the reasons for their peculiar character. This led to the recognition of a sequence of three soil-forming processes, each in keeping with a seasonally dry, but progressively wetter climate, in soils on a probably late Pleistocene terrace landform: churning and calcium carbonate segregation (leading to gil-gaiied Vertisols); clay translocation; ferrollysis. Ferrollysis was identified as the dominant soil-forming process in seasonally wet, noncalcareous Holocene floodplain sediments.

Features indicating ferrollysis in the Bangladesh soils include:

- a seasonal alternation between an acid soil reaction with the presence of exchangeable Al in dry conditions and a near-neutral soil reaction with the presence of exchangeable and soluble Fe^{2+} in wet conditions;
- a net loss of clay from the profile as calculated from texture data as well as from Zr contents of the clay fractions;
- aluminium interlayering with trapped ferrous iron in the interlayers and a low CEC of the clay fractions in the upper horizons;
- the presence of amorphous secondary silica, observed as isotropic sand-sized aggregates, opalescent in incident light, in the upper horizons. Amorphous silica was also observed as 'moth-eaten blankets' and small ($1\mu m$) spherical bodies on a strongly altered cutan (by scanning electron microscopy).

PROBLEM HYDROMORPHIC SOILS IN NORTH-EAST THAILAND

Field work in a problem area for agricultural (irrigation) development led to studies on three aspects of the extremely weathered, seasonally wet, acid and partly saline-acid soils occurring on the extensive 'low terrace' in north-east Thailand. Morphological observations (Brinkman, Jongmans & Miedema, 1977) indicated preweathering of the sediment; clay translocation; clay decomposition and redistribution of iron oxides under seasonally wet conditions; biotic perforation.

The genesis of an example of these soils was further studied by physical, chemical and mineralogical analysis (Brinkman, 1977b). The silt and sand fractions were virtually pure quartz; the heavy mineral fraction comprised resistant minerals and opaque grains, without a clear trend with depth. These observations corroborated the micromorphological indications for a preweathered sediment.

The occasional grains of amorphous silica observed in the upper horizons and the major changes in composition of the clay fractions with depth are marks of soil formation. The clay fractions from most of the profile contained about 60% kaolinite and 10% quartz; those from the surface horizon, 45% kaolinite and 30% quartz. Transmission electron microscopy

showed clear signs of kaolinite dissolution in the surface horizon. Aluminium-interlayered vermiculite comprised about a quarter of the clay fractions in all horizons. It was more completely interlayered near the surface than deeper in the profile and contained small amounts of trapped ferrous iron. Exchangeable cations were largely aluminium. The clay decomposition and interlayering had reduced the cation exchange capacity to extremely low values, particularly in the surface horizon but also in deeper horizons. All these features were interpreted as resulting from long-continued ferrolysis.

Saline-acid, toxic conditions have been locally observed in these soils (Brinkman & Dieleman, 1977). Under semi-natural flooding conditions, most of the land produces a single rice crop with low yield in the monsoon season. Small, slightly higher areas are strongly saline in the upper horizon and on the soil surface by a combination of negligible leaching owing to runoff during the rains and capillary rise of the soil solution when the surrounding land is wet or inundated. The high salinity has displaced exchangeable aluminium into the soil solution in toxic concentrations and lowered the pH to values at which measurable amounts of ferric iron have come into solution as well. Similar, though less extreme, saline and saline-acid toxic patches have appeared in a pilot development project in this area, as a result of excessive water use and wastage during dry-season irrigation of dryland crops. Study of the mechanisms of salinization-acidification, of the possible origins of the salt and of the local hydrology led to advice for the reclamation and use of the different variants of these soils encountered in the area.

SOIL DESCRIPTIONS, ANALYSES AND INTERPRETATION

This chapter contains descriptions and analytical data of several European surface-water gley soils and some well-drained soils from nearby sites in similar materials. The main genetic processes which would explain their features have been inferred from these data. The results from this chapter and from the papers summarized above, as well as data from the literature, have been used as a basis for developing the arguments in the next chapters.

MULTIPLE SOIL-FORMING PROCESSES IN SINGLE PROFILES

Although ferrolysis and cheluviation appear to be mutually exclusive at any one time and place, evidence for both may still be found in single profiles, where the latter process has succeeded the former in surface horizons but not at greater depth. Other soil-forming processes may also have occurred, sequentially or concurrently with ferrolysis or cheluviation. In this chapter examples of multiple processes in single profiles are listed in tabular form and two examples of cheluviation and ferrolysis in single profiles are described in some detail.

PROCESSES TAKING PLACE IN SURFACE-WATER GLEY SOILS, PODZOLS AND PODZOLIC SOILS AND CRITERIA FOR DISTINGUISHING THEIR EFFECTS

On the basis of systematic, tabular descriptions of the processes of cheluviation and ferrolysis, a set of criteria was developed to distinguish between their effects. It has become clear that these processes are mutually exclusive, although cheluviation may follow ferrolysis under certain conditions. Criteria are also given to distinguish between the effects of clay translocation, desilication and ferrolysis. These diagnostic tools should facilitate identification of the marks of well-defined genetic processes in several kinds of soils called by different labels including podzols, podzolic soils, surface-water gley soils and their variants. The criteria mainly refer to the eluvial horizons. These horizons may need to be studied in more detail than has been customary for soil classification.

APPENDIX

The methods that were not summarized or ascribed to an accessible reference in the separate papers, are briefly described or attributed to a published source.

A note explaining the choice of units, following the convention of the *Système Internationale*, and of some of the entities to which they refer, forms the last part of the appendix.

Samenvatting

Er bestaan verschillende verklaringen voor het ontstaan van pseudogleygronden.

Omstreeks 1900 werden deze gronden in Rusland beschreven en gerekend tot de (lemige en kleifge) podzolen, al was het duidelijk dat ze in verscheidene opzichten verschilden van de zandige podzolen, niet alleen in textuur. De 'lemige en kleifge podzolen' hebben ijzer- en mangaanmodules in de gebleekte horizont en in de onderliggende gevleekte horizont; de laatste heeft een laag organische-stofgehalte. De zandige 'podzolen' hebben een gebleekte eluviale horizont zonder ijzer- of mangaanmodules met daaronder een bruine tot zwarte horizont met een hoger organische-stofgehalte.

Tot voor kort werden de pseudogleygronden nog als 'podzolic' beschouwd. De slecht gedefinieerde term podzolizatie werd gebruikt om de vorming van de verschillende soorten 'podzolen', maar ook van enige andere bodems, te verklaren. De laatste decennia is er een tendens om de betekenis van de term podzolizatie te beperken tot cheluvatie: uitloging van bijvoorbeeld aluminium als chelaat. In de Russische literatuur is de term pseudopodzolisatie in zwang gekomen voor de vorming van pseudogleygronden.

De gebleekte uitlogingshorizonten van zandige podzolen zijn ontstaan door cheluvatie van aluminium en ijzer door organische zuren, vaak met vorming van smectiet. Bij cheluvatie blijft de activiteit van aluminium in de eluviale horizont zeer laag. Kleien met aluminium-tussenlagen of aluminiumhydroxyden komen gewoonlijk alleen voor in een onderliggende aanrijkingshorizont. Uitlogingshorizonten van pseudogleygronden bevatten echter geen smectieten maar kleimineralen met aluminium-tussenlagen. Het is dus duidelijk dat het aluminium-hydroxyde-activiteitsprodukt tijdens de vorming van deze horizonten hoog geweest moet zijn, en dat cheluvatie geen dominerende rol gespeeld kan hebben.

In vele pseudogleygronden wordt ingespoelde klei gevonden. Kleiverplaatsing kan textuurverschillen tussen boven- en ondergrond verklaren, maar niet het negatieve saldo van de kleibalans in sommige profielen. De met het seizoen wisselende pH en de bleking en vlekken van de eluviale horizonten van pseudogleygronden kunnen verklaard worden door periodieke reductie en uitspoeling. Er wordt secundaire silica aangetroffen in deze horizonten, en de aluminium-tussenlagen in de kleimineralen bevatten ingesloten ferro-ionen. Deze verschijnselen, evenals de tussenlagen zelf en het negatieve kleisaldo, kunnen gevolg zijn van een bodemvormend proces onder hydromorfe omstandigheden.

In de volgende delen van deze samenvatting worden eerst de reeds verschenen artikelen behandeld en daarna de hoofdstukken en de appendix van dit boek.

FERROLYSE, EEN HYDROMORF BODEMVORMEND PROCES

In dit artikel (Brinkman, 1970) is een hydromorf bodemvormend proces gepostuleerd, beschreven en benoemd: ferrolyse, kleiafbraak (lysis) door een proces berustend op reduc-

tie van ferri-oxyden afgewisseld met oxydatie van ferro-ionen. De meeste deelprocessen van ferrolyse werden aannemelijk gemaakt door verwijzing naar gegevens van anderen betreffende grondmonsters, kleisuspensies en kolomexperimenten.

Het proces is schematisch weergegeven in het diagram voorin dit boek. IJzeroxyden worden gereduceerd tot Fe^{2+} onder microbiële afbraak van organische stof nadat de uitspoelingshorizonten met water zijn verzadigd. Andere kationen worden uitgewisseld voor Fe^{2+} en uitgespoeld, samen met een deel van de ferro-ionen. Tijdens de reductie worden waterstofionen verbruikt; deze worden aangevuld doordat aluminiumionen gedeeltelijk worden geneutraliseerd en gepolymeriseerd. Daarna stijgt de pH van 4-5 naar 6-7. De aluminiumpolymeren worden deels uitgespoeld, deels gefixeerd als octaëdrische fragmenten of incomplete tussenlagen in zwellende kleimineralen. Enig Fe^{2+} dat eerst uitwisselbaar was wordt ingesloten. De kationen-uitwisselcapaciteit van de kleifractie daalt. Wanneer weer zuurstof toetreedt in de uitspoelingshorizonten wordt uitwisselbaar Fe^{2+} weer geoxydeerd tot ferri-oxyden; hierbij ontstaat uitwisselbaar H^+ . De waterstofklei wordt snel omgezet in een aluminium-magnesiumklei door gedeeltelijk oplossen van de kleimineralen. De silica die overblijft lost deels op en kan bij uitdroging weer neerslaan in amorphe vorm. Een deel verdwijnt in oplossing in de volgende natte periode.

AFBRAAKVERSCIJNSELEN IN KLEIHUIDJES

Plasma en kleihuidjes in zure, periodiek natte uitspoelingshorizonten zijn korrelig, isotroop of weinig dubbelbrekend, sterk opaliserend in opvallend licht, en hebben een laag gehalte aan ijzeroxyden in vergelijking met de diepere horizonten. Deze verschijnselen zijn het duidelijkst in georiënteerde klei; ze werden microscopisch, microchemisch en met de röntgendiffractie-microcamera bestudeerd in individuele kleihuidjes (Brinkman et al. 1973).

De röntgendiffractie-foto's gaven aan dat isotrope kleihuidjes in deze gronden meer, zeer fijnkorrelige, kwarts en minder kleimineralen bevatten dan goed dubbelbrekende kleihuidjes. Dit leek te wijzen op nieuwvorming van kwarts bij kleiafbraak. Later bleek echter dat althans de grovere kwarts in de kleifractie grotendeels detritisch was. Hooguit een deel van de kwartstoename bij de kleiafbraak zou dus toegeschreven kunnen worden aan synthese.

Bij microchemische analyse van kleihuidjes met de elektronen-microsonde werden lagere gehalten aan Fe, Mg, K, iets lagere Al- en hogere Si- en Ti-gehalten gevonden in isotrope, korrelige huidjes dan in dubbelbrekende. De kleihuidjes met de hoogste Si-gehalten lichten het sterkst opaliserend op in opvallend licht, waarschijnlijk vanwege fijnverdeelde secundaire silica. Röntgendiffractogrammen van kleifracties uit E-horizonten, die voornamelijk korrelige klei bevatten, gaven veel minder smectiet, meer kwarts en meer klei met tussenlagen te zien dan de B-horizont met voornamelijk dubbelbrekende klei.

PSEUDOCLEYGRONDEN IN BANGLADESH

Bij karteringen in Bangladesh bleken er grote arealen zure, periodiek natte gronden voor te komen. Na beschrijving van hun eigenschappen, het klimaat en de landvormen waarin

ze voorkomen (Brammer & Brinkman, 1977), volgde een detailstudie van de genese van een representatief profiel (Brinkman, 1977a). Hierbij werden sporen van drie bodemvormende processen herkend in gronden van waarschijnlijk laat Pleistocene ouderdom. Deze passen alle bij klimaten met een droog seizoen, maar progressief natter in de natte tijd; zwellen en krimpen en vorming van kalknodules (ontstaan van een vertisol met gilgai); klei-verplaatsing; ferrolyse. Ferrolyse bleek het belangrijkste bodemvormende proces te zijn in periodiek natte, kalkloze Holocene rivierafzettingen.

Ferrolyse in de gronden van Bangladesh wordt gekenmerkt door:

- een lage pH en aanwezigheid van uitwisselbaar aluminium in het droge seizoen afgewisseld met een hogere pH in het natte seizoen bij aanwezigheid van uitwisselbaar en opgelost Fe^{2+} ;
- een negatief kleisaldo zowel op grond van textuuranalyses als van Zr-gehalten in de kleifracties;
- aluminium-tussenlagen met ingesloten tweewaardig ijzer en een lage kationenuitwisselcapaciteit van de kleifracties in de bovenste horizonten;
- amorfe secundaire silica, in de vorm van isotrope aggregaatjes in de zandfracties van de bovenste horizonten. Ook werden met de raster-elektronenmicroscop 'aangevreten dekens' en bolletjes, ongeveer $1\text{ }\mu\text{m}$ groot, van amorfe silica waargenomen op een sterk verweerd kleihuidje.

HYDROMORFE PROBLEEMGRONDEN IN NOORDOOST THAILAND

Veldwerk in een probleemgebied voor landbouwontwikkeling (irrigatie) leidde tot een studie van de extreem verweerde, periodiek natte, zure en deels zoute en zure gronden op het uitgestrekte 'lage terras' van noordoost Thailand. Morfologische waarnemingen (Brinkman et al., 1977) wezen op voorverwerking van het sediment, klei-verplaatsing, kleiafbraak en herverdeling van ijzeroxiden onder periodiek natte omstandigheden en perforatie door bodemfauna.

De genese van een profiel in deze gronden werd verder bestudeerd met fysische, chemische en mineralogische methoden (Brinkman, 1977b). De grovere fracties bestaan bijna geheel uit kwarts; de zware mineralen zijn voornamelijk resistent (zirkoon, toermalijn, opake korrels, rutiel, anataas), zonder duidelijk diepteverloop. Ook dit wijst op voorverwerking.

De enkele amorfe silica-aggregaatjes in de bovenste horizonten en de aanzienlijke verschillen in kleisamenstelling met de diepte duiden op bodemvorming. De kleifracties van de diepere horizonten bevatten ongeveer 60% kaolinit en 10% kwarts; die van bovenin het profiel 45% kaolinit en 30% kwarts. Transmissie-elektronenmicrofoto's tonen duidelijke oplossingsverschijnselen van kaolinit in de bovenste horizont. Vermiculiet met aluminium-tussenlagen vormt ongeveer een kwart van de kleifracties in het hele profiel. De tussenlagen zijn bovenin vollediger dan dieper in het profiel en bevatten wat ingesloten tweewaardig ijzer. Aluminium is het voornaamste uitwisselbare kation. De kationenuitwisselcapaciteit is extreem laag, vooral bovenin het profiel maar ook dieper. Al deze verschijnselen werden verklaard door een lange periode van ferrolyse.

Deze gronden zijn plaatselijk zout en zuur en toxisch voor planten (Brinkman &

Dieleman, 1977). Het grootste deel van het land brengt één kleine rijstoogst per jaar op onder halfnatuurlijke inundatie in de natte tijd. Kleine, iets hoger liggende stukken zijn sterk zout in de bovenste laag en op het oppervlak, door de combinatie van zeer weinig uitspoeling tengevolge van de oppervlakkige afvoer tijdens de regens met een capillaire opstijging van de bodemoplossing wanneer het omringende land nat of geïnundeerd is. Door de hoge zoutconcentratie komt aluminium in toxische concentraties in de bodemoplossing voor en is de pH zover gedaald dat ook meetbare hoeveelheden driewaardig ijzer in oplossing zijn. In een irrigatie-proefproject in dit gebied zijn dergelijke, maar minder extreme, zoute zowel als zoute en zure plekken ontstaan tengevolge van overmatig watergebruik en verspilling bij de irrigatie van een tweede gewas in het droge seizoen. Na beschrijving van de verzoutings- en verzuringsprocessen, de mogelijke bronnen van het zout en de plaatselijke hydrologie werden adviezen opgesteld voor verbetering en gebruik van de verschillende soorten zoute en zure gronden in het gebied.

BODEMBESCHRIJVINGEN, ANALYSES EN INTERPRETATIE

Dit hoofdstuk bevat beschrijvingen en analysegegevens van een aantal pseudogleygronden op verschillende plaatsen in west Europa en van enkele goed ontwaterde gronden in soortgelijk materiaal in hun directe omgeving. Voorts zijn de voornaamste processen aangegeven die hun genese kunnen verklaren.

De volgende hoofdstukken zijn gebaseerd op de resultaten van dit hoofdstuk, op de hierboven samengevatte artikelen en op literatuurgegevens.

MEERDERE BODEMVORMENDE PROCESSEN IN ELK BODEMPROFIEL

Hoewel ferrolyse en cheluvatie elkaar lijken uit te sluiten, kunnen toch beide in één profiel gevonden worden. Cheluvatie is dan op ferrolyse gevolgd in de bovenste horizonten maar niet dieper in het profiel. Ook andere bodemvormende processen kunnen optreden zijn voor, na of tegelijk met ferrolyse of cheluvatie. In dit hoofdstuk zijn voorbeelden hiervan in tabelvorm vermeld, en zijn twee gevallen van ferrolyse en cheluvatie in één profiel beschreven.

PROCESSEN DIE ZICH IN PSEUDOGLEYGRONDEN, PODZOLEN EN 'PODZOLISCHE' GRONDEN AFSPLEN EN CRITERIA OM ZE TE ONDERSCHIEDEN

Op grond van systematische beschrijvingen in tabelvorm van de cheluvatie- en ferrolyse-processen zijn criteria ontwikkeld om hun gevolgen te kunnen onderscheiden. Uit de beschrijvingen is af te leiden dat deze twee processen elkaar uitsluiten, hoewel cheluvatie onder bepaalde omstandigheden wel kan volgen op ferrolyse. Voorts zijn criteria gegeven waarmee ferrolyse onderscheiden kan worden van kleuitspoeling en desilicatie. Hierdoor is het mogelijk geworden om de sporen van verschillende goed gedefinieerde processen te herkennen in gronden met verscheidene namen, zoals podzolen, podzolige gronden, pseudogleygronden. De criteria hebben voornamelijk betrekking op de uitspoelingshorizonten. Deze horizonten lijken meer onderzoek en aandacht waard te zijn dan ze gewoonlijk bij

bodemklassificatie krijgen.

APPENDIX

Van de methoden waarvoor geen samenvatting of verwijzing naar een gemakkelijk toegankelijke bron is gegeven in de eerdere artikelen, staat een korte beschrijving of verwijzing in de appendix. Deze bevat verder een korte uitleg van de gebruikte SI-eenheden en van de term equivalent die - dank zij een recente definitie in overeenstemming met SI - nu in de specificatie bij de eenheid mol gebruikt kan worden.

References

- Abrahamsen, G., K. Bjor, R. Horntvedt and B. Tveite, 1976. Effects of acid precipitation on coniferous forest. p. 37-63 in: Braekke, F.H. (ed.), 1976.
- Alexiades, C.A. and M.L. Jackson, 1965. Quantitative determination of vermiculite in soils. Soil Sci.Soc.Am.Proc. 29: 522-527.
- Avery, B.W., D.C. Findlay and D. Mackney, 1975. Soil map of England and Wales, scale 1:1 000 000. Ordnance Survey, Southampton. 1 map, 68 x 54 cm.
- Bakker, H. de, and J. Schelling, 1966. A system of soil classification for the Netherlands. The higher levels. (Dutch; English summary pp. 171-201). Pudoc, Wageningen. 217 pp., map, appendices 24 pp.
- Baldwin, M., C.E. Kellogg and J. Thorp, 1938. Soil classification. p. 979-1001 in: Soils and Men. U.S.Dept.Agric.Yearb.Agr. U.S.Govt.Pr.Off., Washington, D.C.
- Begheijn, L.Th. and J. van Schuylenborgh, 1971. Methods for the analysis of soils used in the laboratory of soil genesis of the Dept. of Regional Soil Science. Agr. University, Wageningen. 156 pp.
- Begheijn, L.Th., 1979. Improvements for the determination of ferrous iron in soils. Analyst (London) (in press).
- BIPM, 1977. The International System of Units (SI). 3rd edn. H.M.S.O., London. ISBN 0-11-480045-6. 54 pp.
- Bloomfield, C. 1957. The possible significance of polyphenols in soil formation. J.Sci. Food Agric. 8: 389-392.
- Blume, H.P., K.O. Muennich & U. Zimmermann, 1969. Untersuchungen ueber die Auswirkungen des Fichtenreinbaus auf Parabraunerden und Pseudogleye des Neckarlandes. VI. Wasserbewegung und Wasserbilanz. Mitteilgn Ver.Forstl.Standortskd.Forstpflanzenzuecht. 19: 105-111.
- Blume, H.P. (ed.), K.E. Bleich, H. Duemmier, S. Mueller, K.H. Papenfuss, E. Parasher, E. Schlichting, K.F. Schreiber, V. Schweikle, K. Stahr, F. Weller & J. Werner, 1971. Excursionen A und B, gemeinsame Tagung von Kommission V und VI der Internationalen Bodenkundlichen Gesellschaft in Stuttgart-Hohenheim. Mitteilgn Dtsch.Bodenkundl. Gesellsch. 14: 1-105.
- Bornand, M., 1973. Formations quaternaires du bassin rhodanien. Apports de l'étude des paléosols aux problèmes de chronologie quaternaire. Annls.Scient.Univ. Besançon, Géologie, 3ème Série (2): 15-18.
- Bouma, J. and L. van der Plas, 1971. Genesis and morphology of some Alpine pseudogley profiles. J.Soil Sci. 22: 82-93.
- Braekke, F.H. (ed.), 1976. Impact of acid precipitation on forest and freshwater ecosystems in Norway. Research Report FR 6/76, SNFF Project, NISK, 1432 Aas-NLH, Norway.
- Brammer, H. and R. Brinkman, 1977. Surface-water gley soils in Bangladesh: environment, landforms and soil morphology. Geoderma 17: 91-109.
- Brewer, R., 1964. Fabric and mineral analysis of soils. Wiley, New York, London, Sydney. 470 pp.
- Brinkman, R., 1970. Ferrollysis, a hydromorphic soil forming process. Geoderma 3: 199-206.
- Brinkman, R., 1977a. Surface-water gley soils in Bangladesh: Genesis. Geoderma 17: 111-144.
- Brinkman, R., 1977b. Problem hydromorphic soils in north-east Thailand. 2. Physical and chemical aspects, mineralogy and genesis. Neth.J.Agric.Sci. 25: 170-181.
- Brinkman, R., 1979. Clay transformations: aspects of equilibrium and kinetics. Ch. 12, pp. 433-457, in: Bolt, G.H. (ed.), Soil chemistry. Vol. V B. Physico-chemical models. Elsevier, Amsterdam.
- Brinkman, R. and P.J. Dieleman, 1977. Problem hydromorphic soils in north-east Thailand. 3. Saline-acid conditions, reclamation, improvement and management. Neth.J.Agric.Sci. 25: 263-277.
- Brinkman, R., A.G. Jongmans, R. Miedema and P. Maaskant, 1973. Clay decomposition in seasonally wet, acid soils: micromorphological, chemical and mineralogical evidence from individual argillans. Geoderma 10: 259-270.

- Brinkman, R., A.G. Jongmans and R. Miedema, 1977. Problem hydromorphic soils in north-east Thailand. 1. Environment and soil morphology. *Neth.J.Agric.Sci.* 25: 108-125.
- Brown, I.C., T.D. Rice and H.G. Byers, 1933. A study of claypan soils. U.S.Dep.Agric. Tech.Bull. 399. 43 pp.
- Bruckert, S. and F. Jacquin, 1969. Interaction entre la mobilité de plusieurs acides organiques et de divers cations dans un sol à muil et dans un sol à mor (French; English summary). *Soil Biol.Biochem.* 1: 275-294.
- Cain, C.C. and F.F. Riecken, 1958. Sequence relationships of loess-derived forested Planosols in Southeastern Iowa. *Soil Sci.Soc.Am.Proc.* 22: 445-449.
- Cate, R.B., Jr. and A.P. Sukhai, 1965. Salt, acidity and base status in the coastal clays of British Guiana. *Agr. Research in the Guianas*, Nov.-Dec. 1963. Bull. no. 82, Agric.Exp.Sta. Paramaribo, Suriname. p. 133-139.
- Coninck, Fr. de, 1967. Aspects physico-chimiques de la pédogénèse en Campine anversoise. Thesis, Louvain. 153 pp., 36 figures in separate vol. Also, revised text: Coninck, F. de, and A. Herbillon, 1969. Evolution minéralogique et chimique des fractions argileuses dans des Alfisols et des Spodosols de la Campine (Belgique). *Pédologie (Gand)* 19(2): 159-272, diagram.
- Davies, R.I., 1971. Relation of polyphenols to decomposition of organic matter and to pedogenetic processes. *Soil Sci.* 111: 80-85.
- Doeglas, D.J., 1955. A rectangular diagram for comparison of size frequency distributions. *Geol.Mijnbouw* 17: 129-136.
- Dovland, H., E. Joranger and A. Semb, 1976. Deposition of air pollutants in Norway. p. 15-35 in: Braekke, F.H. (ed.), 1976.
- Engelen, E. van, and H.W.A.M. Hurkens, 1975. Die Böden des Hochsolling. Publ. 607, Dept. Soil Science and Geology, Agric. Univ. Wageningen. 55 pp., 3 maps, legend.
- FAO, 1974. FAO-Unesco Soil map of the World. Vol. I. Legend. Unesco, Paris. 59 pp.
- Gerasimov, I.P., 1959. Brown Forest Soils in the U.S.S.R., Europe and the U.S.A. *Sov.Soil Sci.* 1959: 815-823.
- Glinka, K., 1914. Die Typen der Bodenbildung, ihre Klassifikation und geographische Verbreitung. Borntraeger, Berlin. 365 pp., map.
- Halma, G., 1973. Improved efficiency in XRFs routine analysis of geochemical samples - a simple sample changer and an elegant fusion technique. *Colloquium Spectroscop.Int.* Firenze, 1973. II: 626-631.
- Huang, W.H. and W.D. Keller, 1971. Dissolution of clay minerals in dilute organic acids at room temperature. *Am.Mineral.* 56: 1083-1095.
- IUPAC, 1978. Recommendations on the usage of the terms 'equivalent' and 'normal'. *Pure Applied Chem.* 50: 325-338.
- Kanivets, V.I., 1975. Source of accumulation of exchangeable aluminum in soils under the effect of reducing agents during gleying. *Sov.Soil Sci.* 1975: 702-706.
- Kornblyum, E.A. and B.A. Zimovets, 1961. Origin of soils with a whitish horizon in the plains of the Amur region. *Sov.Soil Sci.* 1961: 634-642.
- Kundler, P., 1959. Zur Kenntnis der Rasenpodsole und Grauen Waldböden Mittellusslands im Vergleich mit den Sols Lessivés des westlichen Europas. *Z.Pflanzenernaehr.Dueng. Bodenkd.* 86: 16-36.
- Liverovskiy, Yu.A., I.A. Sokolov and V.O. Targulyan, 1973. Principles of soil-profile and soil-genetic terminology. *Sov.Soil Sci.* 1973, 308-314.
- Petersen, L., 1976. Podzols and podzolization. DSR Forlag, Copenhagen. 293 pp.
- Ponomareva, V.V., 1964 (Russ.); 1969 (English). Theory of podzolization. Izdatelstvo Nauka, Moscow-Leningrad; Israel Program for Scientific Translations, Jerusalem. vi + 309 pp.
- Remmelzwaal, A., 1978. Soil genesis and quaternary landscape development in the Tyrrhenian coastal area of south-central Italy. Thesis, Amsterdam. 309 pp., 2 maps.
- Rode, A.A., 1964. Podzolization and lessivage. *Sov.Soil Sci.* 1964: 660-671.
- Ruhe, R.V., R.B. Daniels and J.G. Cady, 1967. Landscape evolution and soil formation in Southwestern Iowa. Soil Conservation Service, U.S.Dep.Agric.Tech.Bull. 1349. vi + 242 pp., 6 separate plates.
- Schnitzer, M. and J.G. Desjardins, 1968. Chemical characteristics of a natural soil leachate from a humic podzol. *Can.J.Soil Sci.* 49: 151-158.
- Schnitzer, M. and S.I.M. Skinner, 1963. Organo-metallic interactions in soils: 2. Reactions between different forms of iron and aluminum and the organic matter of a podzol B horizon. *Soil Sci.* 96: 181-186.
- Schnitzer, M. and S.I.M. Skinner, 1964. Organo-metallic interactions in soils: 3. Properties of iron- and aluminum-organic matter complexes, prepared in the laboratory and extracted from a soil. *Soil Sci.* 98: 197-203.

- Schuylenborgh, J. van, 1962. On soil genesis in temperate humid climate. I. Some soil groups in the Netherlands. *Neth.J.Agric.Sci.* 10: 127-144.
- Schuylenborgh, J. van, 1963. On soil genesis in temperate humid climate. II. Behaviour of the non-clay fraction. *Neth.J.Agric.Sci.* 11: 10-12.
- Schuylenborgh, J. van and M.G.M. Bruggenwert, 1965. On soil genesis in temperate humid climate. V. The formation of the 'albic' and 'spodic' horizon. *Neth.J.Agric.Sci.* 13: 267-279.
- Slager, S., A.G. Jongmans, R. Miedema and L.J. Pons, 1978. Fossil and recent soil formation in Late Pleistocene loess deposits in the Southern part of the Netherlands. *Neth.J.Agric.Sci.* 26: 308-318.
- Smith, G.D., 1941. Advantages and problems related to the field study of soil development. *Soil Sci.Soc.Am.Proc.* 6: 78-82.
- Smith, G.D., W.H. Allaway and F.F. Riecken, 1950. Prairie soils of the Upper Mississippi valley. *Adv.Agron.* 2: 157-205.
- Soil Survey Staff, 1975. Soil Taxonomy. A basic system of soil classification for making and interpreting soil surveys. U.S.Dep.Agric. Agric. Handbook 436. Washington. 754 pp.
- Swindale, L.D. and M.L. Jackson, 1956. Genetic processes in some residual podzolised soils in New Zealand. *Trans.Int.Congr.Soil Sci.*, 6th, E: 233-239. Paris.
- Tamura, T., 1958. Identification of clay minerals from acid soils. *J.Soil Sci.* 9: 141-147.
- Wernstedt, F.L., 1972. World climatic data. Climatic Data Press, P.O.B. 413, Lemont, Pa. 16851, U.S.A. 523 pp.
- Wilson, A.D. and G.A. Sergeant, 1963. The colorimetric determination of aluminium in minerals by pyrocatechol violet. *Analyst (London)* 88: 109-112.
- Zaydelman, F.R., 1965. Mineral hydromorphic soils of the forest zone. *Sov.Soil Sci.* 1965: 1408-1419.
- Zonn, S.V., 1973. Environmental settings of the processes of lessivage, pseudo-podzolization and podzolization during the Quaternary period in the western and northwestern regions of the U.S.S.R. *Soil Sci.* 116: 211-217.
- Zonn, S.V., A.F. Kostenkova, G.P. Musorok and N.V. Khavkina, 1975. Pseudo-podzolization and its identification from the composition and distribution of free forms of iron. *Sov.Soil Sci.* 1975: 531-546.
- Zyrin, N.G., T.A. Sokolova, L.I. Gavva and M.I. Guseva, 1976. Characteristics of the composition of clay minerals in the subtropical podzols of western Georgia. *Sov.Soil Sci.* 1976: 348-356.

Curriculum vitae

De auteur behaalde in 1954 het diploma Gymnasium β aan het Gemeentelijk Gymnasium te Hengelo (O). In 1961 studeerde hij af (met lof) aan de Landbouwhogeschool te Wageningen in de richting Bodemkunde en Bemestingsleer (vakken regionale bodemkunde, algemene bodemkunde en geologie).

Van 1961 tot 1971 was hij werkzaam als bodemkundige en landevaluatie-deskundige bij de Voedsel en Landbouw Organisatie, tot 1964 in (toenmalig Brits) Guyana, tot 1966 in Bangladesh (Oost Pakistan) en tot 1971 in (West) Pakistan. Sinds 1971 is hij werkzaam als wetenschappelijk hoofdmedewerker aan de Landbouwhogeschool, met enige korte onderbrekingen door buitenlands werk voor FAO en de Dienst Bodemkartering, Suriname.